School of Engineering and Design

Electronic & Computer Engineering

Intelligent Genetic Algorithms for Next-Generation Broadband Multi-Carrier CDMA Wireless Networks

A thesis submitted for the degree of Doctor of Philosophy

Yang Zhang

Brunel University

Supervisor: Dr Qiang Ni

Co-Supervisor: Prof Yonghua Song

August 2008

On January 27, 2004, my grandma and all the families sent me off at Beijing airport. She left us on June 14, 2006.

This thesis is dedicated to the memory of my grandma.

Table of Contents

Abstract

This dissertation proposes a novel intelligent system architecture for next-generation broadband multi-carrier CDMA wireless networks. In our system, two novel and similar intelligent genetic algorithms, namely Minimum Distance guided GAs (MDGAs) are invented for both peak-to-average power ratio (PAPR) reduction at the transmitter side and multi-user detection (MUD) at the receiver side. Meanwhile, we derive a theoretical BER performance analysis for the proposed MC-CDMA system in AWGN channel. Our analytical results show that the theoretical BER performance of synchronized MC-CDMA system is the same as that of the synchronized DS-CDMA system which is also used as a theoretical guidance of our novel MUD receiver design. In contrast to traditional GAs, our MDGAs start with a balanced ratio of exploration and exploitation which is maintained throughout the process. In our algorithms, a new replacement strategy is designed which increases significantly the convergence rate and reduces dramatically computational complexity as compared to the conventional GAs. The simulation results demonstrate that, if compared to those schemes using exhaustive search and traditional GAs, (1) our MDGA-based PAPR reduction scheme achieves 99.52% and 50+% reductions in computational complexity, respectively; (2) our MDGA-based MUD scheme achieves 99.54% and 50+% reductions in computational complexity, respectively. The use of one core MDGA solution for both issues can ease the hardware design and dramatically reduce the implementation cost in practice.

Acknowledgements

Up today, this dissertation is finalized. The writing lasts approximately three months and associated PHD study has been carried on about four years. However, it is not a full-stop of the study. The study will go on along with all my life. It is a time worth to be recorded about what I feel and what I think these days. It was expected it would be great excitement after the work is done, whereas, my heart is quite peaceful at this moment. "You reap what you sow", as people always said. I know what I have paid out these days. At least, I feel no regret to myself and can say to myself "I deserve it".

Actually, there is nothing to be proud of what I have done. What I have done is just what I should do responsible as an overseas student being thousands miles far from my motherland. I am proud to be born as a Chinese and appreciate the motherland brought me up and created opportunities for our generation to study overseas. This writing is dedicated to my beloved dad and mum, who are most adorable people to me in this planet, who are my spiritual supporters, who are the entire of mine and who dedicate the entire of themselves to me. The family is always the peaceful harbor whenever the storm comes.

This writing is also a gift presented to Dr Qiang Ni and Prof Yonghua Song - my whole-life supervisors. The keynote to decide a dissertation's success or not is the selection of research topic. It is not possible to complete this thesis promptly without

help of Dr Qiang Ni. His intensive responsibility, fabulous dedication, abundant professional knowledge and unambiguous direction-sense lead the work moving on in an orderly way. Also, thank-you could not just express my inner appreciation to Prof Yonghua Song, who led me into this field, creates up the comfortable environments and care about every single aspect of my life in this lonely country. They are most admirable people in my heart.

Never forget one's happiness comes from, it comes every single help from all your surroundings. There would be a huge name list in my words. For whom all of you, this writing is the gift to say thank you. Also, special thanks to Nini, thanks for waiting.

Meanwhile, I really appreciate examiners for sharing their precious time with my thesis review.

List of Tables

List of Figures

List of Acronyms

2-D	Two Dimensional
2G	Second Generation
2.5G	2.5 Generation
3G	Third Generation
3GPP	3rd Generation Partnership Project
8PSK	eght-phase shift keying
A/D	Analog to Digital
ACL	Auto-Correlation
ACTs	Advanced Communication Technologies
AMPS	Advanced Mobile Phone System
AWGN	Additive White Gaussian Noise
ARIB	Association of Radio Industries and Business
B3G	Beyond 3G
BER	Bit-Error-Rate
BPSK	Binary Phase Shift Keying
BRAN	Broadband Radio Access Networks
CCDF	Complementary Cumulative Distributive Function
CCL	Cross-Correlation
CD	Conventional Matched Filter Detector
CDMA	Code Division Multiple Access

CSMA	Carrier Sense Multiple Access
CSTT	China Academy Telecommunication Technology
D/A	Digital to Analog
D-AMPS	Digital AMPS
DCS-1800	Digital Cellular System 1800
DF	Decision-Feedback
DFT	Discrete Fourier Transformation
DS	Direct Sequence
EDGE	Enhanced Data Rates for Global Evolution
ETSI	European Telecommunication Standards Institute
FCC	Federal Communication Commission
FDD	Frequency Division Duplex
FDMA	Frequency Division Multiple Access
FEC	Forward Error Control
FH	Frequency Hopping
GA	Genetic Algorithm
GPRS	General Packet Radio Services
GPS	Global Positioning System
GMSK	Gaussian Minimum Shift Keying
GSM	Global System for Mobile
HPA	High-Power Amplifier
HIPERMAN	High Performance Radio Metropolitan Area Network

HSCSD	High-Speed Circuit-Switched Data
ICT	Information and Communication Technology
IDFT	Inverse Discrete Fourier Transformation
IF	Iterative Flipping
IFFT	Inverse Fast Fourier Transformation
IMT	International Mobile Telecommunication
IMT-MC	IMT-Multi-Carrier
ISI	Inter-Symbol Interference
ITU	International Telecommunication Union
JDC	Japanese Digital Cellular
LPF	Low-Pass Filters
MAI	Multi-Access Interference
MAP	Mobile Application Part
MC	Multi-Carrier
MC-CDMA	Multi-Carrier-Code Division Multiple Access
MC-DS-CDMA	Multi-Carrier-Direct Sequence-Code Division Multiple Access
MC-FDMA	Multi-Carrier-Frequency Division Multiple Access
MC-TDMA	Multi-Carrier-Time Division Multiple Access
MDGA	Minimum Distance Generic Algorithm
MT-DS-CDMA	Multitone Direct Sequence-Code Division Multiple Access
MF	Matched-Filter
MMSE	Minimum Mean Square Error

MUD	Multi-User Detection
NMT	Nordic Mobile Telephone
OFDM	Orthogonal Frequency Division Multiplexing
OFCDM	Orthogonal Frequency and Code Division Multiplexing
P/S	Parallel to Serial
PAPR	Peak-to-Average Power Ratio
PDC	Personal Digital Cellular
PDMA	Polarization Division Multiple Access
PIMRC	Personal, Indoor and Mobile Radio Communications
PN	Pseudo-Random
PTS	Partial Transmitted Sequence
S/P	Serial to Parallel
SC	Single-Carrier
SDMA	Space Division Multiple Access
SIR	Signal-to-Interference Ratio
SLM	Selective Mapping
SM	Serial Modulation
SNR	Signal-to-Noise Ratio
TACS	Total Access Communications System
TDD	Time Division Duplex
TDMA	Time Division Multiple Access
TD-SCDMA	Time Division-Synchronous Code Division Multiple Access

TH	Time Hopping
UTRA	Universal Terrestrial Radio Access
WCDMA	Wideband CDMA
WiMAX	Worldwide Interoperability of Microwave Access
WMAN	Wireless Metropolitan Area Network

Chapter 1 Introduction

1.1 Evolution of Wireless Communication

The report of Global Trends and Policies [1] points out that information and communication technology (ICT) has reshaped the world over the past few decades. By connecting various people and areas together, ICT becomes the vital field in national, regional and global development, and decides the future. In particular, wireless communication is one of the most exciting ICT technologies which is penetrating every domain of our daily life. In 1897, Guglielmo Marconi, the dashing Italian, first demonstrated the ability of radio to provide wireless communication with ships sailing in the English Channel. Since then new wireless communication methods and services have been developed and used extensively worldwide. In the early time of the last century, after human speech was first sent wirelessly by Reginald Fessenden, by means of the regulations of the frequency allocation and wireless equipments, the wireless communication industry started to take shape [2]. During the World War I and II, the envelope of wireless communication was further enlarged through numerous operational needs in the military. After the World War II, the driving demand of wireless technology changed from the military purpose to the public use. In late 70's, the first generation mobile communication system emerged and it introduced cellular structure to address the problems of limited available

channel frequencies, high-power transmitters and poor coverage of large areas in other conventional mobile telephone systems. Consequently, each transceiver is connected to a central switching office, which controls and monitors overall system and provides the interface to the local telephone operators. Craig McCaw was one of the pioneers in the mobile telephone field, who then brought the cellular infrastructure from the analog into the digital era which led a revolution: In 1983 the average price of a cellular phone was $3,000, where by 1993 the price had dropped to less that $100. As a consequence, in less than a decade the number of mobile subscribers increased from less than 100,000 to over 16 million in the US and revenues went from less than half a billion to nearly $11 billion [3]. Worldwide, the rapid growth of mobile cellular use, various satellite services, and wireless Internet is generating tremendous changes in the telecommunications and networking field. In the following, let us first review the evolution of wireless communication and motivate the research issues to be addressed in this thesis.

Figure 1.1 illustrates the evolutional process of wireless communication systems from the first generation towards future generations at different stages. Generally, it is a transition process from analog systems to digital systems as well as from low data rate systems towards high data rate systems.

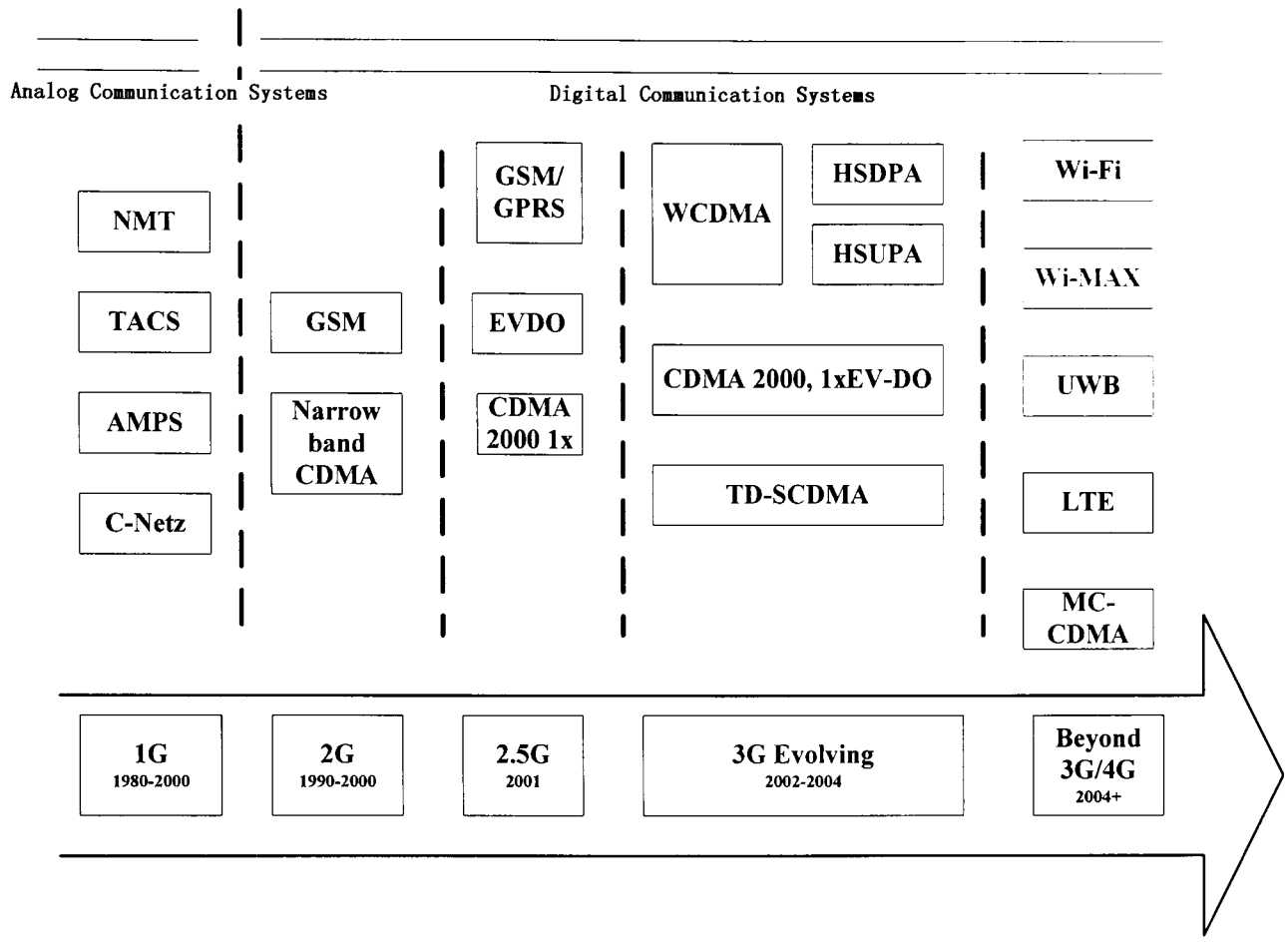

Figure 1.1 Evolution of Wireless Communication Systems

1.1.1 First Generation

The first generation of mobile cellular telecommunications systems emerged in the 1980s. It mainly dealt with voice traffic using analog technology. The frequency-reuse in mobile cellular network increases the system capacity by dividing coverage area into small cells. Some successful standards mutually co-existed in different countries, which were Nordic Mobile Telephone (NMT), Total Access Communications System (TACS), and Advanced Mobile Phone Service (AMPS). Others were mostly used in one country, like C-Netz in West Germany and Radiocomm 2000 in France. NMT was initially applied in Scandinavia and adopted in some countries in central and southern Europe. It came into two variations: NMT-450 and NMT-900. NMT-450 was launched

in market using 450-MHz frequency band earlier than NMT-900 which used 900-MHz band. NMT can support international roaming. AMPS is an American mobile standard that used the 800-MHz frequency band whereas UK used the TACS standard which is quite similar to AMPS but it operated in the 900 MHz. TACS was also adopted in some Middle East countries as well as in southern Europe. AMPS was also launched in some countries including South America, Australia and New Zealand in addition to North America. MCS was the first commercial cellular network in Japan operated by NTT. So far, some areas of the world have already stepped into 3G era, whereas, in a few countries or local districts people are still using first generation networks. However, all the networks may finally be substituted by digital network systems.

1.1.2 Second Generation

It is apparent to differentiate the second generation (2G) mobile cellular system from the first generation. The former is a digital system, whereas the latter is an analog system. The system capacity of the second generation networks is much higher than the first generation systems. One frequency channel is simultaneously divided among several users (either by time division or by code division). The coverage area is further divided into smaller one in which the service area is covered by macro-, micro-, and pico-cells. Consequently, the system capacity is enhanced. There are four main standards for the 2G systems: Global System for Mobile (GSM) communications and its derivatives, Digital AMPS (D-AMPS), narrowband code

division multiple access (CDMA or called IS-95), and Personal Digital Cellular (PDC). GSM is recognized as the most successful and the most deployed 2G system worldwide. Originally, it was a European standard, and soon spread over the world except Americas. North America used Personal Communication System 1900 (PCS-1900; a GSM derivative, also named as GSM-1900) which occupied 1900 MHz frequency spectrum. In South America, Chile is the main user of GSM system. The basic GSM used 900-MHz band and Digital Cellular System 1800 (DCS-1800; also termed as GSM-1800) uses 1800-MHz band. Compared to 900-MHz, 1800-MHz can accommodate more users because normally the coverage of 1800-MHz would be smaller than 900-MHz. Later, the European Telecommunication Standards Institute (ETSI) developed the GSM-400 and GSM-800 specifications. The GSM-400 is mostly applied in remote and nomadic areas which have less population but large cellular coverage and GSM-800 is North America standard. Additionally, D-AMPS (also known as US-TDMA) is also an American 2G standard which is also used in some other countries, like Israel and some Asian countries. D-AMPS is backward compatible with AMPS and has different technical structures with GSM, although it is based on the TDMA scheme as well as GSM.

CDMA, also termed as IS-95 standard, patented by Qualcomm, is another important sub-branch of 2G wireless and mobile communication standard. Different from GSM dividing time slots to different users, CDMA allocates different codes to separate transmissions in the same frequency. Currently, CDMA is commercialized in the

United States, South Korea, Hong Kong, Japan, Singapore, and some other East Asian countries. Especially, this standard is widely used in South Korea.

Personal Digital Cellular (PDC) is the Japanese second generation standard. Originally, it was named as Japanese Digital Cellular (JDC) and later was renamed as PDC to attract more subscribers outside Japan. Unfortunately, the renaming did not bring the overseas market merits as Japanese expected. The standard is commercially used only in Japan. The specification is known as RCR STD-27 and the system operates in the two frequency bands, 800 MHz and 1,500 MHz. It is a mixed analog/digital system. Its physical layer parameters are quite similar to D-AMPS, however its protocol stack is close to GSM. The localized 2G standard urges Japan to develop 3G standards and the major Japanese telecommunications equipment manufacturers are eager to succeed in 3G, because the PDC system capacity is quickly running out.

1.1.3 2.5 Generation

The 2.5 Generation (2.5G) is an intermediate process of the 2G evolving to the 3G. The boundary between 2G and 2.5G is indefinite. Furthermore, some upgrades in 2.5G may have the same performance as those occurring in 3G. Generally, a 2.5G system should include one or all of the following technologies: high-speed circuit-switched data (HSCSD), General Packet Radio Services (GPRS), and Enhanced Data Rates for Global Evolution (EDGE). The main drawback of GSM is

its low air interface data rates. The key technology of HSCSD is to further divide one time slot into several time slots which increase the total data rate. However, one main disadvantage of HSCSD would be the low efficiency in utilizing the scarce radio resources. The solution of GPRS can supply higher data rates up to 115 Kbps or even higher regardless of error correction. Furthermore, GPRS is a packet-switched system which could allow allocating the radio resources in a more flexible way than HSCDS. GPRS is especially suitable for non-real-time applications such as e-mail and web surfing, whereas it does not support well real-time applications as the resource allocation in GPRS is contention-based and thus the maximum delay can not be guaranteed. GPRS is an important step towards a 3G system even the expense of the system is much higher than HSCSD, because the traffic will increasingly become data instead of conventional voice. The third version of 2.5G from GSM is EDGE, which is an acronym of the enhanced data rates for GSM evolution. The idea behind EDGE is a new modulation scheme called eight-phase shift keying (8PSK), which increases the data rates of standard GSM up to threefold and could coexist with the old modulation schemes such as Gaussian minimum shift keying (GMSK). The combination of the above-mentioned three 2.5G systems forms the rudiment of early 3G networks.

In the meantime of GSM evolving towards 2.5G, other 2G standards are also evolving to 2.5G. IS-95 (CDMA) underwent the stage of IS-95B and IS-95C. The transition from IS-95 to 3G is smooth because of the coexistence of air interface between IS-95,

IS-95B, C and its upcoming 3G version. On the other hand, PDC in Japan also evolved to a packet data network (PDC-P) providing a new proprietary service called i-mode, which can be used to access wireless Internet services.

1.1.4 Third Generation

In the same year that Finland launched the first GSM network in 1991, ETSI already started the standardization work for the third generation (3G) mobile communication network. This new system was called the Universal Mobile Telecommunications System (UMTS). ETSI is not the only organization developing 3G network. There are also some other organizations and research bodies involved like European Advanced Communication Technologies (ACTs) and International Telecommunication Union (ITU). A milestone of the 3G radio interface development happened in 1996 and 1997 when both the Association of Radio Industries and Business (ARIB) and ETSI selected wideband CDMA (WCDMA) as the 3G UMTS standard. Later, 3rd Generation Partnership Project (3GPP) involved with most important telecommunication companies started to be responsible for the 3G development work, the motivation of which is to produce the specifications for a 3G system based on the ETSI Universal Terrestrial Radio Access (UTRA) radio interface and the enhanced GSM/GPRS Mobile Application Part (MAP). The UTRA system composes two modes, frequency division duplex (FDD) and time division duplex (TDD). In the FDD mode, the uplink and downlink use separate frequency bands. These carriers have a bandwidth of 5 MHz. The TDD mode uses only one frequency carrier for both

uplink and downlink. The 15 time slots in a radio frame can be dynamically allocated between uplink and downlink directions.

Currently, the most promising 3G standards include the European/Japanese ETSI/ARIB wide-band CDMA (WCDMA) proposal, also known as UTRA FDD, American standard CDMA2000 and Chinese standard TD-SCDMA [4].

WCDMA

By definition, the bandwidth of a WCDMA system is 5 MHz or more. This bandwidth was chosen because:

- It is capable to provide downlink data rates of 144 and 384 Kbps at outdoor environment and 2 Mbps indoors;
- The smallest possible allocation of scarce frequency band should be used;
- This wideband can provide better performance in multi-path and inter-symbol interference (ISI) environment than narrow band.

The WCDMA radio interface proposals can be divided into two groups: synchronous network and asynchronous network. In a synchronous network all base stations are time synchronized to each other which could be realized by means of Global Positioning System (GPS). It is hoped that this could result in more efficient radio interface at the cost of expensive hardware in base stations. However, the practical performance is not that optimistic because GPS receivers' performance is somehow limited in crowded city centers (numerous blind spots) or indoors. Other WCDMA

properties include fast power control in both uplink and downlink, and adaptive spreading for dynamic data rates.

CDMA2000

The CDMA2000 system is based on WCDMA technology and prompted by another major 3G standardization organization namely 3GPP2. In the world of IMT-2000 (umbrella specification of all 3G systems), this proposal is known as IMT-Multi-Carrier (IMT-MC). The CDMA2000 is backward compatible with IS-95 and uses the same core network as IS-95, namely IS-41, because this makes the transition from IS-95 to 3G network much easier and smoother. The chip rate of CDMA2000 is not fixed as that of WCDMA. It will be a multiple (up to 12) of 1.2288 Mcps, giving the maximum rate of 14, 7456 Mcps. In the forward link (downlink) of CDMA2000, there are two configurations. One is the Multi-Carrier configuration, which several narrowband (1.25 MHz) carriers are grouped together. Another configuration of forward link is direct spread, which the whole available forward link bandwidth is allocated to one direct spread wideband carrier. In the reverse link of CDMA2000, only direct spread configuration is used [5].

TD-SCDMA

Time Division-Synchronous Code Division Multiple Access (TD-SCDMA) is a Chinese 3G proposal being pursued by China Academy Telecommunication Technology (CATT), Datang and Siemens AG. It was accepted by ITU as one of the

3G mobile communication standards. The "S" in TD-SCDMA stands for "synchronous", which means that uplink signals are synchronized at the base station in terms of continuous timing adjustments. TD-SCDMA combines the technical advantages of CDMA, FDMA and TDMA. It works at TDD mode through dynamically adjusting the number of time slots allocated for downlink and uplink to easily handle the asymmetric traffic with different data rate requirements. Since it is a TDD mode, there is no need of paired spectrum allocation, and hence the efficiency of utilizing frequency spectrum is dramatically increased. It also uses the time slots to reduce the number of users in each timeslot. The uplink synchronization of all users within one time slot can also improve the system capacity by selecting spreading codes with better orthogonality [6].

1.1.5 Future Generations

In the meantime of standardization and launch into market of 3rd generation mobile communication system, the R&D work for future generations (4G, 5G) also named as beyond 3G (B3G) broadband mobile and wireless access commenced as well. The boundary between the 3G and future generation wireless systems would be obscure in some sense. Nevertheless, some apparent features have been agreed for future generation mobile and wireless networks [7]:

- Supporting various multimedia services;
- Wireless access to broadband fixed networks;
- Seamless roaming among different areas;

- High data rates (2-20 Mbps for 4G and 20-100 Mbps for 5G), high mobility and seamless coverage;
- Several systems coexisting in terms of different service requirements;
- High capacity with low bit cost;
- Open network interface based on IPv6 protocol.

So far, there are several candidate proposals for future generation broadband mobile and wireless access system as shown in Figure 1.1, such as Wireless Fidelity (Wi-Fi) [8], Worldwide Interoperability of Microwave Access (WiMAX) [9], Ultra Wideband (UWB) [10], 3G Long-term Evolution (LTE) [11] and Multi-Carrier-Code Division Multiple Access (MC-CDMA) [12, 13]. Among them MC-CDMA is a relatively new and a promising technique. It proposes to combine Orthogonal Frequency Division Multiplexing (OFDM) [14] scheme with CDMA multiple access technique. The main advantages of MC-CDMA include more robustness in dispersive multi-path mobile wireless environments as compared to CDMA and improved bit-error-rate (BER) performance as compared to OFDM. This thesis aims at investigating some fundamental issues in MC-CDMA system, which will be detailed in the following chapters.

1.2 Motivations of the Thesis

In order for MC-CDMA to be a cogent candidate for future generation mobile and wireless communication in practice, we need to address four important issues of the system. The first one is how to design such a new system effectively. The second one

is the performance analysis of the new system. The last two important issues of MC-CDMA are potential high peak-to-average power ratio (PAPR) and complex multi-user detection (MUD). The drawback of the existing solutions to the last two issues in MC-CDMA is their high computational complexity. Therefore, we propose two novel and similar intelligent genetic algorithms which assist the system in terms of reducing the high computational complexity. The common core of the two algorithms can minish the implementation cost in practical MC-CDMA systems.

1.3 Contributions of the Thesis

The main contributions of this dissertation are:

- We propose a novel intelligent system architecture for MC-CDMA which introduces our intelligent genetic algorithms both at the transmitter and the receiver sides. Such a robust architecture can effectively deal with both the PAPR and MUD problems.
- We derive a theoretical BER performance analysis for the proposed new system in AWGN channel. As a result, we demonstrate that the theoretical BER performance of synchronized MC-CDMA is the same as that of the synchronized DS-CDMA in AWGN channel.
- We propose one core solution Minimum Distance guided Genetic Algorithm (MDGA) suitable for the two issues (PAPR reduction and MUD) of the MC-CDMA system, which can help to reduce the implementation cost of the system dramatically. The advantages of our schemes have been verified through

extensive simulation results.

1.4 Structure of the Thesis

The rest of the dissertation is organized as follows: Chapter 2 reviews the existing multiple access techniques (including CDMA, OFDM and MC-CDMA) as well as the two crucial problems (PAPR reduction and MUD) with the existing solutions. A novel system design of MC-CDMA and its performance analysis are presented in Chapter 3. Chapter 4 and Chapter 5 describe the details of our proposed novel algorithms applied to both PAPR reduction and MUD issues in MC-CDMA as well as the simulation results. The conclusion and future work are highlighted in Chapter 6.

1.5 List of Publications

- Y. Zhang, Q. Ni. "Design of an Intelligent Genetic Algorithm for Peak Average Power Ratio Reduction in a Multi-Carrier Wireless System". 1st Brunel SED Research Student Conference (ReSCon 2008), June 25-26th, 2008. Awarded the Best Presentation Prize.
- Y. Zhang, Q. Ni, H. Chen, Y. Song. "An Intelligent Genetic Algorithm for PAPR Reduction in a Multi-Carrier CDMA Wireless System". IEEE International Wireless Communications and Mobile Computing Conference (IWCMC 08), Crete, Greece, August 6-8th, 2008. Nominated for inclusion in a special issue in Wiley Journal of Wireless Communications and Mobile

Computing.

- Q. Ni, J. Jehanzeb, Y. Zhang, S. Guan. "A Minimum Distance Guided Genetic Algorithm for Multi-User Detection in a Multi-Carrier CDMA Wireless Broadband System". The Fifth IEEE International Conference on Broadband Communications, Networks, and Systems (Broadnets 2008), London, September 8-11th, 2008.

Chapter 2 Literature Review

2.1 Multiple Access Technologies for Single-Carrier Communication Systems

The term "multiple access" refers to the sharing of a communication resource, e.g. time and frequency bandwidth among different users [15]. Multiple access technologies are a kernel in building multi-user mobile and wireless communication networks. Without the coordination provided by multiple access technologies, multiple users in the system could not utilize the channel effectively. Traditional communication systems were based on multiple access technologies with single-carrier modulation, i.e. single-carrier communication systems, in which data frames from different users are modulated, multiplexed and transmitted on a single frequency (i.e. single-carrier). Figure 2.1 shows some conventional single-carrier multiple access technologies.

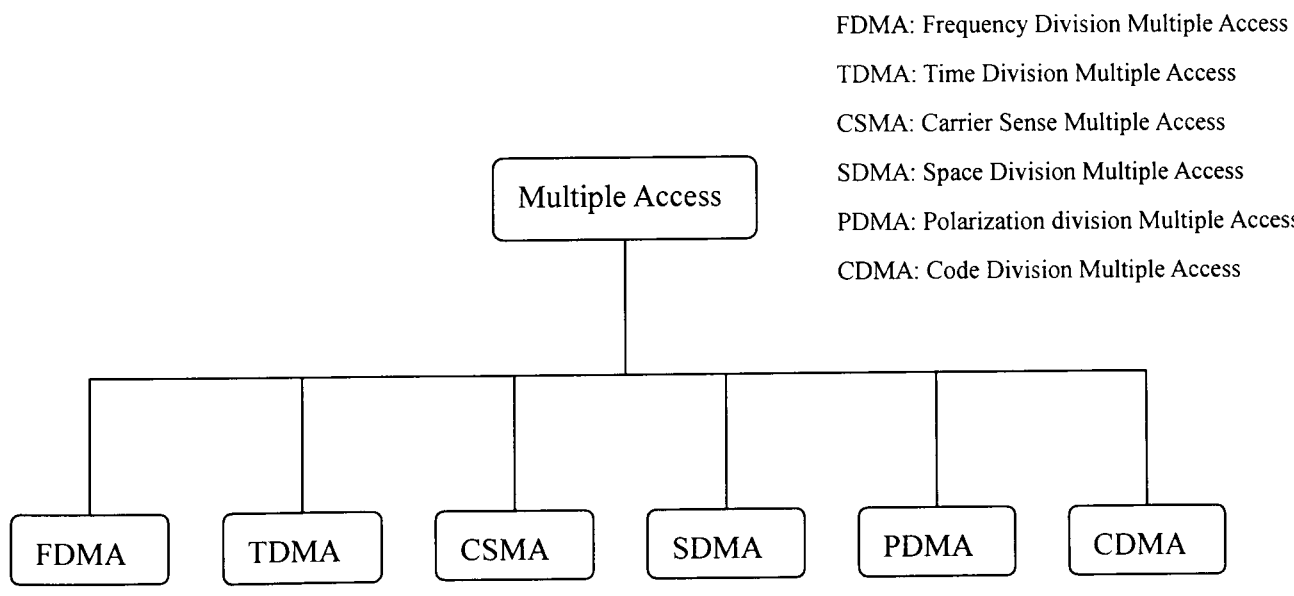

Figure 2.1 Multiple Access Technologies for Single-Carrier Communication Systems

2.1.1 Frequency Division Multiple Access

As an early and simple technology of transmitting telephony signal simultaneously. Frequency Division Multiple Access (FDMA) assigns dedicated frequency channels in sequence to each user as shown in Figure 2.2. During the period of the call, no other user can use the same channel. Band-pass modulation and guard band are normally used to enable frequency separation between different users.

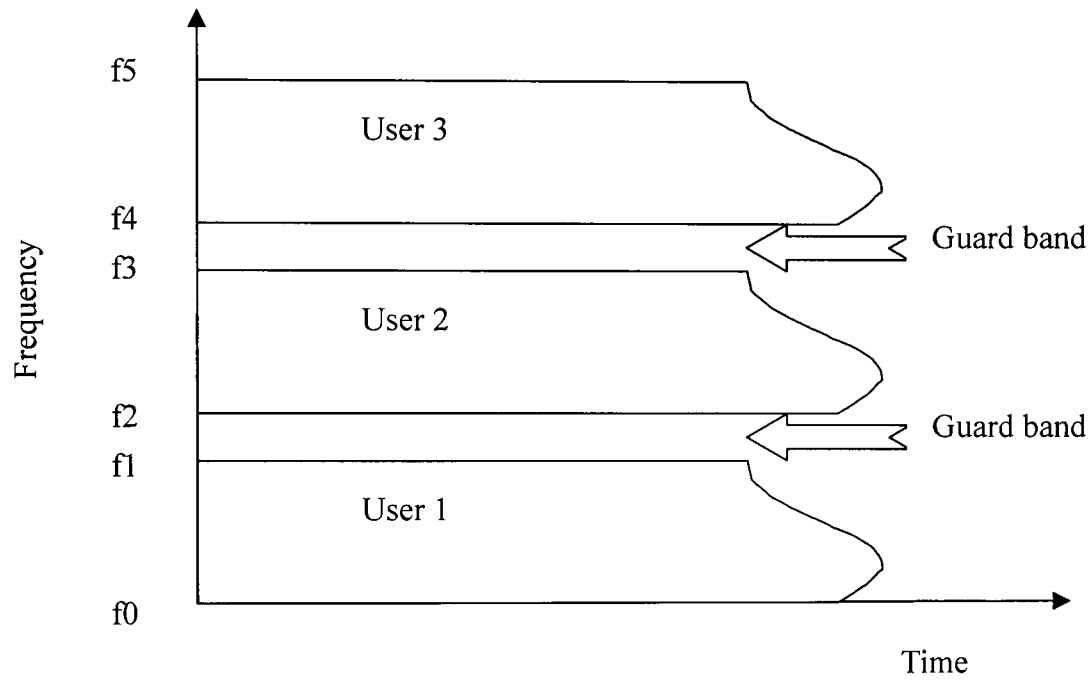

Figure 2.2 Frequency Division Multiple Access

2.1.2 Time Division Multiple Access

In Time Division Multiple Access (TDMA), time domain is divided into a number of slots allocated to each user, as shown in Figure 2.3. Thus, the signals transmitted by various users are separated through different time slots which are isolated by guard time. However, different from FDMA, TDMA must ensure all transmitters and receivers to be synchronized [16].

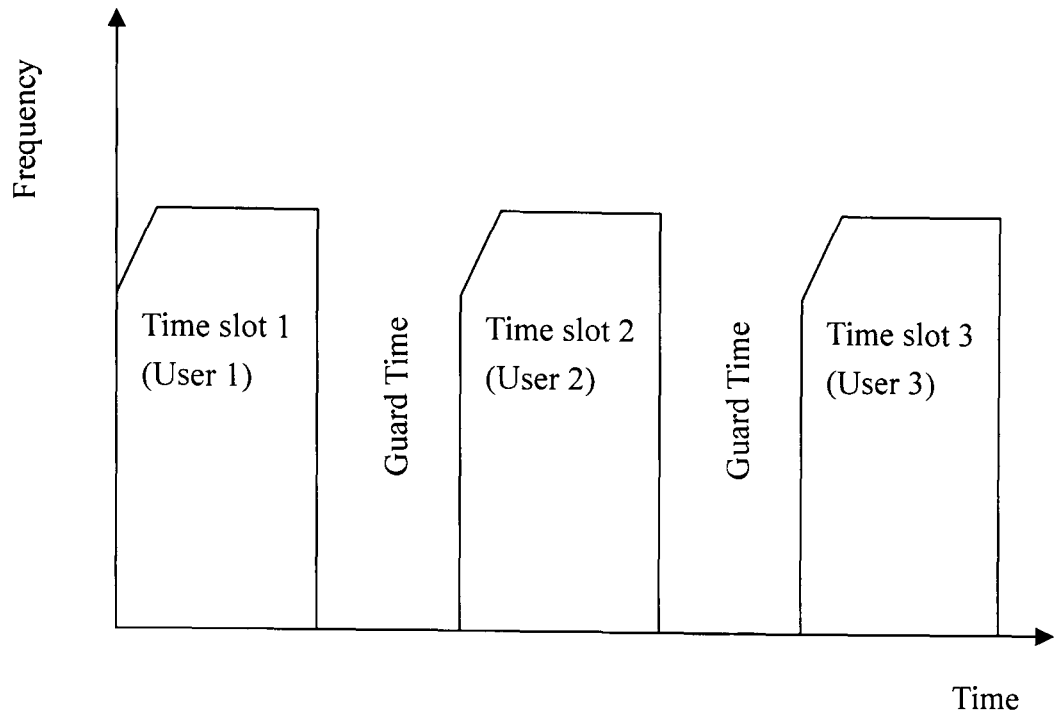

Figure 2.3 Time Division Multiple Access

2.1.3 Carrier Sense Multiple Access

This is one main type of random access mechanisms which originates from the ALOHA system [17] and slotted ALOHA system [18, 19, 20]. Carrier Sense Multiple Access (CSMA) [21] proposes to sense the channel before transmitting data (i.e. listen before talk) to avoid collision with other potential transmissions. In this way, its efficiency of medium utilization is much higher than ALOHA and slotted ALOHA.

2.1.4 Space Division Multiple Access and Polarization Division Multiple Access

In satellite communication system, Space Division Multiple Access (SDMA) is a common scheme that could be used in any centrally controlled demand-assignment

communication networks [22]. The unique feature of such system is its spatial isolation by beam-to-beam coverage, some of which can coexist in the same frequency, called "frequency reuse". Most of the 2G systems used SDMA to assist the multiple access technologies to improve the system capacity [23, 24, 25, 26]. Polarization Division Multiple Access (PDMA) implemented by polarized antenna is used to separate a signal apart from interference from others, where the frequency band could be also reused for orthogonal polarization signals. So it is usually used in combination with SDMA in satellite communications systems, where frequency spectrum could be fourfold reused [27].

2.1.5 Code Division Multiple Access

Code division multiple access (CDMA) is an application of spread-spectrum techniques. Figure 2.4 indicates that in a typical CDMA system, all users can transmit at the same frequency simultaneously and their signals are separated from each other by means of a series of unique spreading codes [28]. Correspondingly, the receiver despreads the signal by correlating assigned code that is identical to the spreading code used at the transmitter.

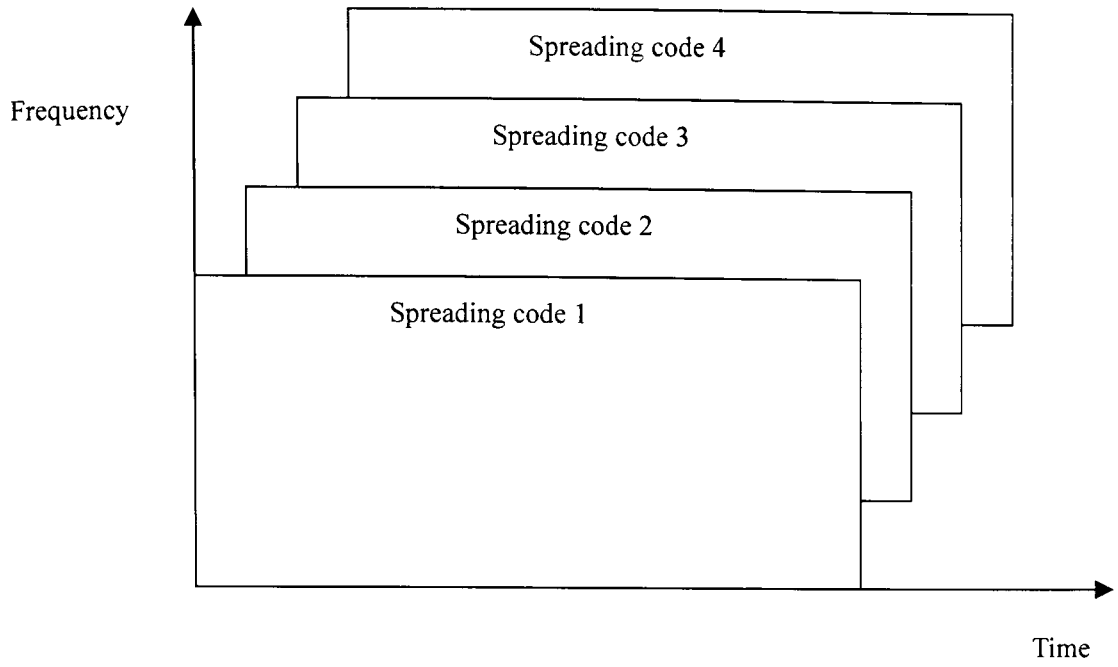

Figure 2.4 Code Division Multiple Access

Figure 2.5 and Figure 2.6 illustrate the spreading and despreading processes, respectively. Spreading signal is the product of data signal and code signal in the spreading process whereas the reverse step is conducted in the despreading process, which the spreading signal is converted back to the data signal by multiplying the same spreading code used in previous spreading process. The time duration of a code bit is called chip duration T_{chip} and the frequency of code signal is called chip rate R_{chip}. Therefore,

$$T_{chip} = 1/R_{chip} \tag{2.1}$$

Note that one chip denotes one spreading sequence symbol which is different from information data symbol.

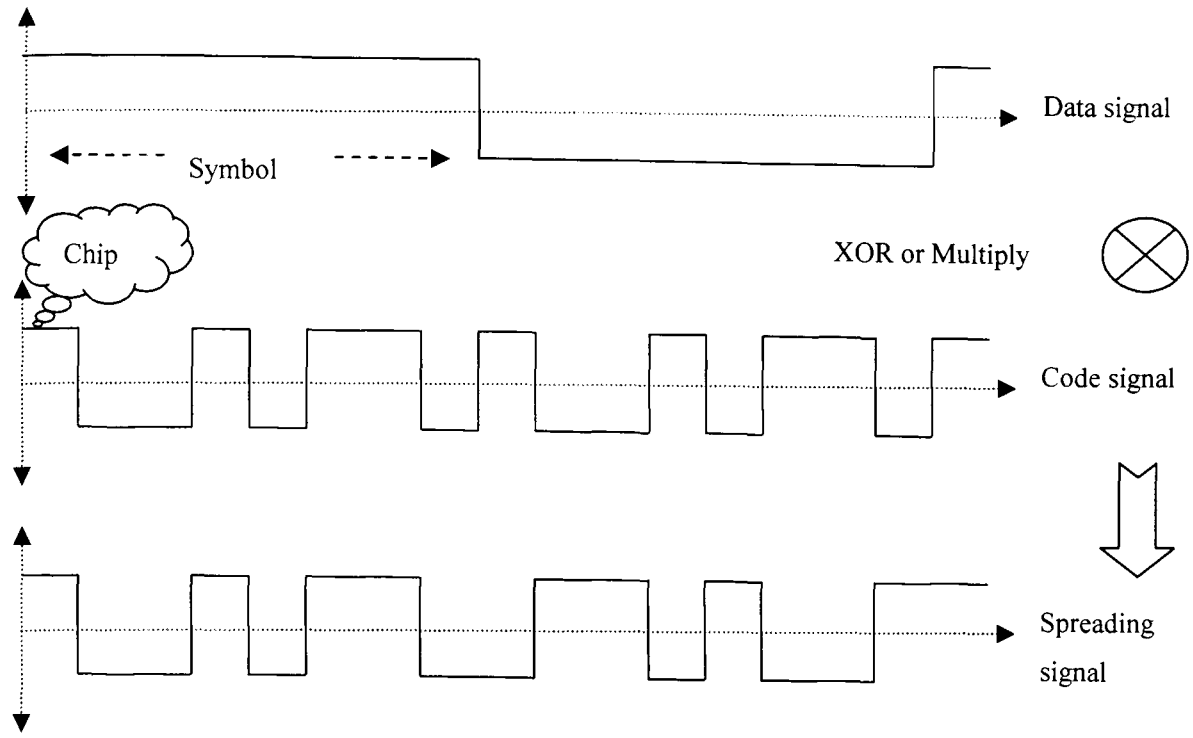

Figure 2.5 Spreading process

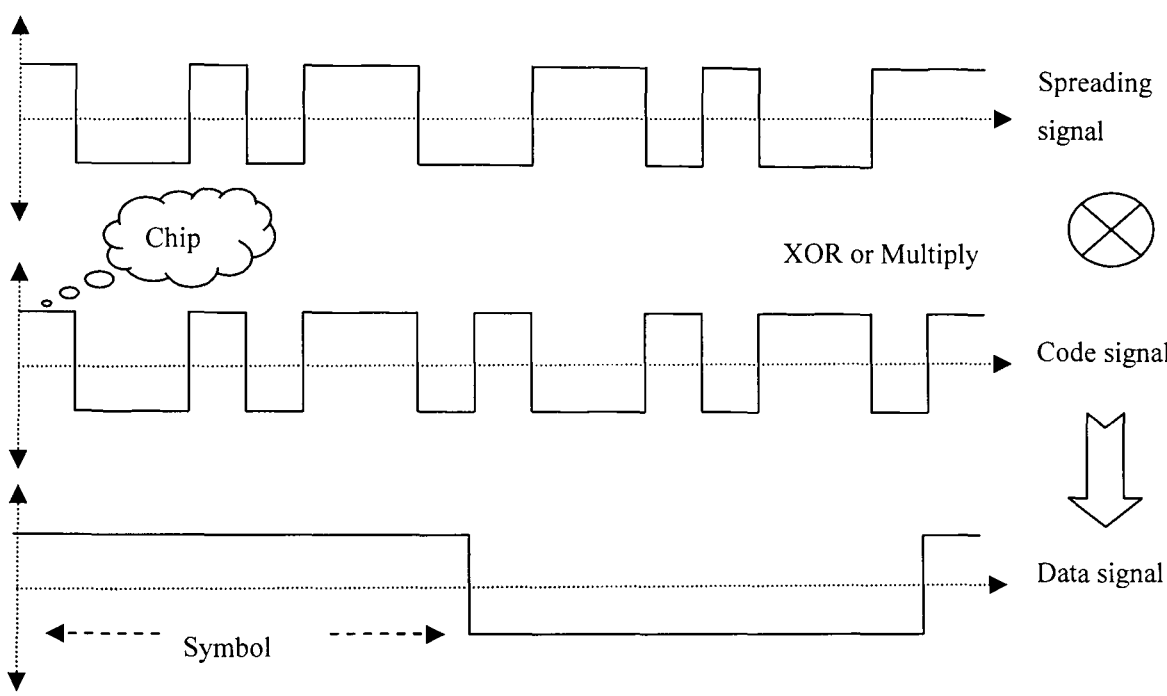

Figure 2.6 Despreading process

As one of the current commercial standards for the 2G systems, CDMA (or more explicitly the IS-95 standard) uses a spreading spectrum technology in its air interface design [29]. Instead of using different time slots to identify different users in TDMA or different frequency bands to separate users in FDMA, CDMA divides multiple

users based on a set of orthogonal codes in a same frequency domain and time domain. The key feature of CDMA is "spreading spectrum", which is implemented by oversampling information signal in the time domain. As a consequence, the transmission bandwidth is wider than the bandwidth of the original information signal. Typically, a pseudo-random (PN) sequence is used to 'spread' the bandwidth of the information signal in frequency domain.

The advantages of CDMA system include:

- Signal hiding and noninterference with conventional systems;
- Anti-jam and interference rejection;
- Privacy;
- Accurate ranging;
- Multiple access;
- Multipath mitigation with the aid of RAKE receiver [30, 31, 32];
- Variable bit rate and adaptive rate transmission [33, 34, 35].

As shown in Figure 2.7, CDMA can be generally classified into three categories, namely Frequency Hopping (FH-) CDMA, Time Hopping (TH-) CDMA and Direct Sequence (DS-) CDMA, respectively. Among them, DS-CDMA is the most popular technical form of CDMA system. As a basic and principle spreading spectrum system, DS-CDMA is achieved by phase modulating the information signal with a PN sequence of zeros and ones, namely chips [4]. In DS-CDMA, the baseband signal is directly modulated by much higher frequency chips, e.g. PN codes.

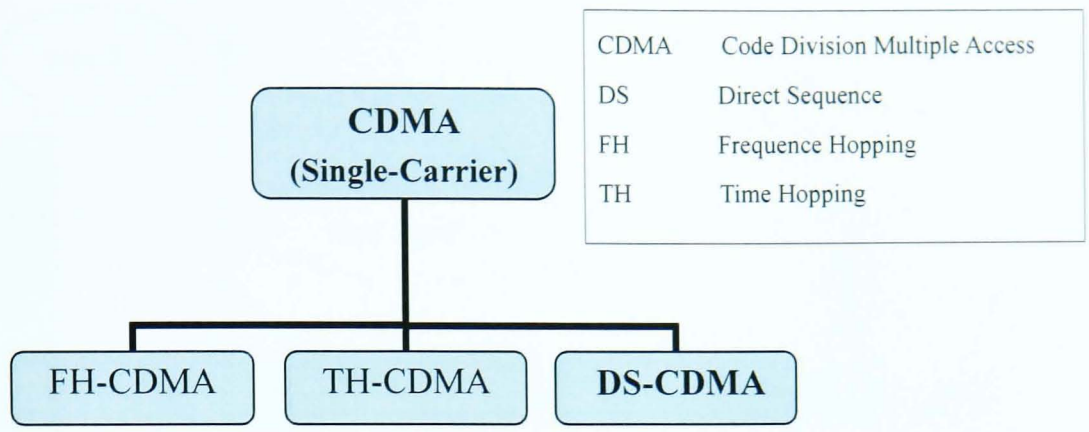

Figure 2.7 Classifications of CDMA technologies

A. Direct-Sequence Code Division Multiple Access

Figure 2.8 depicts the basic concept of spreading spectrum in DS-CDMA system using an example. The data signal of each user is spread by its own spreading code. Both users transmit their spread-spectrum signals within the same frequency domain at the same time, as shown in Figure 2.8 (b). At the receiver, the mixed spread-spectrum signal of both user 1 and user 2 is correlated with user 1's spreading code. Since the cross-correlation property between desired user 1 and user 2 is small, it is possible to recover user 1's original narrowband information signal using the spreading code of user 1 at the receiver side. Thus, user 1's data signal is 'despread' at the receiver, whilst the user 2 retains spread-spectrum signal, like Figure 2.8 (c). After correlation in receiver with the desired user's spreading code, the desired user's signal power is much higher than the others, so the desired signal could be easily detected and detached from the others.

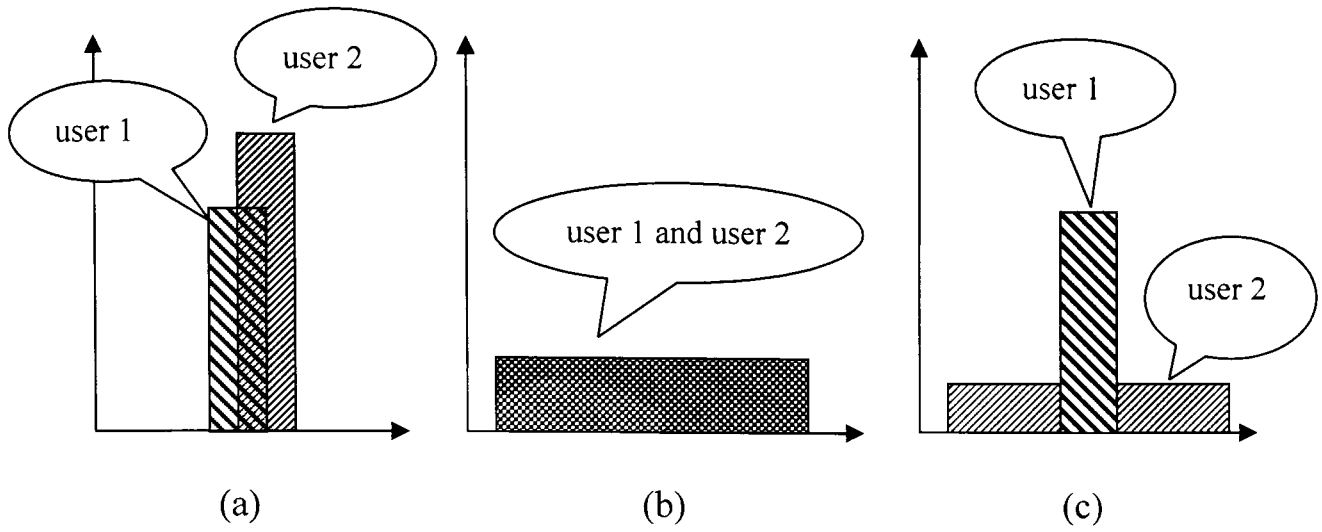

Figure 2.8 Spreading in frequency domain for two-users in DS-CDMA system

It is denoted by Figure 2.9 how DS-CDMA works at the transmitter side. The input data signal could be either an analog signal or a digital one, like Figure 2.9 (a). In the simplest case as shown in Figure 2.9 (b), binary signal is directly multiplied by spreading code signal and the resulting product signal namely chip modulates the wideband carrier. The direct multiplication discloses the essence of the DS-CDMA and that is why its name comes from [28].

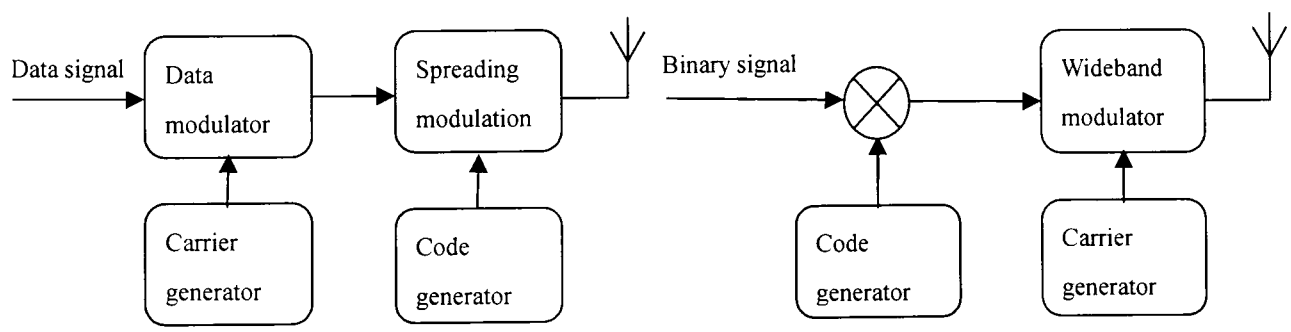

(a) Generic data signal as input (b) Binary data signal as input

Figure 2.9 Block diagram of a DS-CDMA transmitter

B. Spreading Sequences

There are two basic conditions of ideal spreading sequences design for DS-CDMA system. Firstly, the out-of-phase auto-correlation (ACL) of the spreading sequences

should be zero, in order to rectify synchronization error of the spreading sequences. Secondly, it is shown in [36] that the Multiple Access Interference (MAI) highly depends on the cross-correlation (CCL) property between the spreading code of the wanted user and the spreading codes of all the other interfering users. Therefore, our goal is to minimize the cross-correlation property of spreading codes in order to eliminate MAI. Before we compute the correlation values, the binary spreading sequences with chips 0 and 1 are mapped to bipolar spreading sequences with chips -1 and +1, respectively.

Let us consider a DS-CDMA system which supports K users. The users are identified by k=1, 2, …, K. The periodic ACL of the spreading sequence $\left(c^{(k)}\right)$ for the k^{th} user, $R_{kk}(n)$ is defined as:

$$R_{kk}(n) = \sum_{i=1}^{N_s} c_i^{(k)} c_{i-n}^{(k)}, \tag{2.2}$$

where n = $-N_s+1$, $-N_s+2$,…N_s-1, and it stands for cyclic shift between sequences. N_s represents the length of the sequence or the length of the code. The periodic CCL of the two different sequences ($c^{(j)}$ and $c^{(k)}$) is expressed as:

$$R_{jk}(n) = \sum_{i=1}^{N_s} c_i^{(j)} c_{i-n}^{(k)}, \tag{2.3}$$

where n= $-N_s+1$, $-N_s+2$,…,N_s-1. In order to measure whether the spreading code is good or not, $R_{\max}$ is defined in [36]:

$$R_{\max} = \max\left|R_a, R_b\right|, \tag{2.4}$$

and

$$R_a = \max\left|R_{kk}(n)\right| \quad \text{for} \quad 1 \le k \le K, \tag{2.5}$$

which means the maximum value of ACL of the K users, where $-N_s + 1 \le n \le N_s - 1$;

$$R_b = \max\left|R_{jk}(n)\right| \quad \text{for} \quad 1 \le j,k \le K, j \ne k, \tag{2.6}$$

which means the maximum value of CCL among each pair of the K users, where $-N_s + 1 \le n \le N_s - 1$.

Then either of the two threshold criteria, namely Welch [29] and Sidelnikov [29] bounds can be chosen to measure whether a spreading code set is feasible in design of DS-CDMA system. The Welch bound is given by:

$$R_{\max} \ge N_s \sqrt{\frac{K-1}{KN_s - 1}}. \tag{2.7}$$

For the same set of sequences, the Sidelnikov bound is defined as;

$$R_{\max} > (2N_s - 2)^{\frac{1}{2}}, \tag{2.8}$$

As defined in Equation (2.4), $R_{\max}$ is the highest magnitude between the periodic CCL and out-of-phase periodic ACL. A low out-of-phase periodic ACL allows easier code acquisition or synchronization, while a low periodic CCL reduces the MAI. A code set is determined to be optimum if $R_{\max}$ approaches the Welch or Sidelnikov lower bound. Here, K can also represent the number of codes in the set (i.e. the spreading family code set). It is reported in [36] that the larger spreading family code set K, the severer MAI would be. On the other hand, the system capacity is also dependent on the spreading code family size, K. As the family size K increases, more users could be accommodated in the same frequency bandwidth. Therefore, there exists a trade-off between MAI and the system capacity. Consequently, based on

above-mentioned criteria, rational selection of K in spreading code set design is a matter of cardinal significance in DS-CDMA system.

Table 2.1, 2.2 and 2.3 list the properties of different spreading sequence sets of three categories, where m is the order degree of linear generator polynomials. In m-sequence [36], the length of the code ($N_s=2^m-1$) equals to the number of codes in the set. Additionally, N_s could also be treated as the maximum number of users that the system can accommodate without interference theoretically. Also, constructing the both Gold-sequence [36] and Kasami-sequence [36] is derived from a preferred pair of m-sequences, $\underline{x}$ and $\underline{y}$, with identical length N_s. Furthermore, $T^{-n}\underline{y}$ for n=0, 1… N_s-1, represents the periodical shift of $\underline{y}$ by n chip intervals. More explicitly, from respective generator polynomial, the difference between the two spreading codes (Gold vs. Kasami) is that the former one has the size of spreading family Q, defined as

$$Q = N_s + 2 = 2^m + 1, \tag{2.9}$$

with the latter one only has

$$Q = 2^{m/2} \tag{2.10}$$

spreading sequences within one family set, based on the same code length

$$N_s = 2^m - 1. \tag{2.11}$$

Additionally, t(m) and s(m) are correlation values, defined as:

$$t(m) = \begin{cases} 2^{(m+1)/2} + 1 & when\ m\ \ is\ \ odd \\ 2^{(m+2)/2} + 1 & when\ m\ \ is\ \ even, \end{cases} \tag{2.12}$$

and

$$s(m)=\begin{cases} 2^{(m+1)/2}+2 & when \quad m \quad is \quad odd \\ 2^{(m+2)/2}+2 & when \quad m \quad is \quad 2 \bmod 4 \\ 2^{(m+2)/2}+1 \; or \; 2^{m/2}+1 & when \quad m \quad is \quad 2 \bmod 4 \end{cases} \tag{2.13}$$

Spreading sequence	Generator polynomials
m-sequence	$g(x)=g_m x^m+g_{m-1}x^{m-1}+\ldots+g_1 x+g_0$
Gold-sequence	$s_g=\left\{\underline{x},\underline{y},\underline{x}\oplus\underline{y},\underline{x}\oplus T^{-1}\underline{y},\ldots,\underline{x}\oplus T^{-(N-1)}\underline{y}\right\}$
Kasami-sequence	$s_k=\left\{\underline{x},\underline{x}\oplus\underline{y},\underline{x}\oplus T^{-1}\underline{y},\ldots,\underline{x}\oplus T^{-(2^{m/2}-2)}y\right\}$

TABLE 2.1 GENERATOR POLYNOMIALS OF SPREADING SEQUENCES

Spreading sequence	Auto-Correlation (ACL): $R_{kk}(n)$
m-sequence	$\begin{cases} R_{kk}(0)=N_s \\ R_{kk}(n)=-1 \quad for \quad n\neq 0, \end{cases}$
Gold-sequence	$\begin{cases} N_s & for \quad n=0 \\ \{-1,-t(m),t(m)-2\} & for \quad n\neq 0 \end{cases}$
Kasami-sequence	$\begin{cases} N_s & for \quad n=0 \\ \{-1,-s(m),s(m)-2\} & for \quad n\neq 0 \end{cases}$

TABLE 2.2 AUTO-CORRELATION PROPERTIES OF SPREADING SEQUENCE SETS

Spreading sequence	Cross-Correlation (CCL): $R_{jk}(n)$
m-sequence	random, could be very large value
Gold-sequence	$R_{jk}(n)=\{-1,-t(m),t(m)-2\}$ for all n and $j\neq k$
Kasami-sequence	$R_{jk}(n)=\{-1,-s(m),s(m)-2\}$ for all n and $j\neq k$

TABLE 2.3 CROSS-CORRELATION PROPERTIES OF SPREADING SEQUENCE SETS

C. Analytical Performance of DS-CDMA System

Figure 2.10 shows a simple K-user DS-CDMA system. To analyze the BER performance of this DS-CDMA system, the following conditions are assumed:

• BPSK modulation is used;

• All the users are time-synchronized (both senders and receivers);

• All the senders have the same transmitted power;

• The carrier-modulated signal is transmitted through an Additive White Gaussian Noise (AWGN) channel;

• It is shown in [15] that the BER performance of either baseband modulation or bandpass modulation is the same. To simplify the analysis, baseband modulation is used;

• Gold-sequences are used as spreading codes. Each Gold-sequence is assigned to each user pair.

The following notations are defined:

• The number of user pairs (one pair includes one sender and its receiver) is K;

• The frequency of the k^{th} user is denoted by ω_k ;

• The amplitude of the signal of each user is denoted by $A = \sqrt{P}$, where P denotes the average power of the signal;

• The relationship between data bit duration T_b and chip duration T_{chip} is given as $T_b = N_s T_{chip}$;

• Random bipolar ±1 sequences are generated for information signal with the

amplitude of 1. The chips in spreading sequences are also mapped to bipolar ±1 sequences with the amplitude of 1;

• The original information signal of the k[th] sender before spreading is denoted as d_k. Hence, the expected signal received at the receiver k is also assumed to be d_k which was transmitted by the sender k;

• The propagation delay denoted by τ_k is assumed to be zero for all K transmissions.

Without loss of generality, in the following analysis, as an example, the wanted signal at receiver is assumed to be the one from the sender 1 and the received signal from all other (K-1) senders are interferers which may cause MAI.

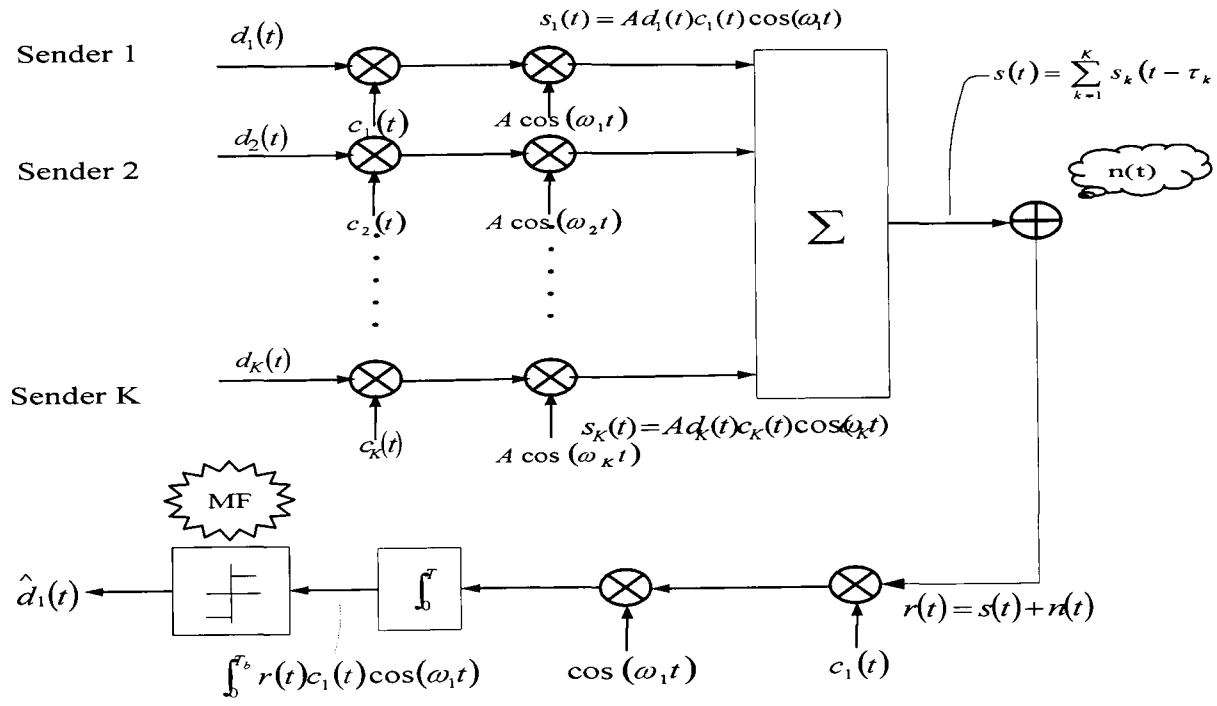

Figure 2.10 System structure of a simple K-users uplink DS-CDMA system

Based on the above assumptions, the received signal can be expressed as

$$r(t) = s(t) + n(t)$$
$$= \sum_{k=1}^{K} s_k(t-\tau_k) + n(t) \qquad (2.14)$$

Using the above definitions, the received signal can be rewritten as

$$r(t) = \sum_{k=1}^{K} \sqrt{P} d_k(t) c_k(t) + n(t) \tag{2.15}$$

Then, this signal is despread with a replica of spreading code of user 1 and sent into a correlator or a matched filter (MF) [37]. The output within one data bit interval is expressed as

$$\begin{aligned} z_1 &= \int_0^{T_b} r(t) c_1(t) dt \,, \\ &= \int_0^{T_b} [\sqrt{P} d_1(t) c_1^2(t) + \sum_{k=2}^{K} \sqrt{P} d_k(t) c_k(t) c_1(t) + n(t) c_1(t)] dt \\ &= D_1 + I_1 + N_1 \end{aligned} \tag{2.16}$$

where D_1 is the wanted signal of user 1 in the output of MF, I_1 is the MAI item caused by the other (K-1) senders, and N_1 is the noise item induced by zero-mean AWGN channel. They are obtained as follow:

First, the received signal component in the output of MF can be calculated as

$$\begin{aligned} D_1 &= \int_0^{T_b} \sqrt{P} d_1(t) c_1^2(t) dt \,, \\ &= \pm \sqrt{P} T_b \,, \text{ if we consider } \; d_1(t) = \pm 1, c_k^2 = 1, \textit{for } k = 1,..K \end{aligned} \tag{2.17}$$

Therefore, the signal power S_{1power} at the output of MF is represented as

$$S_{1power} = D_1^2 = P T_b^2 \tag{2.18}$$

Second, the MAI can be calculated as

$$\begin{aligned} I_1 &= \int_0^{T_b} \sum_{k=2}^{K} \sqrt{P} d_k(t) c_k(t) c_1(t) dt \\ &= \sqrt{P} \sum_{k=2}^{K} \int_0^{T_b} d_k(t) c_k(t) c_1(t) dt \end{aligned}$$

$$= \pm\sqrt{P}T_b \sum_{k=2}^{K} R_{k,1}(0), \tag{2.19}$$

where the normalized periodic cross-correlation item $R_{k,1}$ between the spreading codes of the sender 1 and the sender k is defined as

$$R_{k,1}(0) = \frac{1}{T_b} \int_0^{T_b} c_k(t) c_1(t), \tag{2.20}$$

Without loss of generality, $R_{k,1}(0)$ could be denoted as $R_{k,1}$. Hence if we define

$$I_{k,1} = \pm\sqrt{P}T_b R_{k,1} \tag{2.21}$$

as the independent interference to the sender 1 from the k^{th} sender, so the total interference power from the (K-1) senders is written as

$$M_1 = \sum_{k=2}^{K} I_{k,1}^2 \tag{2.22}$$

where

$$\sum_{k=2}^{K} I_{k,1} = I_1 . \tag{2.23}$$

Third, the noise component at the output of user 1's MF can be calculated by

$$N_1 = \int_0^{T_b} n(t) c_1(t) dt . \tag{2.24}$$

Additionally, since $n(t)$ is the AWGN with zero-mean and constant variance $\sigma^2 = \frac{N_0}{2}$ [15], so the average power of integral noise product, W_1 is given by

$$W_1 = E\left(N_1^2\right) = E\left(\int_0^{T_b} n(t) c_1(t) dt \int_0^{T_b} n(\tau) c_1(\tau) d\tau \right)$$

$$= \int_0^{T_b} \int_0^{T_b} E\left(n(t)n(\tau)\right) c_1(t) c_1(\tau) dt d\tau$$

$$= \int_0^{T_b} \int_0^{T_b} \frac{N_0}{2} \delta(t-\tau) c_1(t) c_1(\tau) dt d\tau$$

$$= \frac{N_0}{2} \int_0^{T_b} c_1^2(\tau) d\tau$$

$$= \frac{N_0}{2} T_b \tag{2.25}$$

where $E(N_1^2)$ denotes the expectation of N_1^2. $E\big(n(t)n(\tau)\big)$ is the auto-correlation of $n(t)$ which can be calculated by [37]

$$E\big(n(t)n(\tau)\big) = \frac{N_0}{2}\delta(t-\tau). \tag{2.26}$$

Consequently, the equivalent signal-to-interference ratio (SIR) of the user 1 is presented as

$$SIR_1 = \frac{S_{1power}}{W_1 + M_1}$$

$$= \frac{PT_b^2}{\frac{N_0 T_b}{2} + PT_b^2 \sum_{k=2}^{K} R_{k,1}^2}$$

$$= \left[\frac{N_0 T_b}{PT_b^2} + \frac{PT_b^2 \sum_{k=2}^{K} R_{k,1}^2}{PT_b^2} \right]^{-1}$$

$$= \left[\frac{N_0}{2E_b} + \sum_{k=2}^{K} R_{k,1}^2 \right]^{-1}$$

Following the same way, for any user j in the system, the general SIR can be expressed as

$$SIR = \left[\frac{N_0}{2E_b} + \sum_{k=1, k\neq j}^{K} R_{k,j}^2 \right]^{-1} \tag{2.27}$$

Using the Gaussian Q-function $Q(x)$ [37], the theoretical BER performance in bit-synchronized DS-CDMA system can be determined by

$$BER = Q\left(\sqrt{SIR}\right) \tag{2.28}$$

Substituting Equation (2.27) into (2.28), therefore we have

$$BER = Q\left(\left(\left(\frac{2E_b}{N_0}\right)^{-1} + \sum_{k=1,k\neq j}^{K} R_{k,j}^2\right)^{-\frac{1}{2}}\right) \tag{2.29}$$

where $\frac{E_b}{N_0}$ denotes the bit energy power noise density ratio which is the same as signal-to-noise ratio (SNR) per bit defined in [37].

A DS-CDMA system applies spreading sequences in the time domain and uses RAKE receivers to optimally combine the time-dispersed energy in order to combat the effects of multi-path fading. However, it is hard for CDMA to achieve a high chip rate with the order of tens of MHz in order to gather energy from low time dispersion at the cost of high clock rate, high power consumption as well as increased implementation complexity [38]. Hence, CDMA itself is not suitable for supporting high data rate in next-generation broadband wireless access. In order to conquer these problems, a range of novel techniques combing CDMA and OFDM were recently proposed which will be introduced in Section 2.2.2.

2.2 Multiple Access Technologies for Multi-Carrier Communication System

Compared to conventional Single-Carrier (SC) communication system, most of recent research interests are focusing on Multi-Carrier (MC) communication system, which is identified as the cogent candidate for future 4G mobile and wireless communication systems. The basic principle of MC communication system is that it partitions the single high data rate channel into multiple parallel orthogonal low data rate

sub-channels (or called subcarriers), which can be realized by using a so-called Orthogonal Frequency Division Multiplexing (OFDM) technology [39, 40, 41, 42]. Since the symbol rate of an MC communication system on each subcarrier is much lower than that of SC system, the symbol duration through each subcarrier is accordingly enlarged against propagation delay spread. Therefore, one promising advantage of MC communication systems is to reduce or eliminate the side effect of propagation delay spread in order to simplify the complexity of equalizer. Furthermore, if the guard band between transmitting MC symbols is reasonably selected and designed, the equalizer could even be wiped off from the system [42].

2.2.1 Orthogonal Frequency Division Multiplexing

OFDM is defined as a physical layer modulation technique that divides a high data rate signal into multiple low data rate subcarriers in parallel [43]. Figure 2.11 illustrates the conception of OFDM as a modulation scheme in two dimensions. In OFDM one single user occupies all frequency resource at the transmitted symbol duration. A number of parallel information data symbols are simultaneously modulated and transmitted by different subcarriers within OFDM symbol duration. Moreover, the subcarrier frequencies are carefully chosen in order to be mutually orthogonal to each other with overlapping over the symbol duration as shown in Figure 2.12. Thereby, the frequency bandwidth resource is efficiently exploited. Additionally, the symbol rate of parallel transmissions in OFDM is lower than that of serial transmission in SC communication systems, so the symbol duration is increased

accordingly. Therefore, an OFDM symbol is more robust to inter-symbol interference (ISI) and multi-path fading than SC modulated signal so that frequency-domain channel equalizer can be eradicated, which is a significant merit of the system. OFDM is a low-complex bandwidth-efficient modulation scheme and hence will be a promising candidate [44] for next-generation high-speed wireless communication. The practical applications of OFDM include high-speed modems, digital audio broadcast, digital video broadcast, and high-speed wireless access systems, etc [44]. A number of advantages of using OFDM for future wireless communication can be summarized as follow:

- Multi-path delay spread tolerance;
- Effectiveness against channel distortion;
- Throughput increment;
- Invulnerability against impulse noise;
- Frequency diversity.

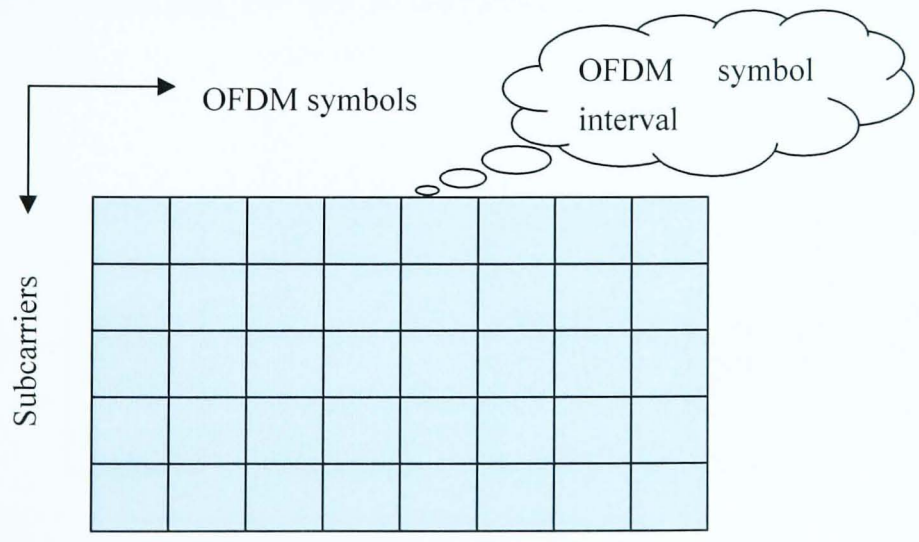

Figure 2.11 OFDM conception

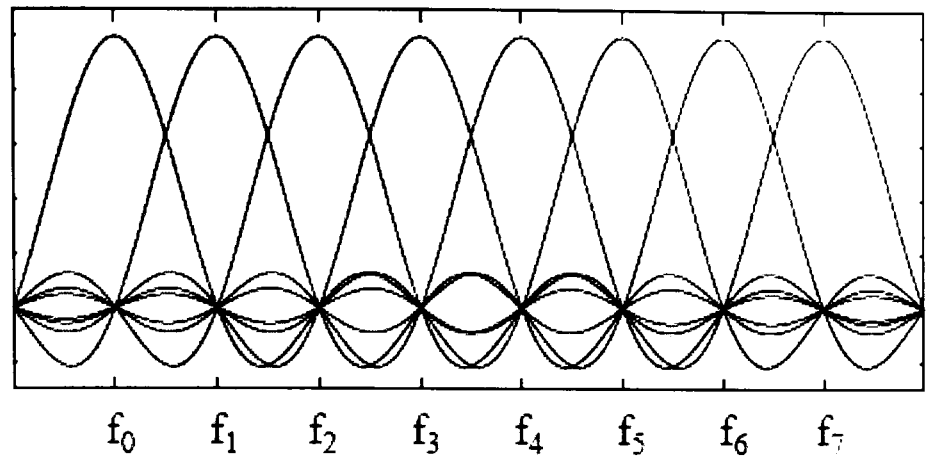

Figure 2.12 The frequency spectrum of OFDM subcarriers

Figure 2.13 illustrates the block diagram of OFDM transmitter. The input data signal is firstly converted from serial to parallel. Then each subcarrier is modulated using Inverse Discrete Fourier Transformation (IDFT) or Inverse Fast Fourier Transformation (IFFT). Guard-interval is added on the serial symbol after parallel-to-serial conversion of the IFFT output to resist the effect of ISI and multi-path interference. Next, the serial OFDM symbol is converted from digital to analog and then sent into the propagation channel.

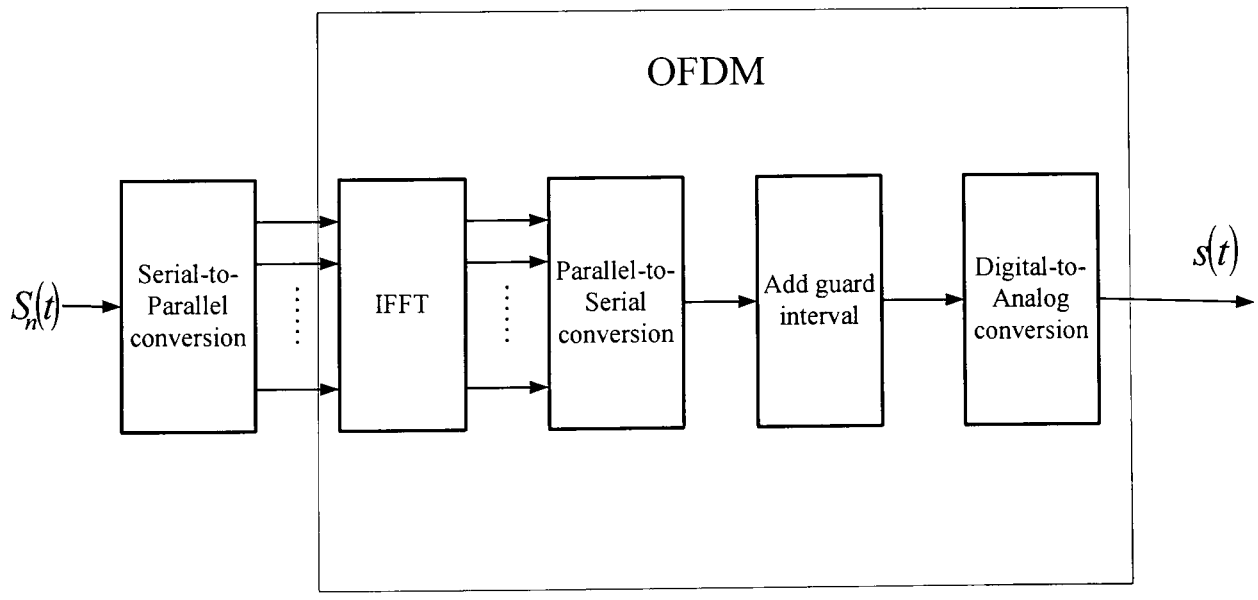

Figure 2.13 The block diagram of OFDM transmitter

As an example, we assume that BPSK modulation is used. A serial of parameters are

defined as follows:

• BPSK modulated information signal is denoted by $S_n(t)$, where n=1, 2, …, N_c and N_c denotes the number of data symbols within a frame.

• A bit duration is denoted by T_b.

• The frame duration is denoted by T_s, thus we have

$$T_s = N_c T_b, \tag{2.30}$$

• Subcarrier frequency is denoted by f_n, where

$$f_n = \frac{n}{T_s}, \quad n = 0, 1, ...N_c - 1 \tag{2.31}$$

Hence, the spacing of subcarrier frequencies Δf is calculated by

$$\Delta f = \frac{1}{T_s}. \tag{2.32}$$

• Maximum multipath spread delay is denoted by $\tau_{\max}$.

• Guard interval between OFDM symbols is represented as T_{guard}. In order to resolve the propagation delay in guard interval, a cyclic guard interval is required to add at both the front and the end of an OFDM symbol, denoted by

$$T_{guard} \geq \tau_{\max}. \tag{2.33}$$

After adding guard interval, the frame duration changes as

$$T_s^{'} = T_{guard} + T_s \quad . \tag{2.34}$$

By fulfilling preceding assumptions, the complex envelope of OFDM symbol is formed as

$$s(t) = \frac{1}{\sqrt{N_c}} \sum_{n=0}^{Nc-1} S_n(t) e^{j2\pi f_n t} \quad , 0 \leq t \leq N_c T_b \quad . \tag{2.35}$$

where $\frac{1}{\sqrt{N_c}}$ is the normalized factor of power.

Furthermore, the energy density spectrum is given by

$$|S(f)|^2 = \frac{1}{N_c}\sum_{n=0}^{N_c-1}\left|S_n T_s \frac{\sin(\pi(f-f_n)T_s)}{\pi(f-f_n)T_s}\right|^2 . \tag{2.36}$$

Figure 2.14 gives an example about normalized energy density spectrum of 16 subcarriers for an OFDM symbol, which is calculated by Equation (2.36). If we sample the modulated signal $s(t)$ at the time nT_b with the interval T_b, where $n = 0,1,...N_c - 1$. So we have the sampled data formed as

$$s(nT_b) = \frac{1}{\sqrt{N_c}}\sum_{n=0}^{N_c-1} S_n e^{j2\pi f_n(nT_b)} \tag{2.37}$$

After normalization, the modulated signal $s(t)$ becomes a sequence of samples of discrete signal expressed as

$$s(n) = \frac{1}{\sqrt{N_c}}\sum_{n=0}^{N_c-1} S_n e^{j2\pi f_n n} \tag{2.38}$$

Thus, the modulation or multiplexing of data source symbols could be implemented by IDFT or IFFT elaborated in [44]

$$s(n)^{(T)} = IFFT\left(S_n^{(T)}\right), \quad n = 1,2,...,N_c \tag{2.39}$$

where $(\bullet)^{(T)}$ denotes transposition of a vector sequence.

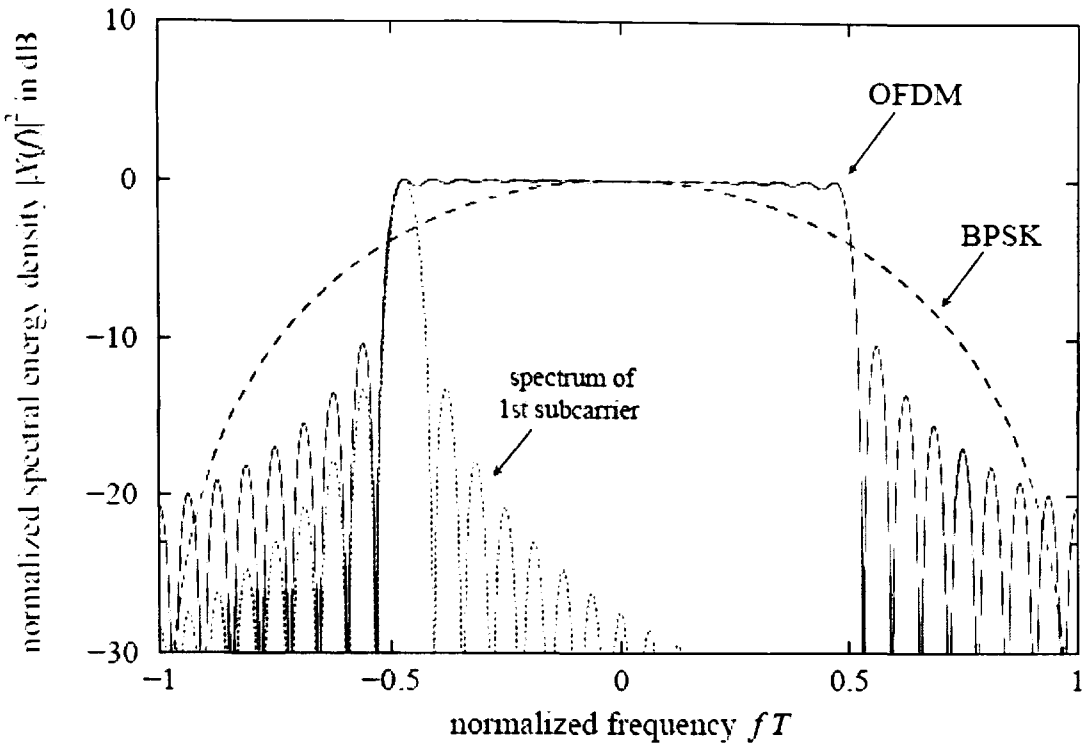

Figure 2.14 Normalized energy density spectrum vs. subcarrier frequency of an OFDM symbol with the symbol duration $T_s = N_c T_b$

2.2.2 Multifarious MC Communication Systems

As mentioned in the above section, OFDM is a very efficient modulation scheme. However, OFDM itself is not a multiple access technique to accommodate multiple users. Hence, people decide to combine it with various multiple access techniques to support MC communication. Figure 2.15 lists the categories of MC communication systems. The three main categories are Multi-Carrier-Frequency Division Multiple Access (MC-FDMA) [45, 46], Multi-Carrier-Time Division Multiple Access (MC-TDMA) [46, 47, 48] and Multi-Carrier-Code Division Multiple Access (MC-CDMA) [49, 50, 51] respectively. Within MC-CDMA, Multi-Carrier-Direct Sequence-Code Division Multiple Access (MC-DS-CDMA) [52, 53, 54, 55, 56, 57], Orthogonal Frequency and Code Division Multiplexing (OFCDM) [58, 59, 60,

61 , 62] and Multitone Direct Sequence-Code Division Multiple Access (MT-DS-CDMA) [63, 64, 65] are variations of the basic MC-CDMA [49, 50, 51], in which multiple access is engendered by CDMA spreading scheme. Actually, the difference between those MC-CDMA variations is the fashion how OFDM is combined with CDMA.

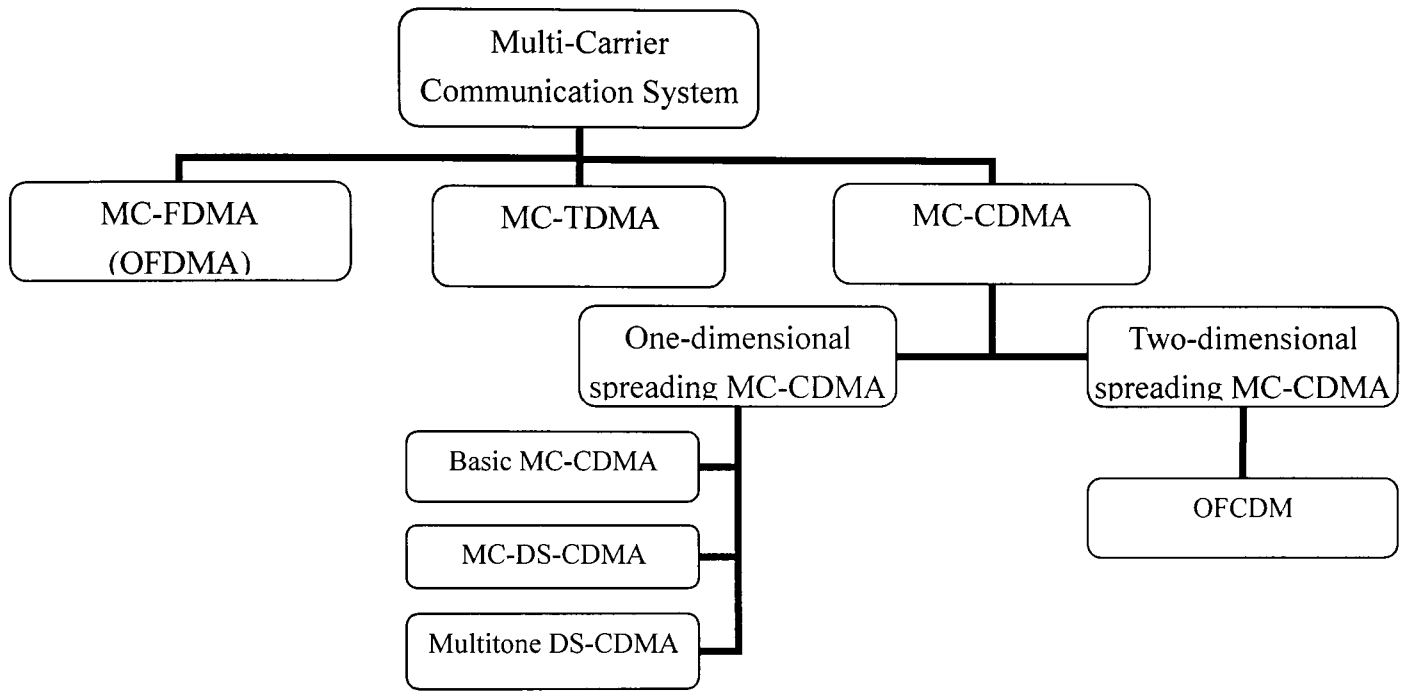

Figure 2.15 Categories of MC communication systems

The simple schematic Figure 2.16 shows the basic conception of MC-FDMA also termed as Orthogonal Frequency Division Multiplexing Access (OFDMA) in some references [66, 67, 68]. Each user can flexibly transmit the user data using an amount of subcarriers simultaneously which is isolated by the guard band. The subcarriers modulated by user data sequence are mutually orthogonal to each other so as to avoid MAI and ISI.

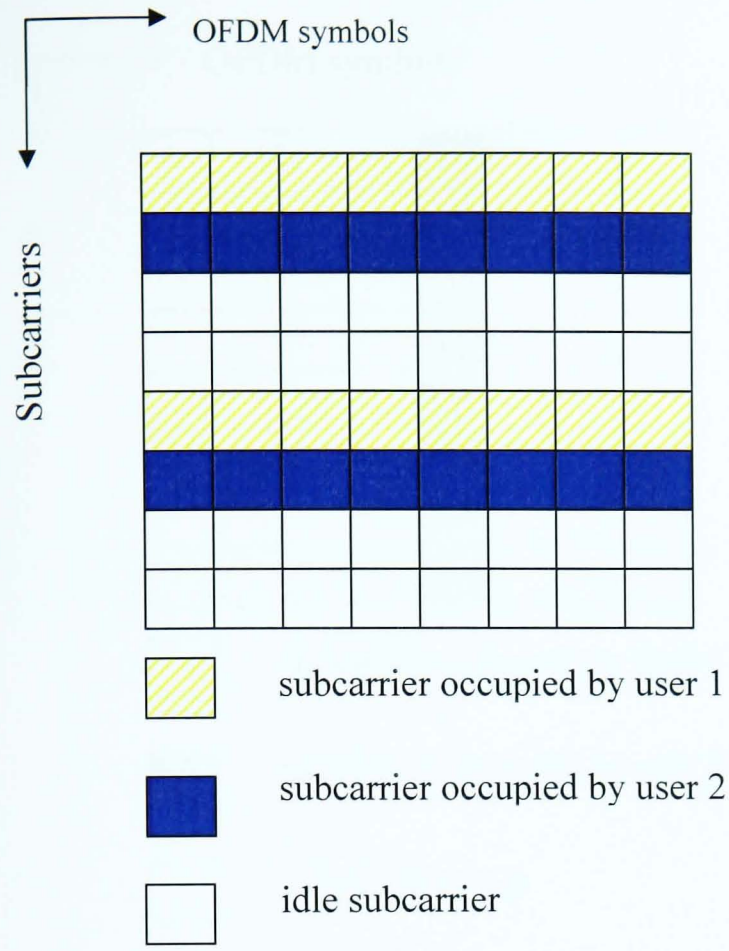

Figure 2.16 MC-FDMA conception

Compared to MC-FDMA, MC-TDMA divides different time slots for each user to transmit user signal using all subcarriers. As shown in Figure 2.17, similar to conventional TDMA system, the orthogonality between each user is achieved in the time domain by isolated time slots.

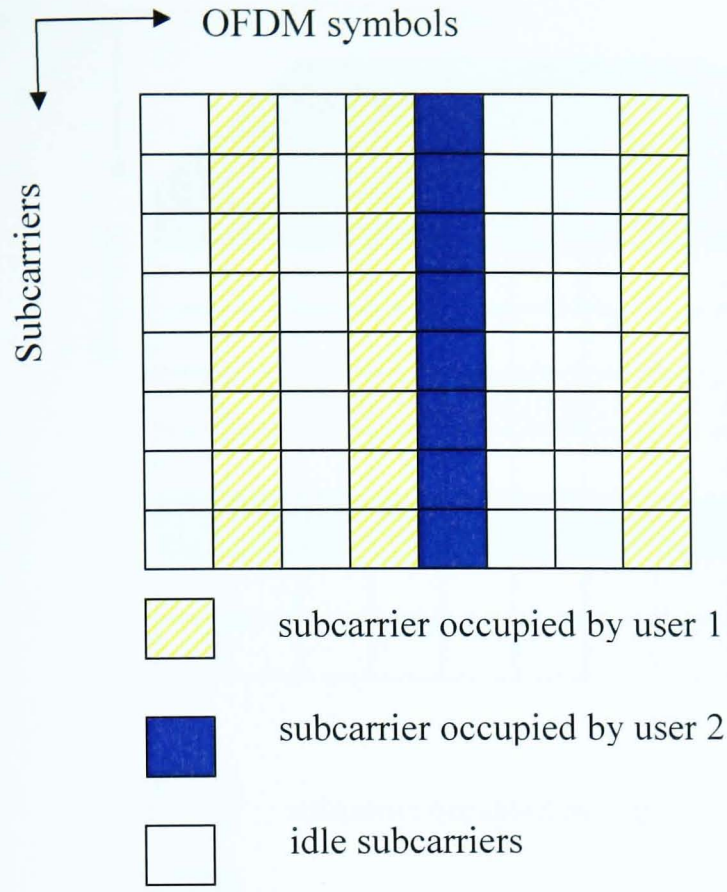

Figure 2.17 MC-TDMA conception

The configuration of MC-CDMA is depicted in Figure 2.18. MC-CDMA spreads frequency bandwidth for each subcarrier using different spreading code assigned to each user. One major advantage of MC-CDMA over Single-Carrier CDMA is that it can lower the symbol rate in each subcarrier so that longer symbol duration makes it easier to quasi-synchronize the transmission. As abovementioned, there are several different ways in terms of combination of OFDM and CDMA to implement MC-CDMA. Nevertheless, all these systems conform to both the fundamental theory of OFDM and CDMA illustrated in Figure 2.18. Next, various modified versions of MC-CDMA systems are presented.

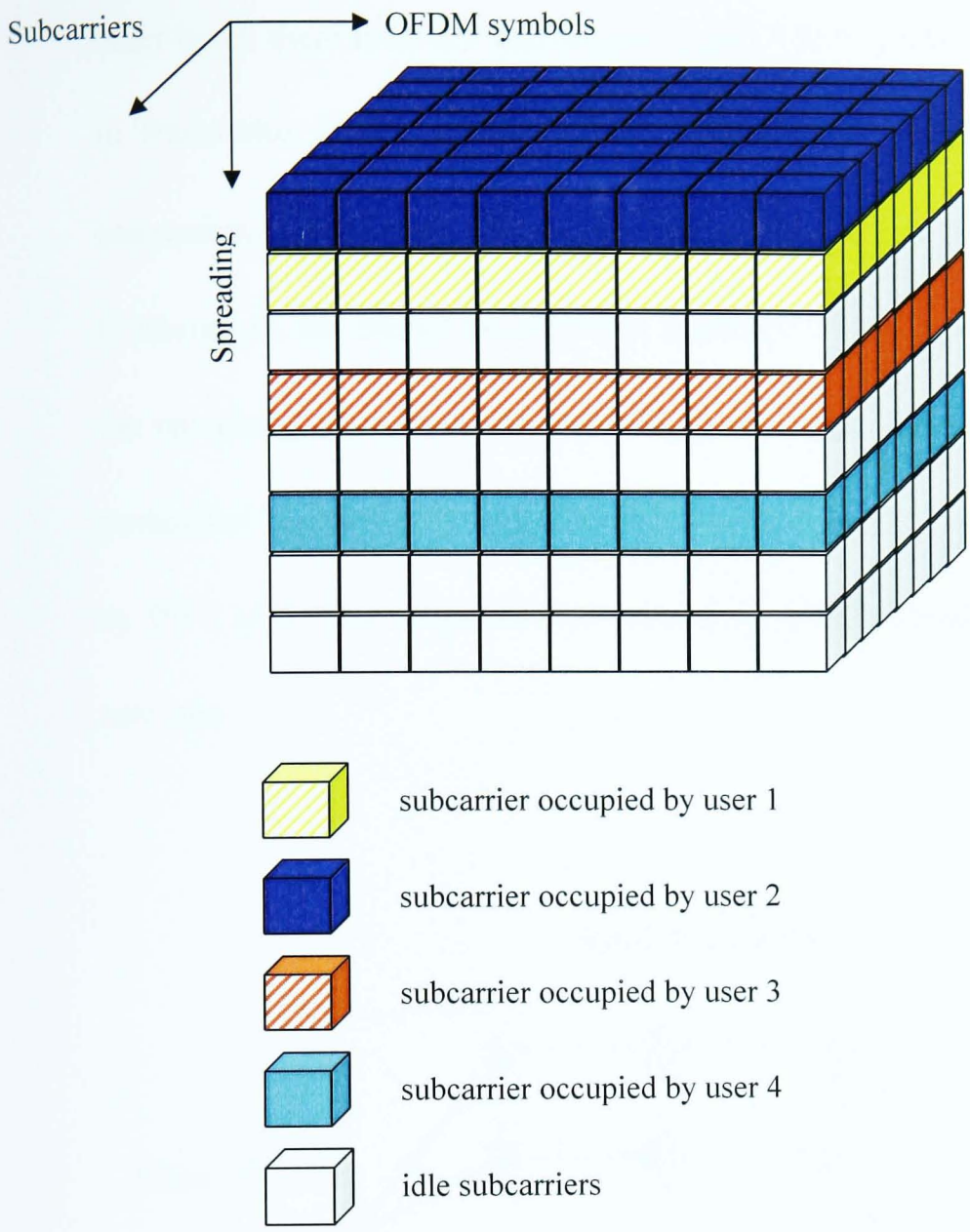

Figure 2.18 MC-CDMA conception

First, let us look at basic MC-CDMA system. There are two basic MC-CDMA transmitter implementations, namely basic MC-CDMA transmitter I and transmitter II as shown in Figure 2.19 and Figure 2.20, respectively.

The only difference between MC-CDMA transmitter I and transmitter II shown in block diagram is the serial-to-parallel (S/P) convergence. In MC-CDMA transmitter I, there is no S/P conversion, hence data bit is multiplied with different chip. On the

other hand, there is an S/P conversion in MC-CDMA transmitter II. It is worth to note in Transmitter II the serial data bit is spread by chip sequence $c_k(i)$ before the S/P conversion, where i=0,…,N_p-1. N_p denotes the number of subcarriers in the system. Furthermore, the output parallel chip sequence is used to modulate subcarriers. Then, the remaining process is the same for both cases. In both cases, each subcarrier is modulated by each chip and then summed up together, which could be implemented by IFFT [69]. The output is converted from parallel-to-serial and then sent through antennas.

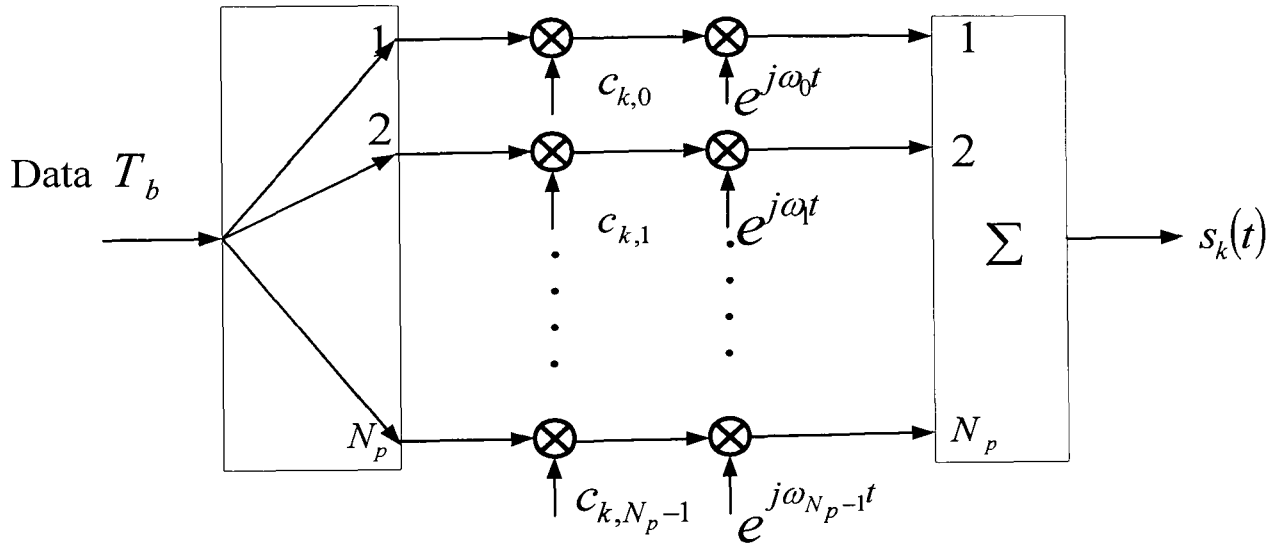

Figure 2.19 Basic MC-CDMA transmitter I

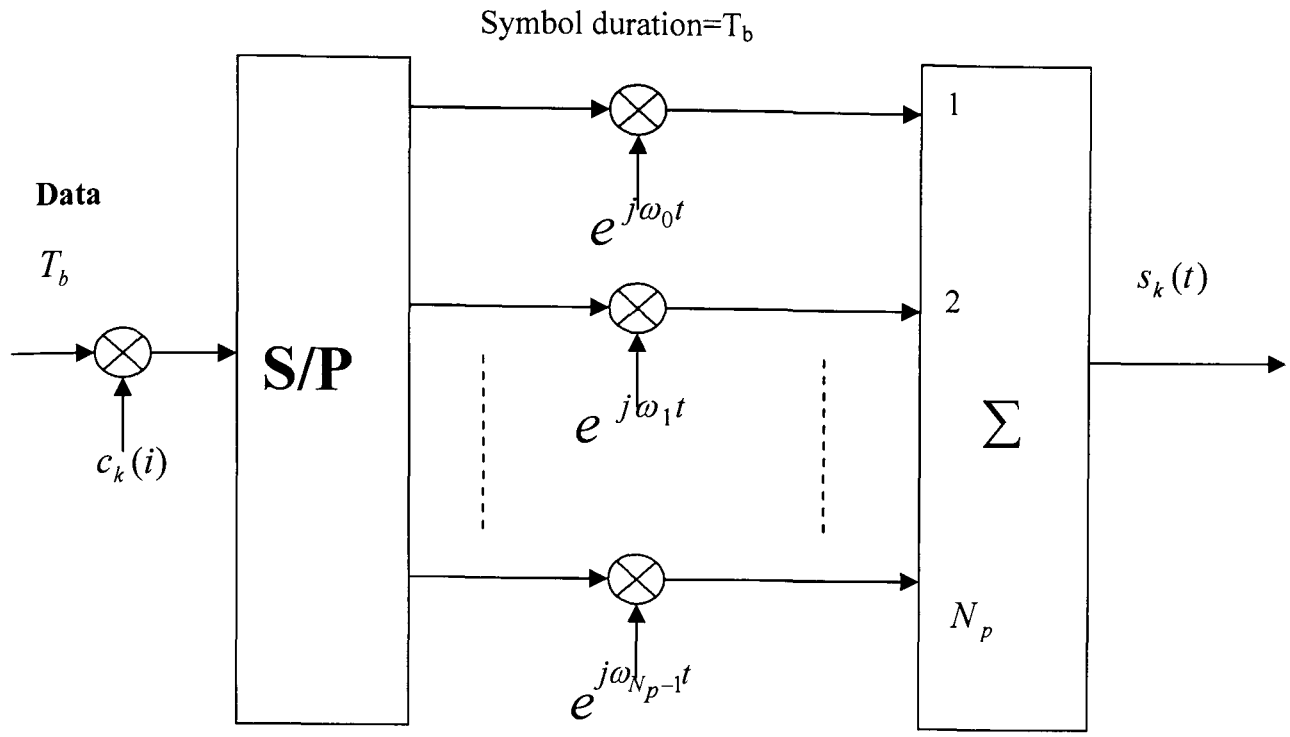

Figure 2.20 Basic MC-CDMA transmitter II

The receiver structure corresponding to basic MC-CDMA transmitter (both I and II) is shown in Figure 2.21. Due to the orthogonality of subcarriers and spreading codes for the different users, the received signals can be demodulated and despread sequentially. Then, they are passed into low-pass filters (LPF) before summation. The main advantage of the basic MC-CDMA system denoted in Figure 2.19, Figure 2.20 and Figure 2.21 would be that the receiver can efficiently utilize the scattered signal energy from the different subcarriers so as to recover the signal data with better BER performance over other MC-CDMA schemes [65].

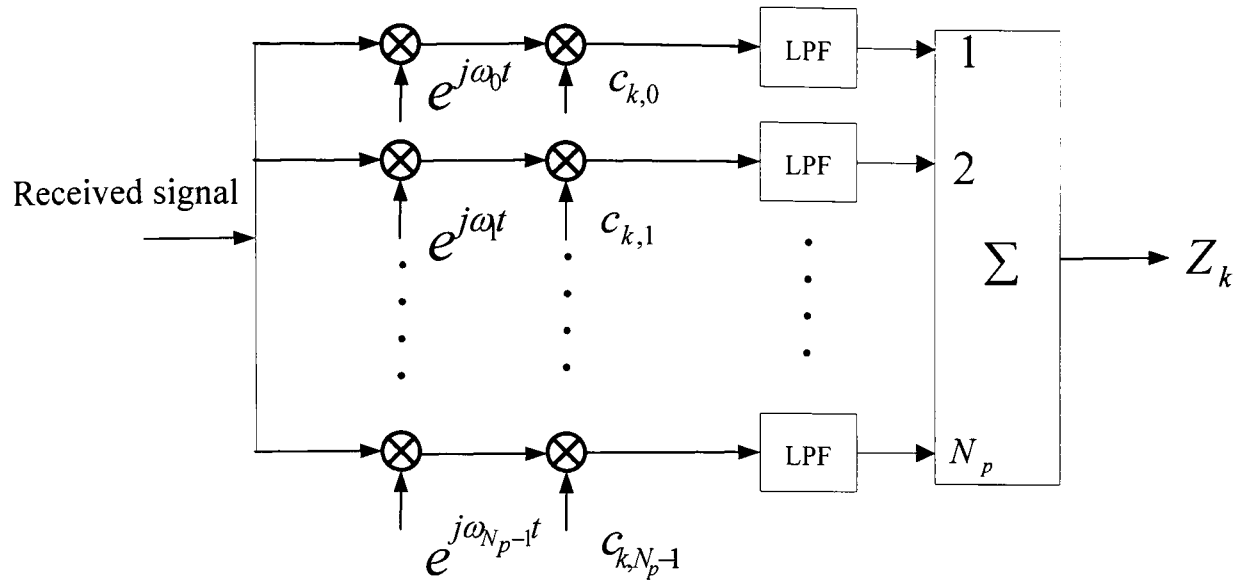

Figure 2.21 The receiver block diagram of basic MC-CDMA I and II

The spectrum of the transmitted signals with eight subcarriers is shown in Figure 2.22 for both the basic MC-CDMA system I and II. Based on these two types of transmitters, the subcarrier frequencies are designed to be orthogonal to each other with overlapping areas.

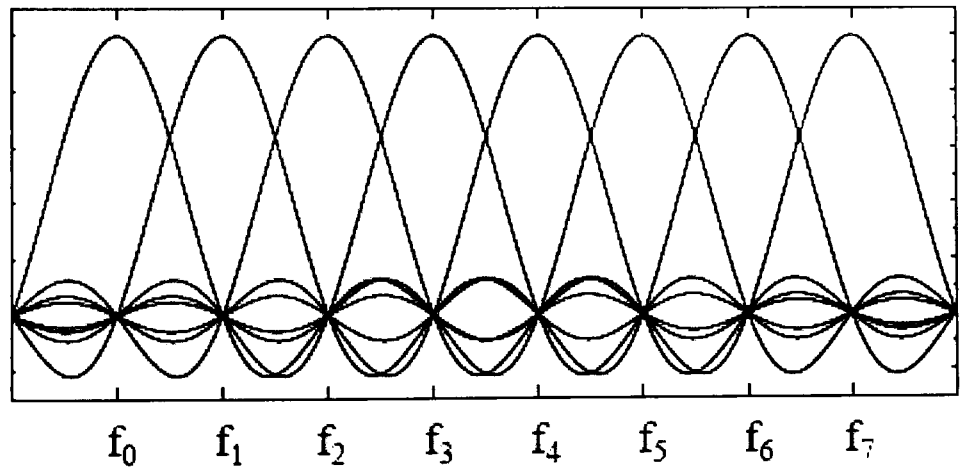

Figure 2.22 The spreading frequency spectrum of basic MC-CDMA system I & II

Also there are two versions of MC-DS-CDMA system implementations. The concept of MC-DS-CDMA transmitter I [70, 71] is displayed in Figure 2.23. The user data bit

is spread by the unique spreading code before modulating each subcarrier. Therefore, each subcarrier is modulated by spreading code sequence with the chip duration.

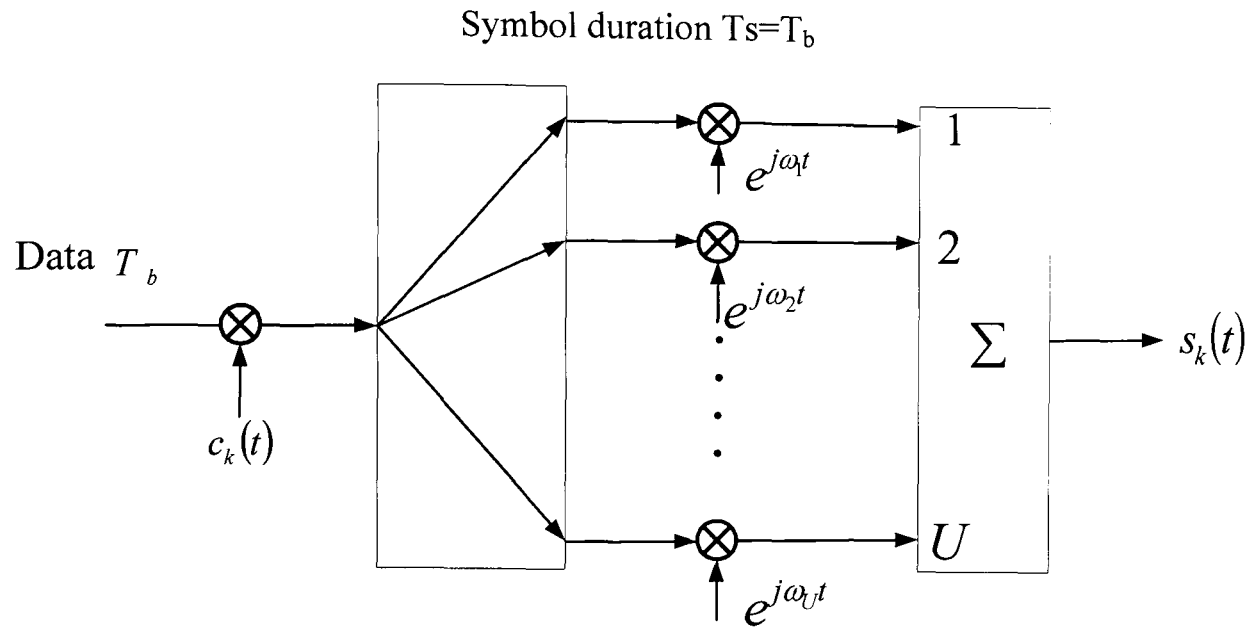

Figure 2.23 The transmitter block diagram of MC-DS-CDMA system I

The receiver block diagram of the MC-DS-CDMA system I is shown in Figure 2.24. Compared to conventional DS-CDMA receiver, the MC-DS-CDMA system I uses U Single-User Matched Filters (MFs) to detect the data bit in each subcarrier and then combine them together to acquire the processing gain using frequency diversity. Here U is equivalent to N_p in the basic MC-CDMA system. Major advantages of this system are its robustness against multi-path fading due to its frequency diversity and invulnerability to frequency-selective fading due to non-overlapping of each subcarrier.

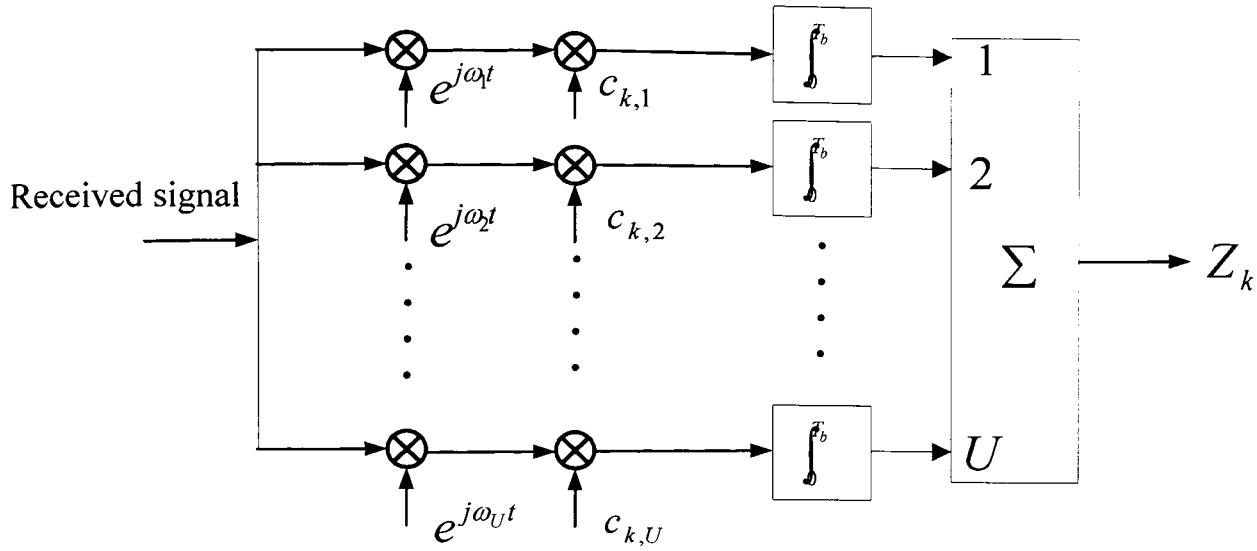

Figure 2.24 The receiver block diagram of the MC-DS-CDMA system I

Additionally, the subcarrier frequencies are orthogonal to each other without overlapping in order to avoid liaising distortion shown in Figure 2.25. Thus the entire bandwidth is eight-fold of the subcarrier frequency bandwidth as shown in Figure 2.25.

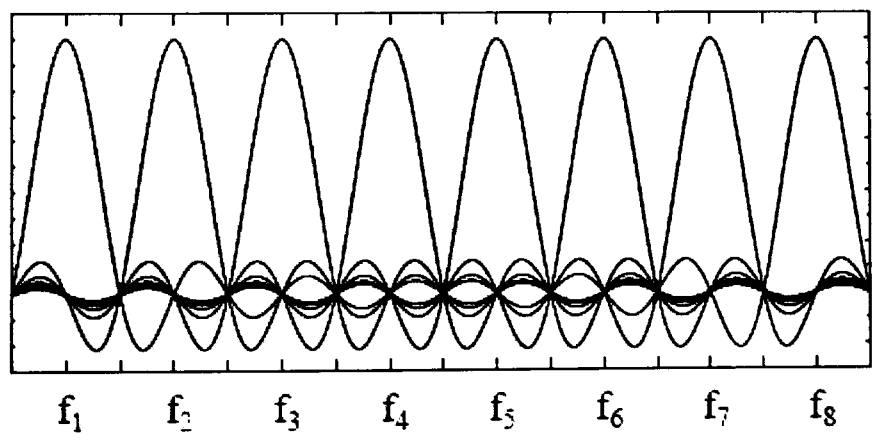

Figure 2.25 The spreading frequency spectrum of the MC-DS-CDMA system I

As a variation from MC-DS-CDMA system I, the transmitter of MC-DS-CDMA system II as shown in Figure 2.26 spreads each serial-to-parallel converted data bit

using given spreading code designated for each user. Compared with bit-wise process in transmitter I, a frame-wise data bits are converted in this fashion.

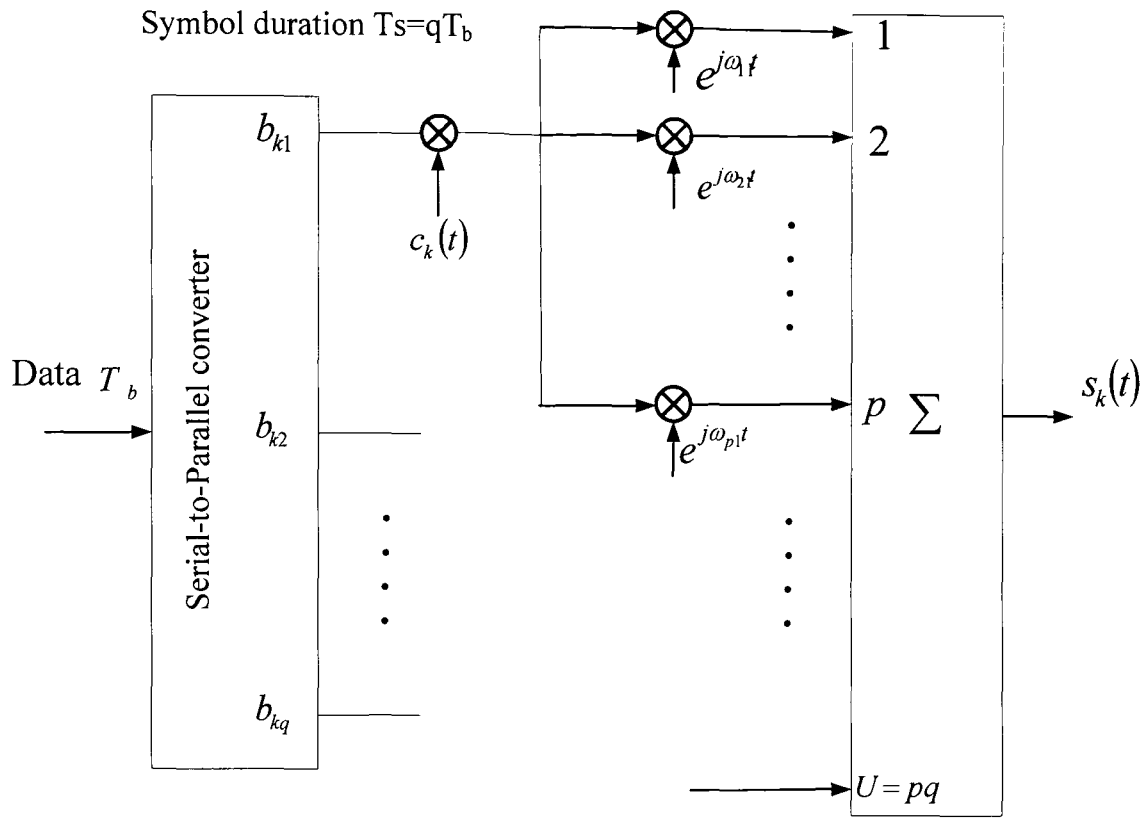

Figure 2.26 The transmitter block diagram of the MC-DS-CDMA system II

The receiver block diagram of the MC-DS-CDMA II [72, 73, 74, 75] system is shown in Figure 2.27. The receiver uses an MF to detect the received signal in each subcarrier and the outputs of a bunch of MFs associated with the same data bit are coherently detected. Next, the parallel-to-serial converter is used to recover original serial data sequence. Furthermore, a RAKE receiver could be employed to mitigate the frequency-selective fading. The MC-DS-CDMA can support higher processing gain, less performance degradation due to multi-path interference and flexible frequency/time diversity compared with DS-CDMA at the cost of high complexity and additional forward error control (FEC) technology.

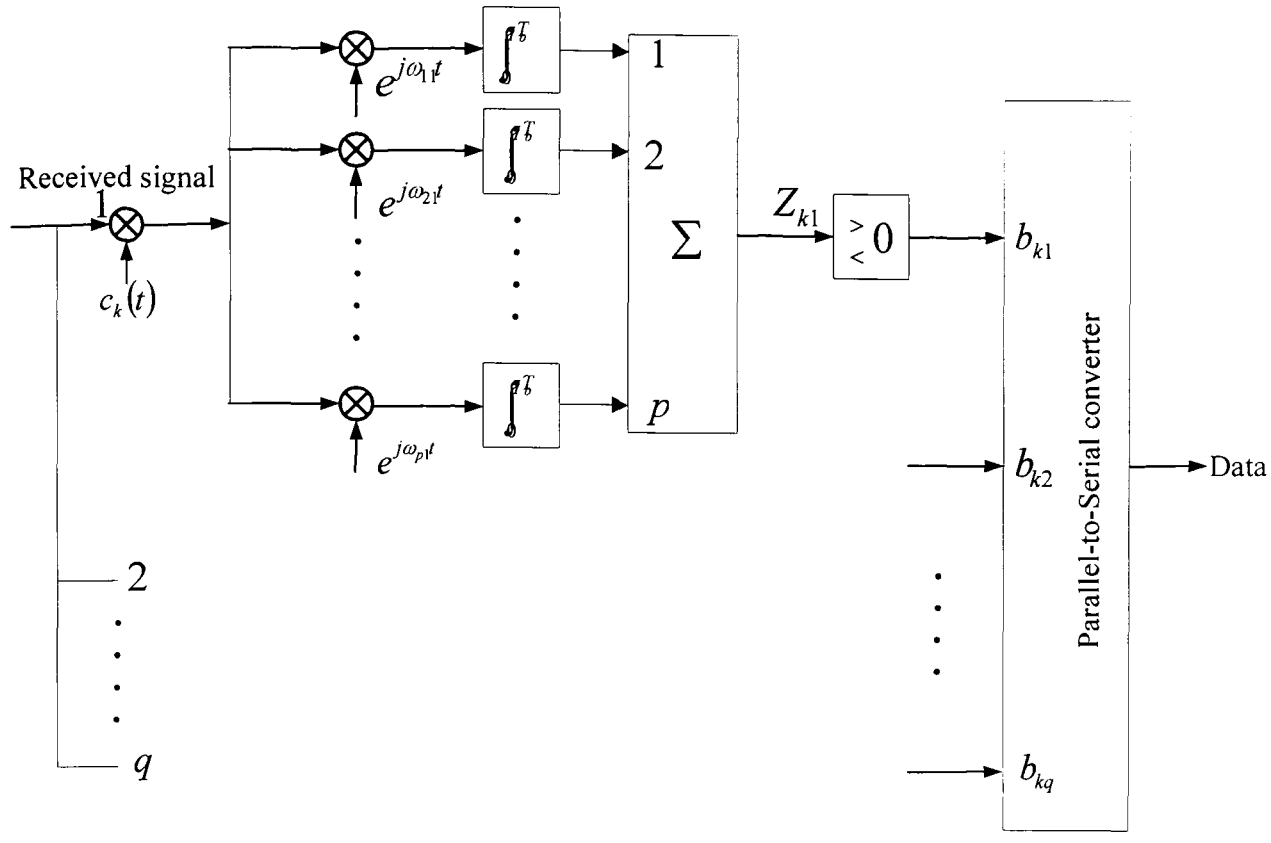

Figure 2.27 The receiver block diagram of the MC-DS-CDMA system II

In contrast to the $U = p$ subcarriers in the MC-DS-CDMA system I, the entire frequency bandwidth is divided as $U = pq$ subcarriers in the MC-DS-CDMA system II as depicted in Figure 2.28, where p and q are defined as the number of subcarriers allocated to transmit same user bit and the number of user bits per frame, respectively.

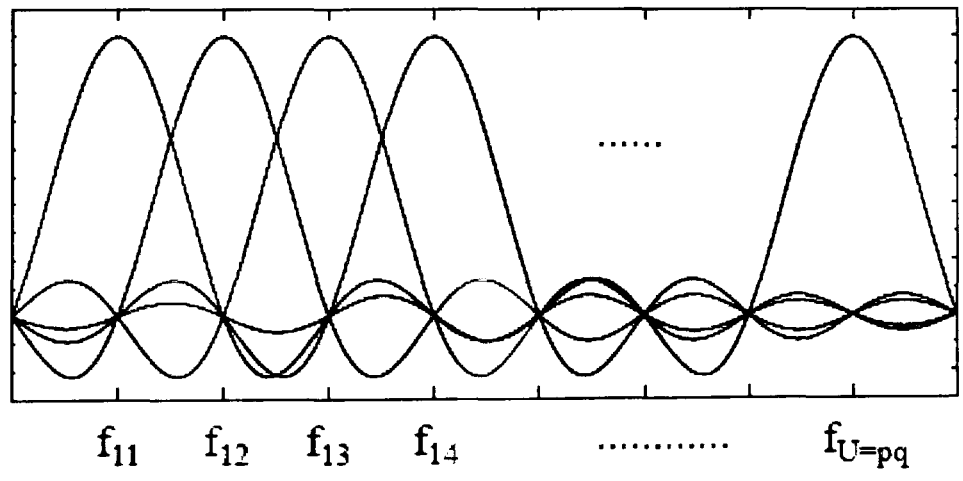

Figure 2.28 The spreading frequency spectrum of the MC-DS-CDMA system II

Figure 2.29 illustrates a block diagram of Multitone DS-CDMA transmitter [64]. Signal is converted from serial to parallel and then multiplexed before being spread.

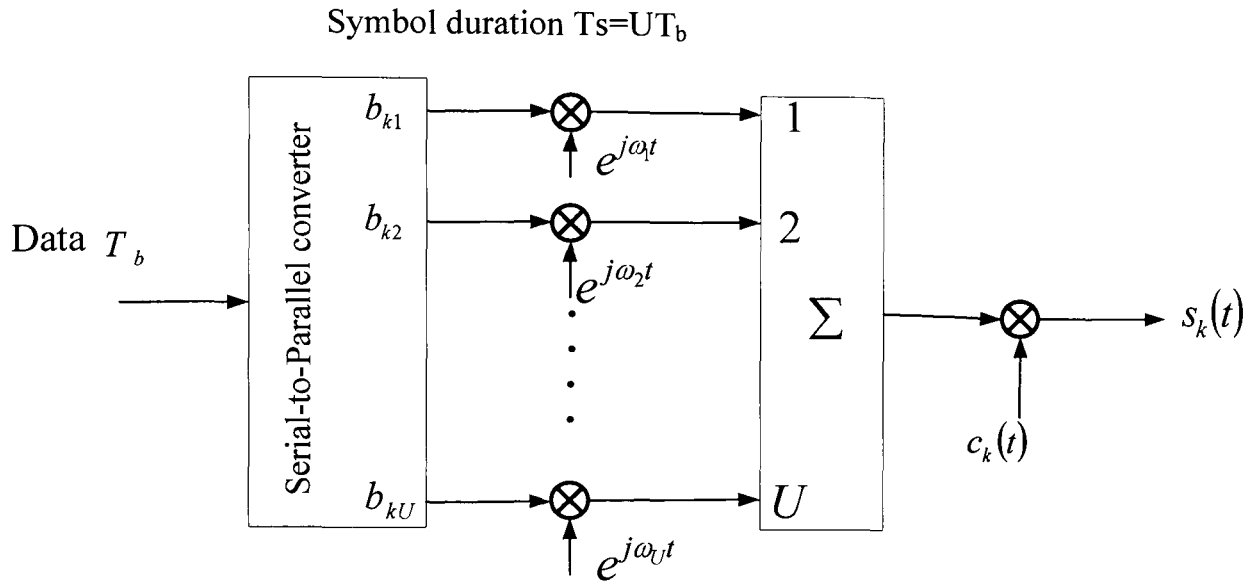

Figure 2.29 The transmitter block diagram of the Multitone DS-CDMA system

The receiver of Multitone DS-CDMA system as shown in Figure 2.30 applies U RAKE combiners with high complexity to detect received chips on each subcarrier for each user. Due to spreading of orthogonal subcarriers in transmitter, the inter-subcarrier interference is an intrinsic disadvantage of the system. Therefore, a high-complexity RAKE receiver is needed for Multitone DS-CDMA system [65].

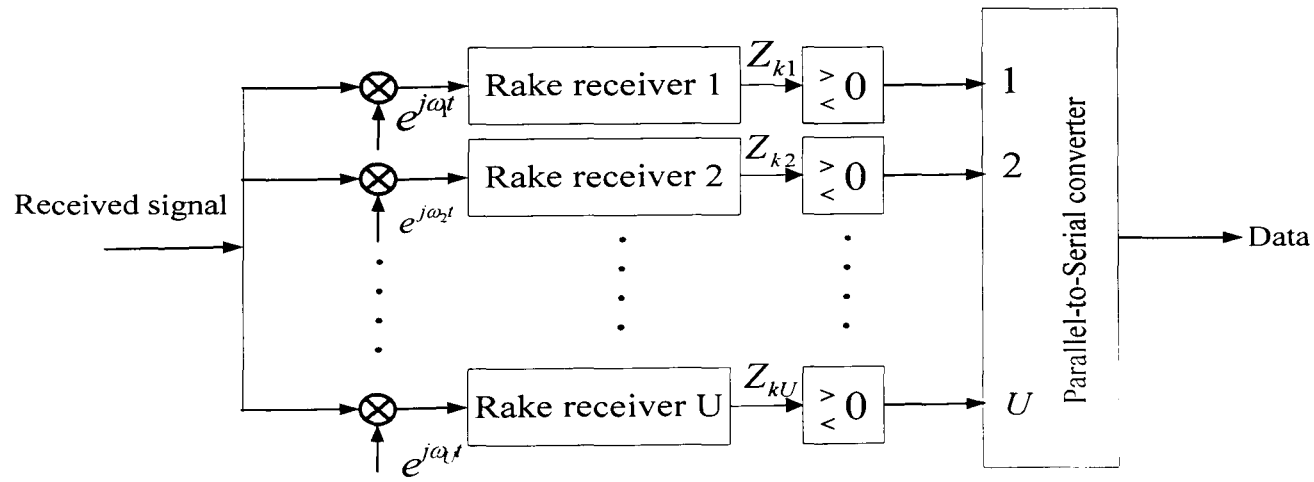

Figure 2.30 The receiver block diagram of the Multitone DS-CDMA system

Consequently, as shown in Figure 2.31, the frequency domain is spread but the minimum spacing of subcarrier frequencies is compressed as compared to basic MC-CDMA system I and II.

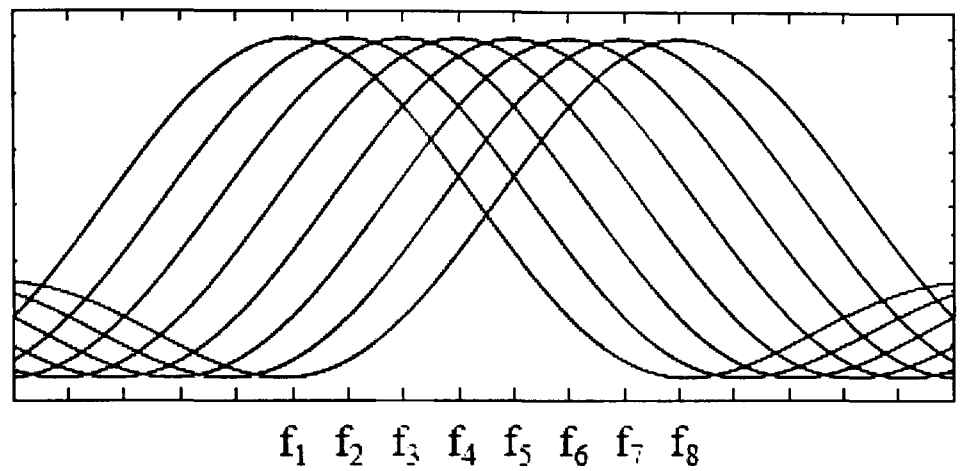

Figure 2.31 The spreading frequency spectrum of the Multitone DS-CDMA system

Since the power of chips in a symbol based on spreading only in frequency domain is vulnerable to frequency-selective fading, where orthogonality between each code is destroyed, to perform spreading also in time domain was proposed in [76]. Then two dimensional (2-D) spreading both in frequency and time domains, namely OFCDM, is investigated in [77]. Figure 2.32 illustrates a simplified block diagram of an OFCDM transmitter. Two-dimensional spreading is processed in each subcarrier. A two-dimensional spreading factor is defined as $N_{2D} = N_t \times N_f$ in [77], where N_t and N_f denotes spreading factor in time domain and frequency domain, respectively. The frequency spectrum is similar to Figure 2.22 but the bandwidth and the spacing of subcarrier frequencies is proportional to N_f and N_t. respectively.

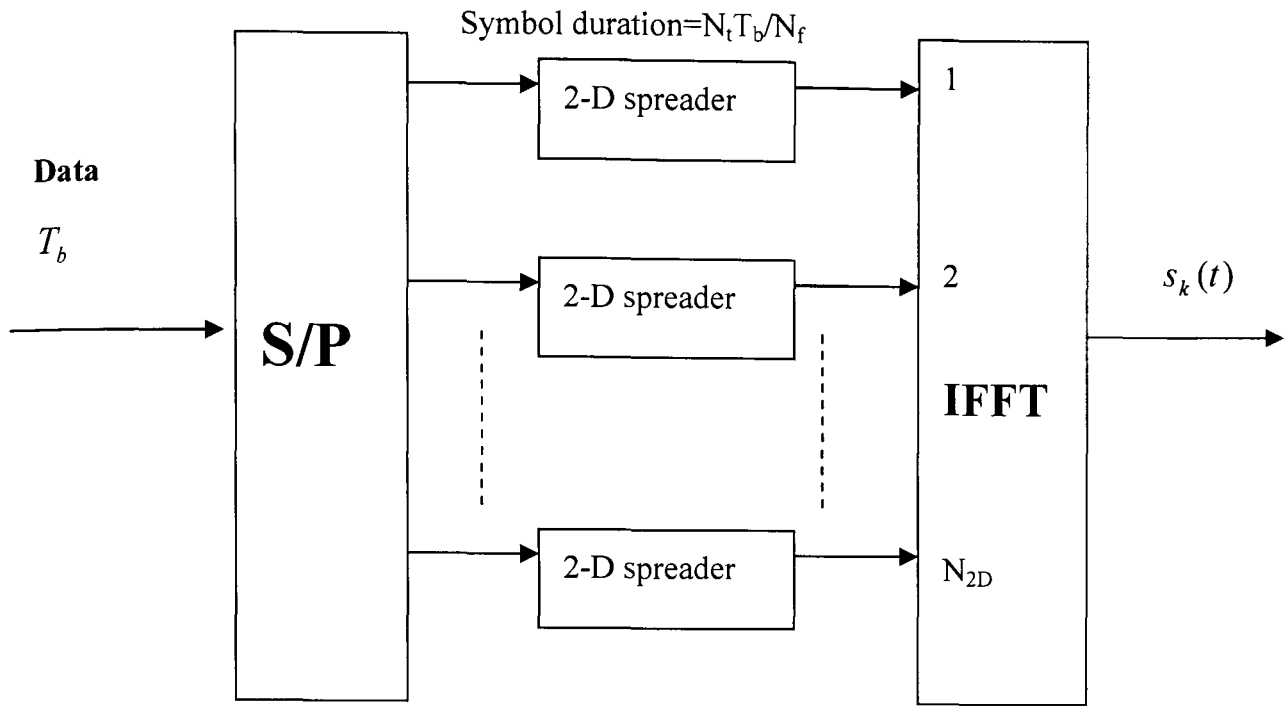

Figure 2.32 The transmitter block diagram of OFCDM

Figure 2.33 is the reverse process of the Figure 2.32, which depicts the simplified receiver block diagram of OFCDM.

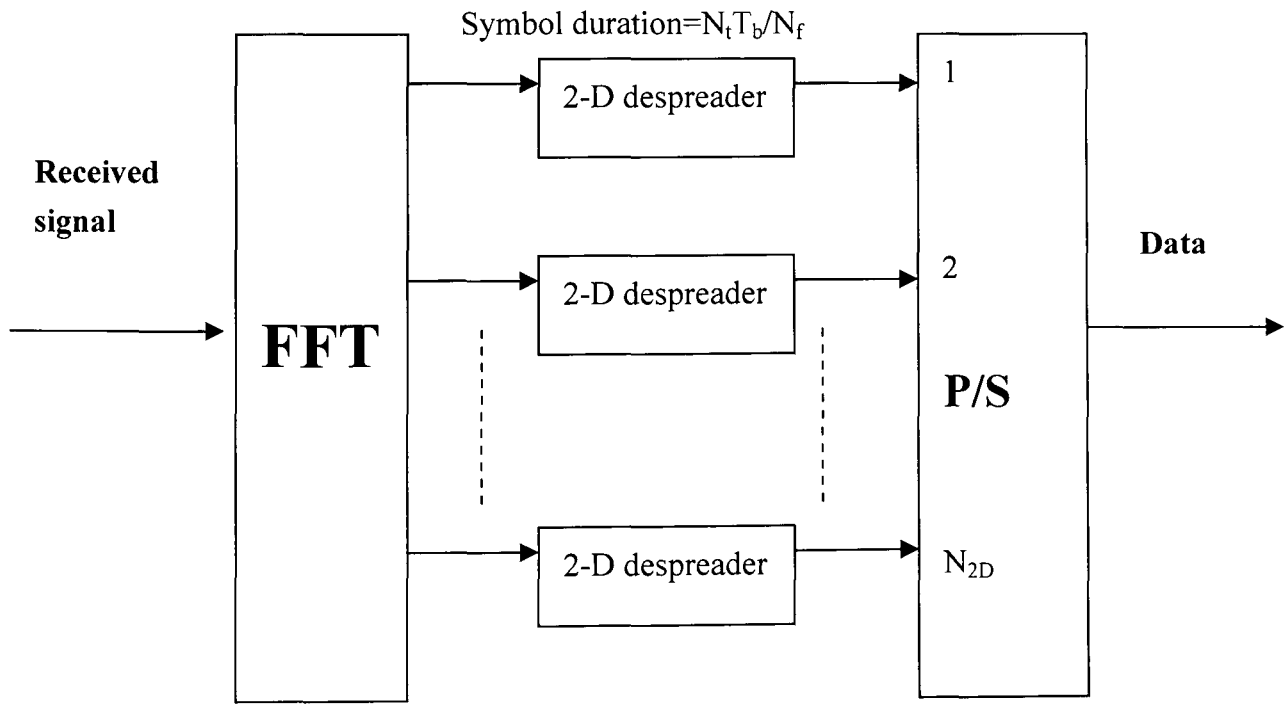

Figure 2.33 The receiver block diagram of OFCDM

Among the MC communication systems introduced above, basic MC-CDMA is the most typical system which combines OFDM and CDMA together. Hence, without loss of generality, the basic MC-CDMA (I or II) will be selected as our research reference model throughout the thesis.

In an MC-CDMA system, two significant research problems need to be addressed, which are peak-to-average power ratio (PAPR) [42] reduction and multi-user detection (MUD) problems. In the following sections, the principles about the two problems and some existing solutions will be surveyed.

2.3 PAPR Reduction and MUD in MC-CDMA System

2.3.1 PAPR Problem

In MC-CDMA system, the signal independently modulated by OFDM scheme over a number of subcarriers can engender a large peak-to-average power ratio (PAPR) when being added up coherently. This is because when N_p subcarriers are added together with the same phase, they will produce a peak power which is N_p times higher than an average power, as illustrated in Figure 2.34. High PAPR will cause in-band distortion, out-of-band frequency radiation and BER performance deterioration, when modulated signal is passed into high-power amplifier (HPA) in the transmitter of MC-CDMA [42].

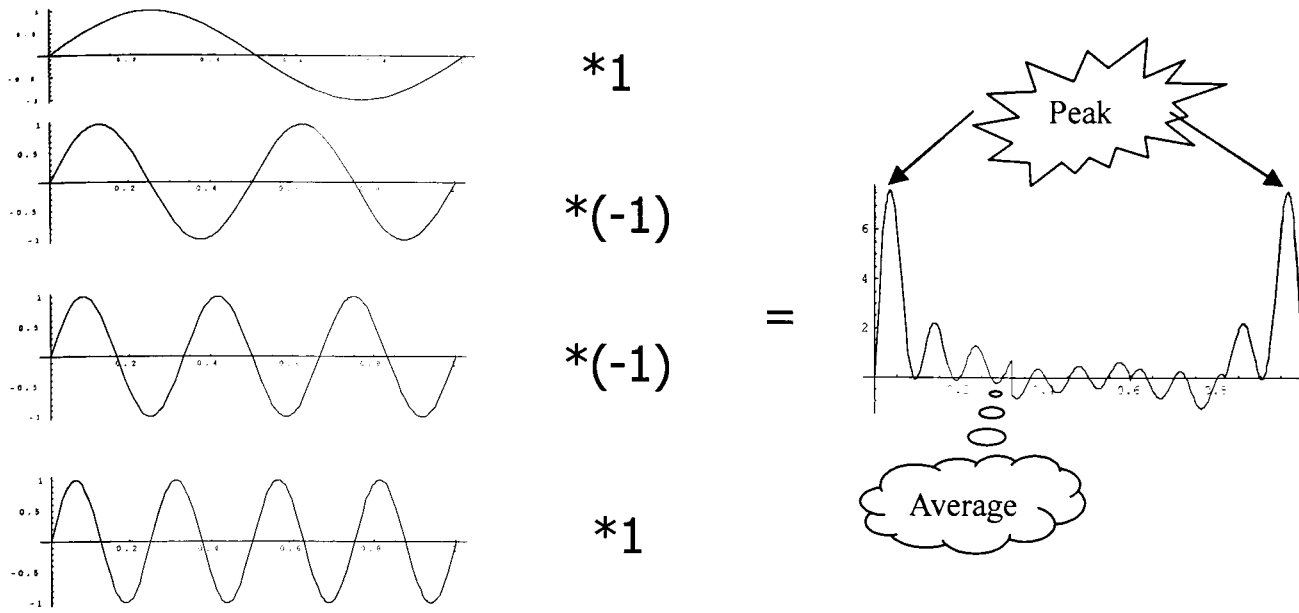

Figure 2.34 Illustration of the reason why PAPR is high in an MC system

Normally, a Rapp model [78] as shown in Figure 2.35 with a parameter p=2 is used to approximate the amplitude-to-amplitude conversion characteristic of a realistic low-cost solid-state power amplifier. The ratio of output to input amplitude in this model with parameter p is given by

$$\left|\frac{V_{out}}{V_{in}}\right| = \frac{1}{\left[1+\left|V_{in}/V_{out}\right|^{2p}\right]^{1/2p}} \tag{2.40}$$

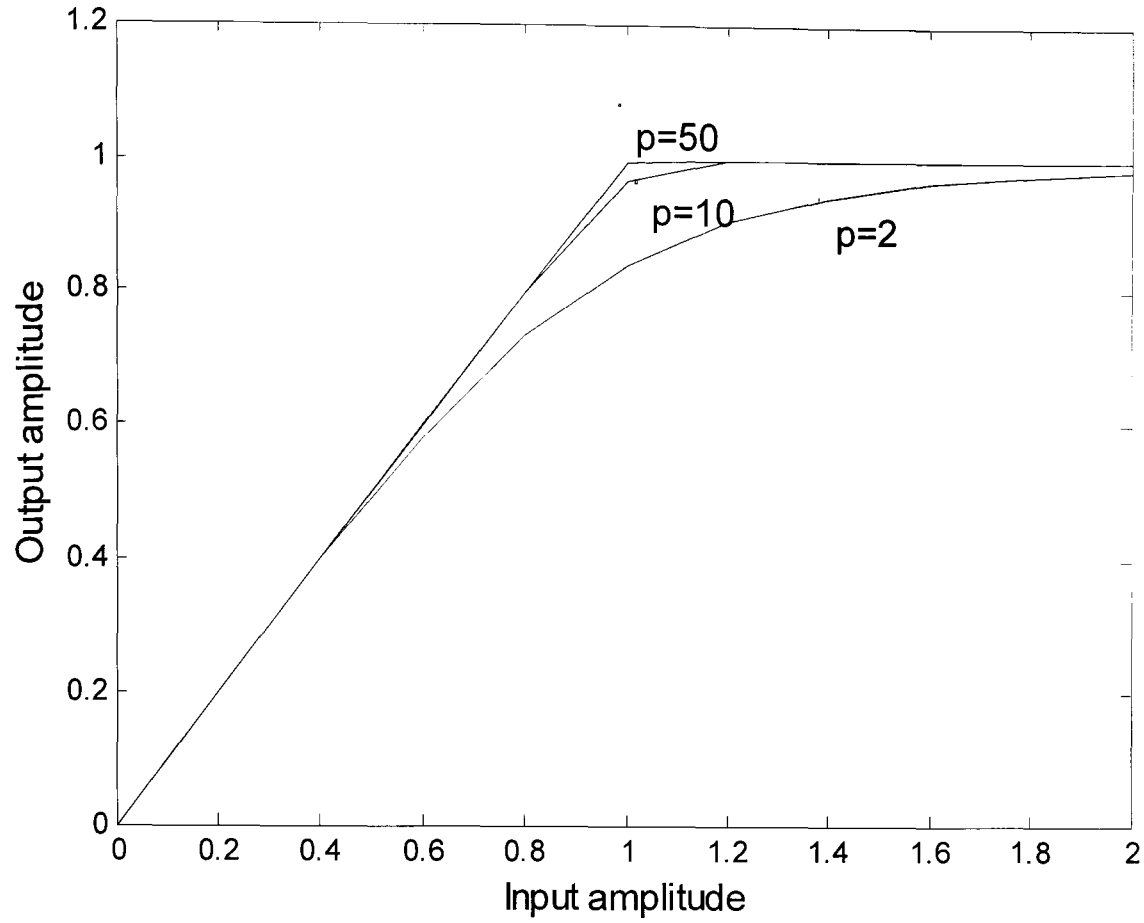

Figure 2.35 Rapp model of HPA nonlinearity

The back-off of HPA is defined as the ratio of maximum saturation output power to actual average output power [78]. Large back-off of HPA will have more possibilities to make input signal work in the linear amplifying area. Hence, the system performance degradation caused by nonlinear effect of HPA will be counteracted. However, the cost of HPA is increased dramatically as well as the required greater back-off. Additionally, HPA is the most expensive component in the radio transmitter. Therefore, one important motivation of PAPR reduction schemes focused on input signal is to avoid the large back-off of HPA. Generally, there are four main categories of PAPR reduction schemes: distortion technique (e.g. clipping, peak windowing & μ-law companding) [79, 80, 81, 82, 83, 84], coding technique (e.g. block coding) [85], scrambling technique (e.g. selected mapping (SLM) & partial transmit

sequences (PTS)) [86, 87, 88], and Discrete Fourier Transform scheme (DFT) [89].

2.3.2 Existing Solutions of PAPR Reduction

A. Clipping, Peak Windowing and μ-law Companding

The evident motivation to select clipping [79] for PAPR reduction is due to the simplicity of the implementation. Since the large peak power occurs with a very low probability, clipping could be an effective approach to mitigate the PAPR. However, deliberately clipped signal in time domain would induce the significant in-band distortion in frequency domain and out-of-band power radiation, also would degrade the bit-error-rate (BER) performance. If we normalize the average signal power for each subcarrier, the total average power of an MC signal is N_p, whereas the peak power is N_p^2. Therefore, the root mean square (rms) power of the signal denoted by σ is $\sqrt{N_p}$ for baseband signal and $\sqrt{N_p/2}$ for bandpass signal, respectively. As defined in [79], the normalized clipped level, namely clipping ratio (CR) is

$$CR = A/\sigma \tag{2.41}$$

where A is clipped level for the MC signal s_k. Hence, the signal after clipping will be:

$$c_k(t) = \begin{cases} -A, & if \quad s_k(t) \le -A \\ s_k(t), & if \quad -A < s_k(t) \le A \\ A, & if \quad s_k(t) > A \end{cases} \tag{2.42}$$

Figure 2.36 shows a block diagram of clipping followed by filtering. Filtering is normally applied after clipping to prohibit the spectral splatter but may also produce more peaks in time domain and hence may engender the peak re-growth. Therefore, a number of repeated clippers and filters may be introduced so as to compensate this

problem [90]. However, it may introduce high implementation cost into the system and in-band clipping noise which may cause some BER performance degradation.

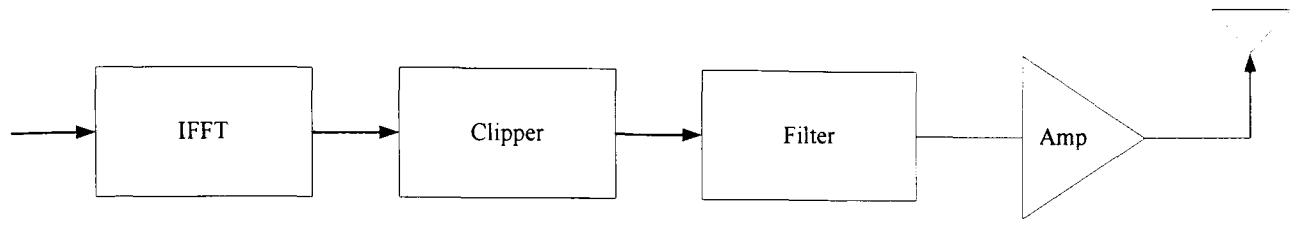

Figure 2.36 Block diagram of clipping and filtering approach

Second, since clipping in time domain usually causes out-of-band radiation, some peak windowing techniques (e.g. cosine, Kaiser and Hamming window functions [80]) are introduced to replace clipping in time domain. In [80], as the window width increases, the out-of-band radiation decreases. However, the window should not be too long in the time domain, unless it would bring in high in-band distortion and noise.

Third, μ-law companding was proposed in [81, 82, 83, 84] to increase the average signal power so as to reduce PAPR. However, companding also induces the out-of-band re-growth which needs filtering or shaping before compression.

B. Block Coding Scheme

The idea of the coding scheme [91] is to choose the code words with relatively low PAPR values as the selected code words to be transmitted from a number of possible code words. Table 2.4 lists the PAPR values corresponding to the four code words on different subcarriers.

d_{dec}	d_1	d_2	d_3	d_4	PAPR(dB)
0	0	0	0	0	16
1	1	0	0	0	7.07
2	0	1	0	0	7.07
3	1	1	0	0	9.45
4	0	0	1	0	7.07
5	1	0	1	0	16
6	0	1	1	0	9.45
7	1	1	1	0	7.07
8	0	0	0	1	7.07
9	1	0	0	1	9.45
10	0	1	0	1	16
11	1	1	0	1	7.07
12	0	0	1	1	9.45
13	1	0	1	1	7.07
14	0	1	1	1	7.07
15	1	1	1	1	16

TABLE 2.4 PEAK POWER DURING A SYMBOL PERIOD FOR ALL POSSIBLE DATA WORD D_N

The reduction of PAPR using block coding scheme is at the expense of an increase in the bandwidth for the same data rate and a reduction in energy per transmitted bit for the same transmit power. However, the increased bandwidth is small and, in comparison to SC scheme, this is compensated by the high spectral efficiency of the MC schemes. The reduction in energy per transmitted bit is also small and this could be offset by the error detection/correction potential of the block coding, which can be exploited in reduction of BER in conjugation of clipping approach. The supreme constraint of the block coding approach applied on PAPR reduction is the trade-off among coding rate, the PAPR performance and encoding/decoding in error correction. The performance of the reduction of the PAPR is reciprocally proportional to the

coding rate, which the performance degrades as the coding rate increases. However, in order to match with the code words designed for the encoding/decoding in error correction, the coding rate should be lower than the required one for optimum PAPR reduction performance. Furthermore, low coding rate is not suitable for the system with high data rate transmission. Therefore, block coding is a sub-optimum scheme applied for PAPR reduction, which is only suitable for the low data rate MC system with a small number of subcarriers.

C. Selective Mapping and Partial Transmit Sequence

Selective mapping (SLM) and partial transmit sequence (PTS) can be generalized as one generic category, namely scrambling [42], since they can be implemented in a similar way. In the SLM approach, M statistically independent sequences are generated from same information and those sequences with lowest PAPR values are selected for transmission. The implementation of SLM is depicted in Figure 2.37. M candidate sequences are generated by multiplying the information sequence by M random sequences with length of N_p. If the complementary cumulative distributive function (CCDF) of the original information signal is $\Pr(\text{PAPR}>\text{PAPR}_0)$, then the CCDF of the best of M random sequences is given as $\Pr(\text{PAPR}>\text{PAPR}_0)^M$.

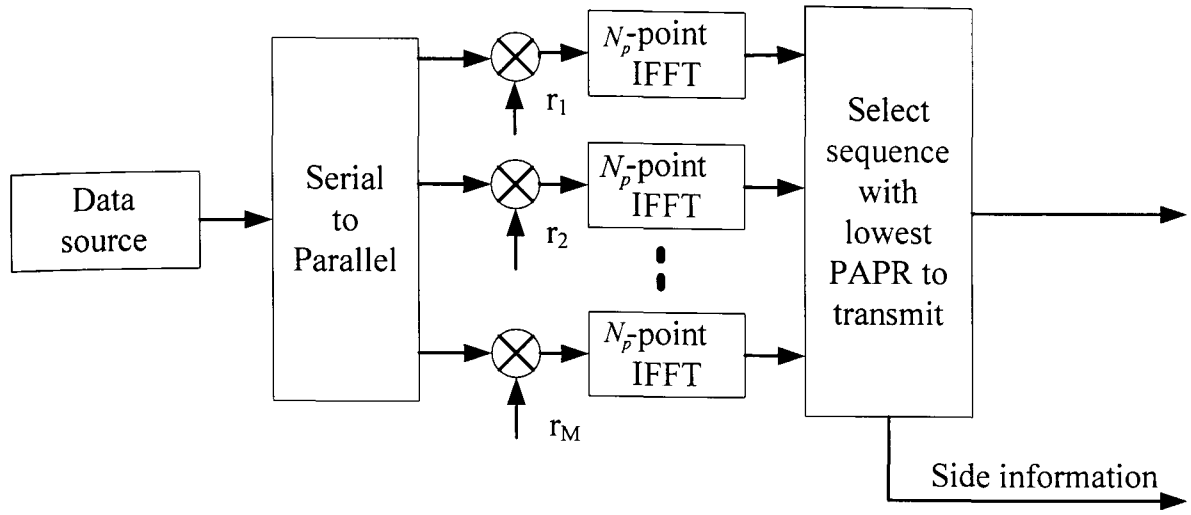

Figure 2.37 Selective mapping approach

As shown in Figure 2.38, the PTS scheme divides the input symbol block into M disjoint sub-blocks and multiplies them with a set of phase factors for phase rotation. The phase factors are given as $b_w = e^{jw\theta}$, where $w = 0,1,...,W-1$, $\theta = \frac{2\pi}{W}$ and W is a random integer. Each sub-block is transformed into partial transmit sequence using IFFT and then rotated by its allocated phase factor. Therefore the crucial objective is to optimally combine the sub-blocks and corresponding phase factors in order to transmit the superimposed symbol block with the lowest PAPR.

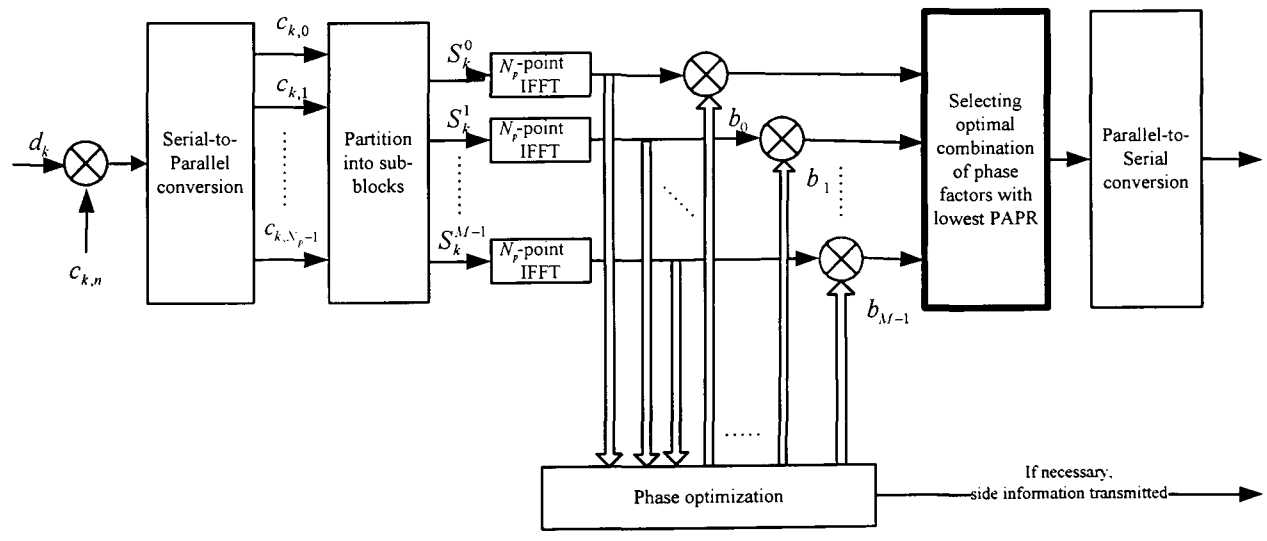

Figure 2.38 The transmitter model of PTS scheme

However, the drawbacks of both SLM and PTS schemes are high computational complexity, extra IFFT implementations and slight side information need to be

transmitted. Therefore, the receiver should have the knowledge about side information sent from the transmitter in order to correctly recover the original signal.

D. Discrete Fourier Transform (DFT) Scheme

DFT-precoded [89] or namely serial modulation (SM) [92] scheme is proposed to reduce the PAPR in Multi-Carrier system. As shown in Figure 2.39, the DFT-spreading block is disposed to precede the IFFT modulation in the transmitter of MC-CDMA to achieve low PAPR value performance by multiplying DFT-spreading matrix F with the S/P converted Multi-Carrier block signal, where DFT-spreading matrix F is given by

$$F_{n,m} = \frac{1}{N_P} e^{-2\pi nm/N_P}, 0 \le n, m \le N_P - 1 \tag{2.43}$$

The essential of the DFT-precoded Multi-Carrier system to reduce PAPR is somehow a simple conversion from Multi-Carrier system to Single-Carrier. Consequently, the PAPR of the transmitted signal is significantly shrunken.

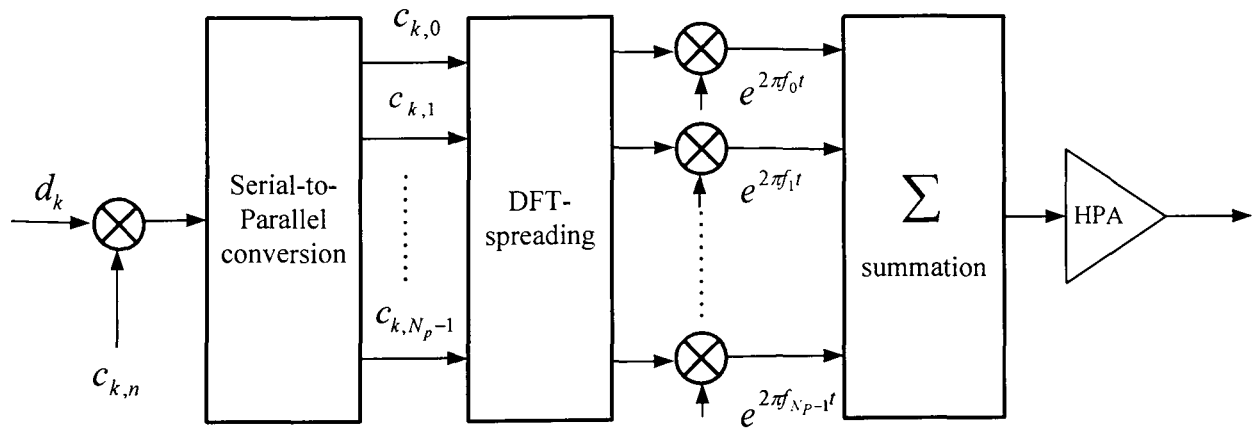

Figure 2.39 Transmitter block diagram of MC-CDMA system with DFT spreading

2.3.3 Multi-User Detection

In Chapter 2.1.5, we explained the cause of MAI in a DS-CDMA system. Similarly, unwanted MAI may also cause high BER in MC-CDMA which significantly degrades the system performance. Therefore, eliminating the MAI effect generated from different users is a vital research issue for MC-CDMA systems. In contrast to inefficient conventional receiver [29] consisting a bank of MFs assuming each user is the only present and treats the interferences as noise, the maximum-likelihood (ML) multi-user detector (MUD) [93] utilizes the spreading code information allocated to all users to coherently and efficiently detect the wanted signal for each user. Verdu [16] proposed MUD as a joint detection of all users in CDMA system to reduce MAI problem. The idea of MUD is to treat MAI as a part of information, not as noise. In this way, it could improve the system performance significantly. Hence, MUD has received much attention for both CDMA and emerging MC-CDMA systems [16, 94, 95]. With an optimal MUD detector [16], the receiver should consider all possible combinations of the transmitted signal and check which one could maximize the joint correct decision probability of the bits received from all the users.

In conventional receiver with only single-user MF, no knowledge about signature waveform and timing for each interfered user can be available, so the interference engendered by crosstalk from different spreading codes has to be treated as noise in detector. In the abovementioned optimum MUD based receiver, it can exploit the knowledge of the spreading codes for all users and utilizes the observations from all

users at the receiver as sufficient statistics to jointly estimate the transmitted data. The main advantage of MUD is that the BER performance could be improved through peeling off the obstacle from the MAI as compared to the conventional single-user MF which treats the MAI as only noise by invoking the central limit theory [37]. However, the optimal MUD detector proposed by Verdu becomes impractical due to very high computational complexity when there is a large number of users. This is because that the system has to check every possible combination of the bit vector sent. For example, if there are K users in the system, the total number of possibilities becomes 2^K. Hence, the computational complexity of the optimal detector increases exponentially with the number of users. Therefore, recent research work focuses on looking for suboptimal MUD solutions which could be feasible in practice. Therefore, it is an interesting research topic to acquire an acceptable suboptimal solution with acceptable low computational complexity. In the following section, we review the existing sub-optimum detectors.

2.3.4 Existing Solutions of Sub-Optimal MUD

A. De-Correlating Detector

The advantage of de-correlating detector [16, 94] than conventional single-user MF detector is the robustness to the near-far problem with linear computational complexity, where means the complex power control can be neglected. Figure 2.40 depicts a decorrelating receiver structure and the output of the K MFs can be obtained:

$$Z = [Z_1, Z_2, \ldots Z_K]^T$$
$$= \Re d + n \tag{2.44}$$

where "$\Re$" is the correlation matrix of user spreading signatures and d is the vector of synchronous transmitted bits for all users at the transmitter.

$$\Re = \begin{bmatrix} 1 & \rho_{12} & \cdots & \rho_{1K} \\ \rho_{21} & 1 & \cdots & \rho_{2K} \\ \vdots & \vdots & \vdots & \vdots \\ \rho_{K1} & \rho_{K2} & \cdots & 1 \end{bmatrix}, \tag{2.45}$$

$$d = \left[\sqrt{E_1} d_1, \ldots, \sqrt{E_K} d_K\right]^T \tag{2.46}$$

and "ρ_{jk}" is the cross-correlation between the codes given by

$$\rho_{jk} = \int_0^{T_b} c_j(t) \cdot c_k(t) dt \tag{2.47}$$

and the noise vector item of the output of MFs with elements $n = [n_1\ n_2 \ldots . n_K]^T$ has a covariance

$$E\left(nn^T\right) = \frac{1}{2} N_0 \Re \tag{2.48}$$

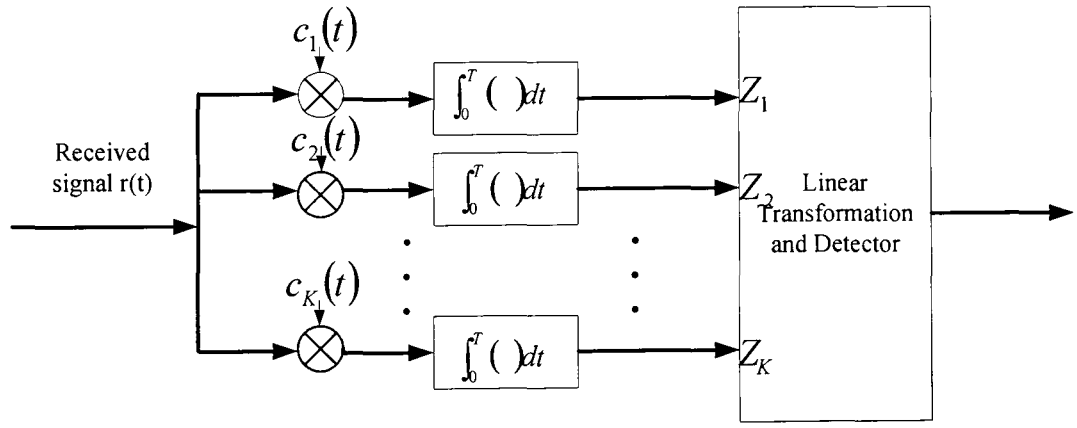

Figure 2.40 Receiver structure for decorrelating receiver

If we apply the inverse of the correlation matrix to the output of MFs then we can completely get rid of the MAI.

$$Z_{Decorrelator} = \Re^{-1}(\Re d + n)$$

$$= (\Re^{-1}\Re)d + \Re^{-1}n$$

$$= d + \Re^{-1}n \tag{2.49}$$

$$\hat{d} = \mathrm{sgn}(Z_{Decorrelator}) \tag{2.50}$$

Although the de-correlating detector can remove the effect of MAI from the desired signal, the item $(\Re^{-1}n)$ in the above equation causes severe problem in low SNR values. This problem is similar to zero-forcing equalizer that perfectly removes ISI. The resulting noise power is always greater than or equal to the noise power at the output of the conventional single-user MF detector [94]. Another disadvantage of the de-correlating detector is that the inversion of the Correlation Matrix "$\Re$" becomes difficult for a large number of users. One good property of this detector is aforementioned that it is near-far effect resistant regardless of knowledge of the user signal's amplitudes. From Figure 2.41, we can see that the de-correlating detector performs worse than conventional MF detector at low SNR conditions because of the increased noise term due to $(\Re^{-1}n)$.

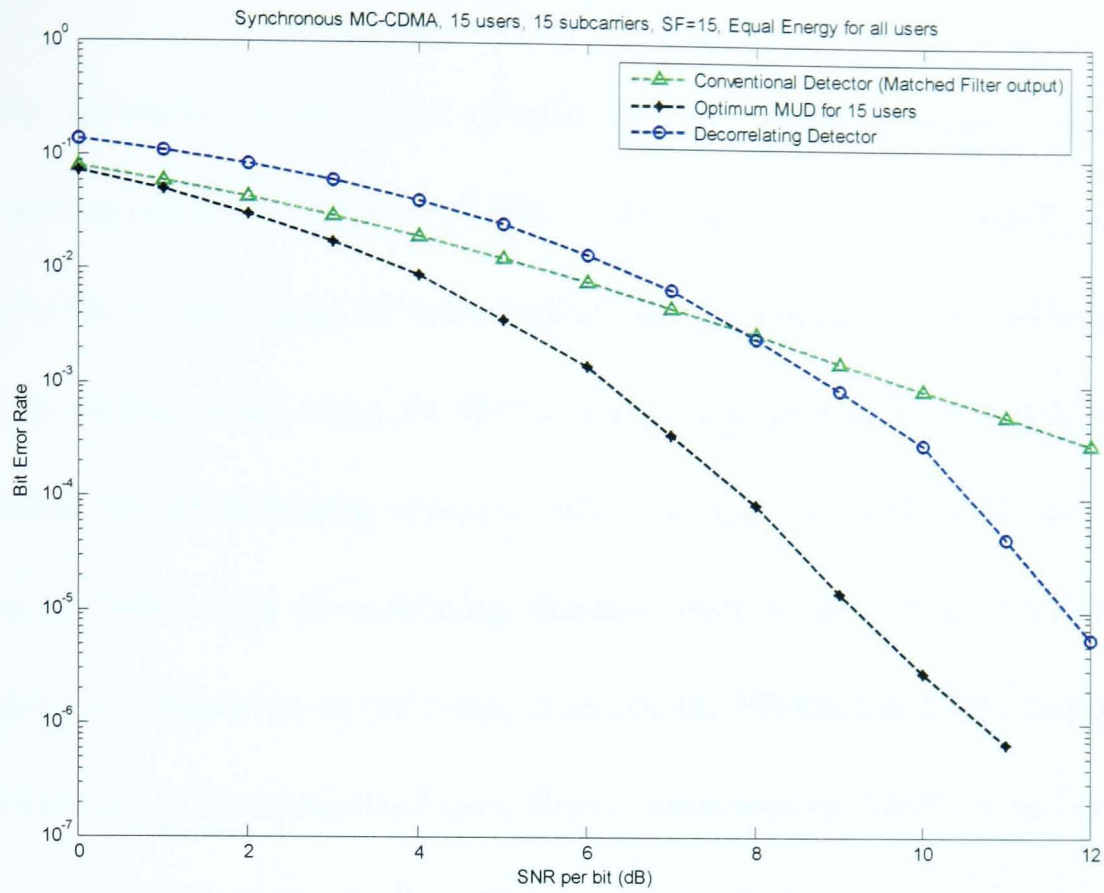

Figure 2.41 The performance of De-Correlating MUD for Synchronous 15-user MC-CDMA receiver

B. Minimum Mean Square Error Detector

The Minimum Mean Square Error (MMSE) assisted MUD [94, 95] is a detector with linear computational complexity which takes into account both the background noise power and the knowledge of cross-correlation matrix of users' spreading codes. The MMSE detector operates through minimizing the mean square error (MSE)

$$J(d) = E\left[\left(d - Z_{MMSE}\right)^T \left(d - Z_{MMSE}\right)\right] \tag{2.51}$$

to have a reasonable estimate of the transmitted data by means of Z_{MMSE}, where the optimum choice of Z_{MMSE} is given by

$$Z_{MMSE} = \left(\Re + \frac{1}{2} N_0 I\right)^{-1} \left(\Re d + n\right) \tag{2.52}$$

where I is the identity matrix. Hence, the output of detector is then expressed as:

$$\hat{d} = \mathrm{sgn}(Z_{MMSE}) \tag{2.53}$$

The only difference of estimation criterion between MMSE (Equation (2.52)) and de-correlating detector (Equation (2.49)) is the item $\frac{1}{2}N_0 I$. The MMSE detector considers the varied impact of noise against user interference as the different SNR values. In another word, when the SNR is high, the performance of MMSE detector approaches the de-correlating detector, where in the low SNR case, the MMSE detector is better than de-correlating detector, because the additive noise is the dominant term. However, as the linear criterion, the MMSE inevitably produces the biased estimate of the transmitted data. Hence, some residual MAI can not be totally removed after detection. Additionally, a significant drawback of this detector compared with the de-correlating detector is that it requires estimation of the received amplitudes of all users and hence the performance of MMSE detector is more vulnerable to the near-far problem, which needs a more complex power control algorithm.

C. Decision-Driven MUD

There are many non-linear MUD methods in contrast to the above linear detectors. Decision-driven MUD [16, 96] also namely decision-feedback (DF) MUD is one of them. It is analogous to the decision-feedback equalizers used for ISI suppression. The simple approach of decision-driven MUD schematically shown in Figure 2.42 executes as: Decision is firstly made about an interfering user's bit, and then the result is fed back to the receiver to assist being subtracted from received waveform. The resulting waveform become de-interfered signal provided the decision was correct;

otherwise it will double the effect of the interferer, and result will be discarded. Then the decision will be re-assumed iteratively until the correct result is acquired at the receiver. Even the decision-driven MUD could have better solution than linear MUDs, the disadvantage is its high computational complexity.

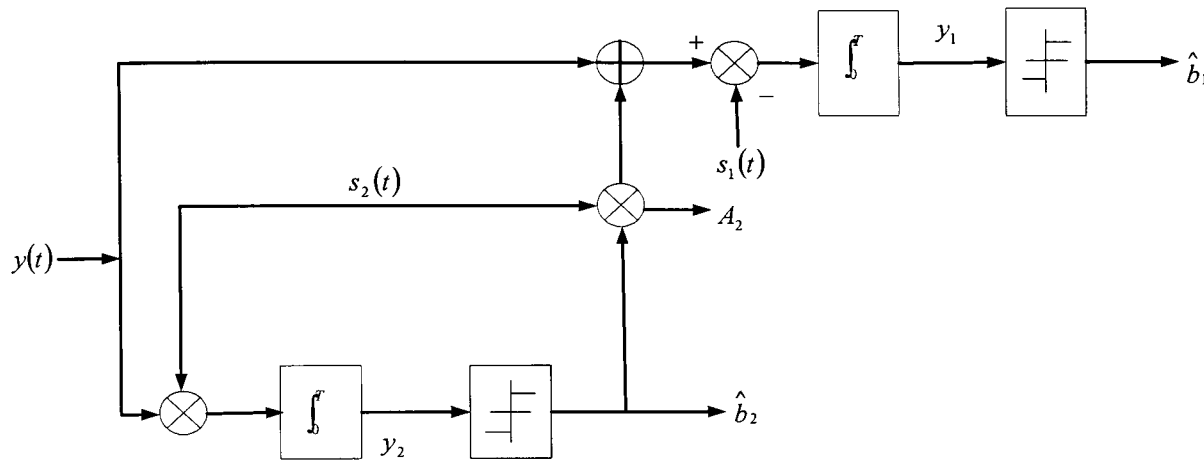

Figure 2.42 Schematic block diagram of decision-driven MUD for two synchronous users

Chapter 3 Intelligent System Design and Performance Analysis for MC-CDMA System

Partial transmitted sequence (PTS) scheme applied in the transmitter of MC-CDMA system is deemed as a promising candidate to efficiently reduce the PAPR value engendered by superimposing the large number of subcarriers without sequelae such as out-of-band frequency spectrum radiation, in-band distortion and complex implementation coding scheme. However, no technology is panacea. The drawback of PTS implementation is that its salient computational complexity increases exponentially with the number of sub-blocks. In MC-CDMA system, the extra information about sub-block's partition and phase factors allocated for sub-blocks in conjugation of the spreading sequences for all users can be provided to receiver as side information by the users via some control channels. Therefore, the focus of the issue becomes how to reduce the computational complexity in the transmitter while keeping an ideal near-optimum solution. Additionally, as aforementioned, the MAI in the receiver will dominantly deteriorate the accurate detection performance with a large SNR in MC-CDMA system. Optimum MUD was proposed to resolve the MAI in practice, but the considerable computational complexity is also the primary obstacle. Therefore, coherently reducing the large computational complexity for both PAPR reduction at transmitter and optimum MUD at receiver for MC-CDMA system would be our research emphasis. Genetic algorithm (GA) [97] is an intelligent search mechanism derived from the principles of genetics and natural selection. In this

Chapter, we first propose a novel intelligent system architecture based on a unified GA to reduce dramatically the computational complexity of both issues. Then we derive an analytical BER performance for the proposed MC-CDMA system. After that, we carry on a detailed performance analysis for the two sub-components of the system: PAPR reduction and MUD. Based on our analysis, in the next two Chapters, we will present in detail the two novel intelligent genetic algorithms (MDGAs) for both issues.

3.1 Intelligent System Design for MC-CDMA

Theoretically, applying PTS scheme and optimum MUD at the transmitter and the receiver of an MC-CDMA system can reduce the impediments from PAPR and MAI, respectively. However, they can not be used in practice due to their common inherent drawbacks, which are the large computational complexity increasing exponentially with the number of sub-blocks and users in the cell, respectively. How to reduce the large amount of computational complexity while maintaining the optimum performance as much as possible becomes the key issue for emerging MC-CDMA system. Our proposed novel intelligent GA namely Minimum Distance Genetic Algorithm (MDGA) can efficiently address this intractable issue. In this section, conventional GA is first reviewed and then followed by the system design of MDGA assisted MC-CDMA and the theoretical analysis.

3.1.1 Genetic Algorithm

In GA, the evolution is carried on under specified selection rules to a state that maximizes the "fitness" (or minimizes the cost function) for all individuals of population in each generation. The method was initially proposed by John Holland (1975) and then popularized by one of his students, David Goldberg, who was able to solve a difficult problem involving the control of gas-pipeline transmission (Goldberg, 1989) [98]. Recently, GA is deemed as an effective tool to cope with multi-objective combinatory optimization problem. GA is an iterative procedure maintaining a constant-size population of candidate solutions during each iteration step, namely a generation. The objective of GA is to reduce the large amount of computational complexity through promptly locating the global optimum. The mechanism of GA mimics biological evolution by iteratively forming and evaluating new generation in order to blaze a fast trail in searching space from random beginning to global optimum. Some benefits of GA applied in multi-objective combinatory optimization problem include:

1. Application to the optimization with continuous or discrete variables.
2. Transparency to the derivative information.
3. Simultaneous operation for a wide sampling from the cost surface.
4. Ability to handle a large number of variables.
5. Well suited for parallel computing.
6. Coping with extremely complex cost surfaces as well as the ability to avoid being stuck at a local optimum.

7. Multiple optimum solutions.
8. Ability to optimize the encoded variables.
9. Application to various types of the data (e.g., numerical data, experimental data, or analytical functions).

Unfortunately, GA can not work efficiently in some situations such as convex analytical functions with only a few variables or large population processed in a serial computing. As mentioned in [98], GA shines when the epitasis (a biological term for gene interaction and interpreted as the variable interaction here) is medium to high. Additionally, apart from the consideration of the benign environment to which GA applied, the trade-off between the convergence rate and the convergence region is the most important metric to measure the performance of GA. Our proposed novel GA would adaptively adjust this trade-off so as to obtain the optimum performance.

In order to achieve best performance of GA, the following parameters need to be investigated:

1. Population matrix: Each row in population matrix is termed as "chromosome" or "gene". The number of the chromosomes (the length of the column) in the matrix is defined as the population size which is kept constant along with each generation. Initial population matrix is generated randomly.
2. Variable encoding and decoding: Converting continuous values into binary representation, and vice versa.

3. Cost function: Also termed as the objective function or fitness function. The cost could be interpreted as a mathematical result, an experimental result or a game verdict. Fitness implies a maximization problem, while cost is normally referred to as the minimization. However, the maximization problem can be easily converted as a minimization problem by looking for the minus of fitness. Thus, they are equivalent. The cost is measured based on each chromosome in the population matrix of each generation.
4. Natural selection: Based on some rules, to mimic the natural biological selection process. A fraction of the fittest chromosomes are survived and selected to continue mating, where the chromosomes with highest cost are discarded.
5. Selection process: To distinguish from 4, the selection process is also termed as pairing or matching. Two chromosomes are selected from the mating pool which is composed by all survivors from natural selection to produce two new offspring. Pairing takes place in the mating pool until the positions of all discarded chromosomes are replaced by new born offspring. Some common selection rules include pairing from top to bottom, random pairing, weighted random pairing and tournament selection etc.
6. Crossover: The most important re-combination operator in GA is crossover. Crossover also namely mating is the creation of offspring from the parents selected in the pairing process, which is normally conducted by single-point crossover, two-point crossover or uniform crossover. Under the crossover

operator, two chromosomes exchange portions of their genes to produce two new offspring. For example, if the chromosomes are represented by binary strings, crossover can be implemented by choosing a point at random, called the crossover point, and exchanging the segments based on this point. Let X_1 = 100:01010 and X_2= 010:10100, and suppose that the crossover point has been chosen as indicated. The resulting new offspring would be Y_1 = 100:10100 and Y_2 = 010:01010. The crossover rate controls the percentage of population chosen for mating. The higher the crossover rate, the more frequently new offspring are introduced into the population. Hence, if the crossover rate is too high, high-performance chromosomes will be discarded very quickly. Whereas if the crossover rate is too low, the search may stagnate due to the low exploration rate.

7. Mutation: Random mutation alters a certain percentage of the bits of designated chromosomes in the matrix. The mutation creates the searching diversity which can avoid being stranded in local minimum. Generally, it has two patterns, constant mutation rate and dynamic mutation rate.
8. Elitism: Elitism strategy is used to keep attributes of the individuals having the highest fitness values during the course of evolution. Elitism is invoked to counterpart the excessive randomness engendered by mutation. Since the mutation normally after crossover would obliterate the best attributes provided by the chromosomes with fittest values, especially when the fittest chromosome is already optimum solution.

9. Incest protection: In order to prevent same chromosome pair from coexisting in the mating pool, which would debase the efficiency of the GA, two or more same chromosomes happened in the mating pool is termed as incest. If the incest happens, we can simply discard one chromosome from mating pool or substitute it by the fittest chromosome picked from discarded group in the population.
10. Convergence: The ending condition of the GA. The number of generations of the evolution depends on whether an acceptable solution is reached or the pre-defined number of iterations is exceeded. The GA should be stopped at the point when all the chromosomes and corresponding costs become the same if there are no further mutations.

By illuminating the primary components of GA, the process of GA is schematized in Figure 3.1.

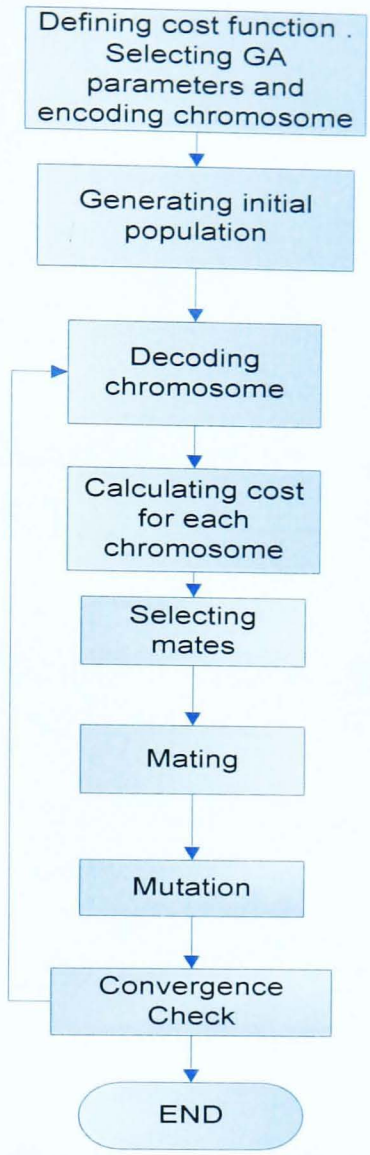

Figure 3.1 Flow chart of Genetic Algorithm

3.1.2 Our System Design

In this section, we show a new system design of MC-CDMA combined with our proposed MDGA blocks. The block diagram of the transmitter side is shown in Figure 3.2, and the receiver side is shown in Figure 3.3.

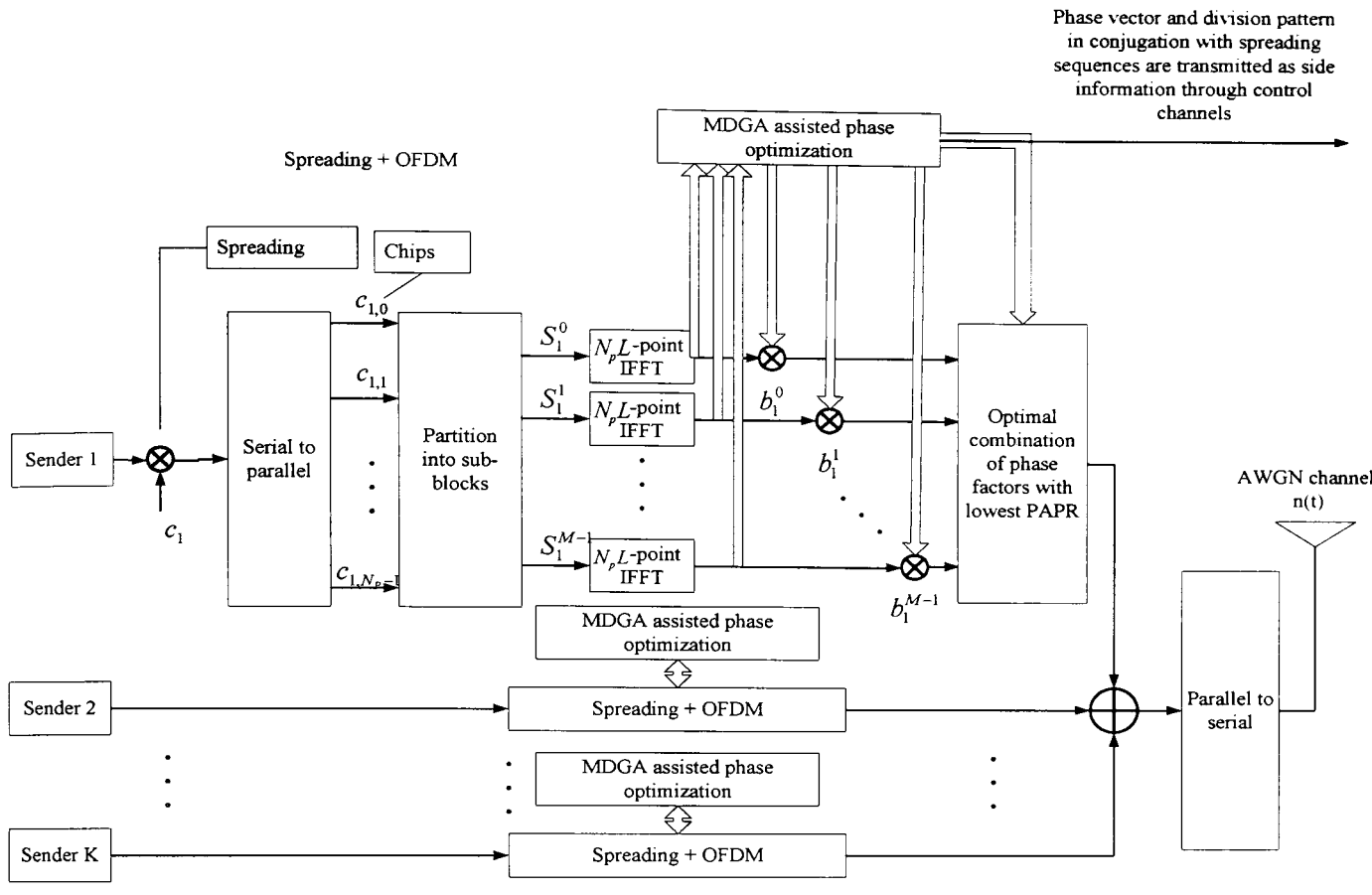

Figure 3.2 The block diagram of PTS based MC-CDMA transmitter assisted by MDGA

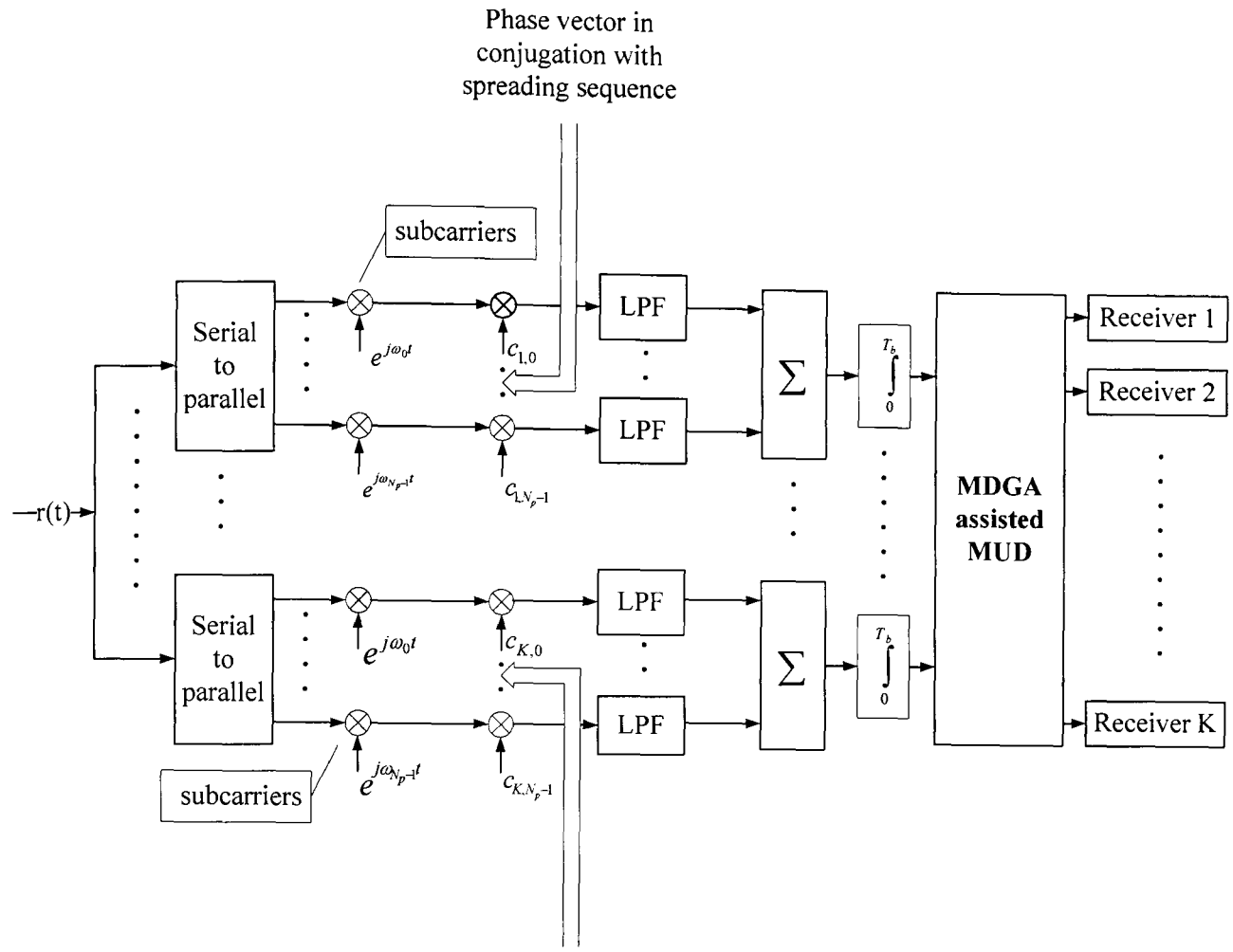

Figure 3.3 The block diagram of the MUD based MC-CDMA receiver manipulated by MDGA

In practice, it is worth to note the chip sequences for despreading acquired from control channel are not any more the original user's chip sequence in the MC-CDMA receiver (Figure 3.3). They are also rotated by associated phase factors, which corresponding modification is conducted in the transmitter side, and transmitted through control channels as side information. Therefore, the correlation matrix $\Re$ defined in Equation (2.45) also needs to be adjusted accordingly, which represents the cross-correlation property between new rotated chip sequences. However, for the

simplicity of the research, we assume the chip sequence keep constant with the original version, which means the effect of side information is ignored at the MC-CDMA receiver.

3.2 Analytical System BER Performance Analysis

3.2.1 Problem Statement and Assumptions

We consider a synchronous MC-CDMA transmitter model as shown in Figure 3.2. Instead of applying spreading sequences in time domain, we apply them in the frequency domain through serial-to-parallel conversion, mapping each chip of a sequence to an individual OFDM subcarrier. Hence, each OFDM subcarrier has identical data rate of the original information and OFDM modulation compensates the increased chip rate due to applying spreading sequences in time domain. After a sequence of chips spreading in frequency domain of each user information data, each individual chip from each different user is imposed on a same subcarrier, which means each subcarrier transmits a bunch of chips from each user simultaneously.

Figure 3.3 shows a simplified receiver schematic of MC-CDMA system followed by MDGA based MUD. The received signal is firstly de-modulated and then despread in the frequency domain. The output is passed through a bunch of low-pass-filters (LPFs) and then summed parallel in order to make a decision by an MF.

Before analyzing the system performance in more detail, we assume the following conditions:

- Uplink transmission channel.
- BPSK modulated information signal.
- Similar to Section 2.1.5 C, perfect power control is assumed for all the users and the power of transmit signal is the same for all the users.
- The carrier-modulated signal is transmitted through an AWGN channel.
- All the users are transmitting signals to a single base station within one cell, which means no cross-cell interference in the system.
- Similar to Section 2.1.5 C, Gold-sequences are chosen as spreading codes.
- All the users are time-synchronized.
- The number of chips is assumed to be equivalent to the number of subcarriers.

The following notations are used:

- The total number of senders and receivers in the system is 2K where half are senders and another half are the corresponding receivers. The k^{th} receiver is expected to receive the data signal from the k^{th} sender.
- N_P: Number of subcarriers, also the number of chips in our assumed case, which means a fraction of the symbol corresponding to a chip of the spreading code is transmitted through a different subcarrier.
- P denotes the average power of the signal.
- $d_k(t)$: Transmitted binary bit of the k^{th} sender, {+1, -1}.

- $c_{k,n}$: Frequency-domain representation of the k^{th} sender's spreading sequence over the n^{th} subcarrier. In PTS scheme, the binary phase-rotated chip of the k^{th} sender over the n^{th} subcarrier is denoted as $\underline{c}_{k,n}$.
- $c_k = \{c_{k,0}, c_{k,1}, \ldots, c_{k,Np-1}\}^T$: Frequency-domain representation of the k^{th} sender's spreading code. In the thesis, all chips of the spreading sequence to be transmitted are assumed as ±1.
- T_b: Binary bit duration.
- T_c: Chip duration.
- $\omega_n = 2\pi f_n$, where f_n (n=0, …, N-1) are the subcarrier frequencies and $f_n = f_0 + n\Delta f$,where the spacing between two adjacent subcarrers is defined as $\Delta f = 1/T_b = 1/N_P T_c$.
- W_b (Hz): null-to-null bandwidth of the binary baseband data signal defined as $1/T_b$.
- W_c (Hz): null-to-null bandwidth of each subcarrier signal given by $1/T_b$.
- SG: Spectral gain, which is defined as the ratio between the bandwidth required by the MC scheme without overlapping and the actual bandwidth of the corresponding MC scheme.
- Random bipolar sequences ±1 are generated for information signal with the amplitude of 1. The chips in spreading sequences are also mapped to bipolar ±1 sequences with the amplitude of 1.

3.2.2 BER Analysis for MC-CDMA

Similar to Section 2.1.5 C, the desired signal to be detected at receiver 1 is the one from sender 1 and all other (K-1) senders are interferers which cause MAI. As shown in Figure 3.2, the MC-CDMA transmitter spreads the original data stream over N_P subcarriers using a given spreading code of $c_k(t) = \{c_{k,0}, c_{k,1}, \ldots, c_{k,Np-1}\}$ in the frequency-domain. The chip rate on each of the N_P subcarriers becomes the same as the input data rate. Therefore, compared to chip rate in DS-CDMA, the chip rate in MC-CDMA is N_P times reduced, and hence the multipath fading effect is significantly mitigated. Regarding Figure 3.2, the *k*th MC-CDMA user's transmitted signal can be expressed as:

$$s_k(t) = \sqrt{\frac{2P}{N_p}} \sum_{n=0}^{N_P-1} d_k(t) c_{k,n} \cos(2\pi f_n t) \tag{3.1}$$

In our MC-CDMA system model, the subcarrier frequencies are chosen to be orthogonal to each other, which is given by

$$\int_0^{T_b} \cos(2\pi f_i + \phi_i) \cdot \cos(2\pi f_j + \phi_j) dt = 0, \ for\ i \neq j. \tag{3.2}$$

The spectrum of the transmitted MC-CDMA signal is shown in Figure 2.22. If 50% overlapping of each subcarrier frequency bandwidth is assumed, then the spectral gain of the MC-CDMA system is given by:

$$SG = \frac{N_P(2/T_b)}{(N_P+1)(1/T_b)} \tag{3.3}$$

which approximates two when N_P goes infinity.

According to the assumption of the bit-synchronous uplink MC-CDMA system, the received signal could be expressed as

$$r(t) = \sum_{k=1}^{K} s_k(t) + n(t)$$

$$= \sqrt{\frac{2P}{N_P}} \sum_{k=1}^{K} \sum_{n=0}^{N_P-1} d_k(t) \underline{c}_{k,n} \cos(2\pi f_n t) + n(t) \tag{3.4}$$

At the receiver side, the received signal is firstly demodulated from each subcarrier frequency and then despread in the frequency domain. For example when receiver 1 is considered, the decision variable Z_1 can be expressed as

$$Z_1 = \int_0^{T_b} \sum_{n=0}^{N_P-1} r(t) \cos(2\pi f_n t) \underline{c}_{1,n} dt$$

$$= \int_0^{T_b} \sum_{n=0}^{N_P-1} \left(\sqrt{\frac{2P}{N_P}} \sum_{k=1}^{K} \sum_{m=0}^{N_P-1} d_k(t) \underline{c}_{k,n} \cos(2\pi f_m t) + n(t) \right) \cos(2\pi f_n t) \underline{c}_{1,n} dt$$

$$= \int_0^{T_b} \left(\sqrt{\frac{2P}{N_P}} \sum_{n=0}^{N_P-1} \sum_{k=1}^{K} \sum_{m=0}^{N_P-1} d_k(t) \underline{c}_{k,n} \underline{c}_{1,n} \cos(2\pi f_n t) \cos(2\pi f_m t) + \sum_{n=0}^{N_P-1} n(t) \cos(2\pi f_n t) \underline{c}_{1,n} \right) dt$$

$$= \int_0^{T_b} \left(\sqrt{\frac{2P}{N_P}} \sum_{n=0}^{N_P-1} \sum_{m=0}^{N_P-1} d_1(t) \underline{c}_{1,n}^2 \cos(2\pi f_n t) \cos(2\pi f_m t) + \sqrt{\frac{2P}{N_P}} \sum_{k=2}^{K} \sum_{n=0}^{N_P-1} \sum_{m=0}^{N_P-1} d_k(t) \underline{c}_{k,n} \underline{c}_{1,n} \cos(2\pi f_n t) \cos(2\pi f_{ni} t) \right.$$

$$\left. + \sum_{n=0}^{N_P-1} n(t) \cos(2\pi f_n t) \underline{c}_{1,n} \right) dt \tag{3.5}$$

Considering that $d_k(t) = \pm 1$, $\underline{c}_{1,n}^2 = 1$ and Equation (3.2), Equation (3.5) can be rewritten as:

$$Z_1 = \int_0^{T_B} \left(\pm \sqrt{\frac{2P}{N_P}} \sum_{n=0}^{N_P-1} \cos^2(2\pi f_n t) \pm \sqrt{\frac{2P}{N_P}} \sum_{k=2}^{K} \sum_{n=0}^{N_P-1} \underline{c}_{k,n} \underline{c}_{1,n} \cos^2(2\pi f_n t) + \sum_{n=0}^{N_P-1} n(t) \cos(2\pi f_n t) \underline{c}_{1,n} \right) dt \tag{3.6}$$

Due to transition of the trigonometric function $\cos^2(2\pi f_n t) = \frac{1 + \cos 4\pi f_n t}{2}$ and the integration of the high frequency component tends to be zero as

$$\int_0^{T_b} \cos 4\pi f_n t \approx 0 \tag{3.7}$$

Therefore, Equation (3.6) can be represented as

$$Z_1 = \int_0^{T_b} \left(\pm \frac{N_P}{2} \sqrt{\frac{2P}{N_P}} \pm \frac{N_P}{2} \sqrt{\frac{2P}{N_P}} \sum_{k=2}^{K} \sum_{n=0}^{N_P-1} \underline{c}_{k,n} \underline{c}_{1,n} + \sum_{n=0}^{N_P-1} n(t) \cos(2\pi f_n t) \underline{c}_{1,n} \right) dt$$

$$= D_1 + I_1 + N_1 \tag{3.8}$$

where D_1, I_1, N_1 denote signal, interference and noise and they are calculated as follow:

$$D_1 = \int_0^{T_b} \left(\pm \frac{N_P}{2} \sqrt{\frac{2P}{N_P}} \right) dt = \pm \frac{N_P T_b}{2} \sqrt{\frac{2P}{N_P}} \tag{3.9}$$

$$S_{1power} = D_1^2 = \frac{N_P T_b^2 P}{2} \tag{3.10}$$

where S_{1power} is the power of the signal.

$$I_1 = \int_0^{T_b} \left(\pm \frac{N_P}{2} \sqrt{\frac{2P}{N_P}} \sum_{k=2}^{K} \underline{c}_k \underline{c}_1 \right) dt \tag{3.11}$$

Without loss of generality, the summation of chip product $\sum_{n=0}^{N_P-1} \underline{c}_{k,n} \underline{c}_{1,n}$ was replaced by phase-rotated spreading chip sequence product $\underline{c}_k \underline{c}_1$ and we also define $\underline{R}_{k,1}$ as the normalized cross-correlation product of the phase-rotated spreading chip sequence between the kth sender and the 1st sender, which is given by

$$\underline{R}_{k,1} T_b = \int_0^{T_b} \underline{c}_k \underline{c}_1 \ . \tag{3.12}$$

Accordingly, the interference in Equation (3.11) can be formulated as

$$I_1 = \pm \frac{N_P T_b}{2} \sqrt{\frac{2P}{N_P}} \sum_{k=2}^{K} \underline{R}_{k,1} \ . \tag{3.18}$$

Hence, the power of the interference is calculated as

$$M_1 = \sum_{k=2}^{K} \frac{N_P T_b^2 \underline{R}_{k,1}^2 P}{2} \tag{3.19}$$

The noise component in Equation (3.8) is given by

$$N_1 = \int_0^{T_b} \left(n(t) \sum_{n=0}^{N_P-1} \underline{c}_{1,n} \cos(2\pi f_n t) \right) dt \tag{3.20}$$

since $n(t)$ is the AWGN with zero-mean and constant variance $\sigma^2 = \frac{N_0}{2}$ [37], so the average power of noise term, M_1 is given by

$$\begin{aligned}
W_1 = E(N_1^2) &= E\left(\int_0^{T_b} \left(n(t) \sum_{n=0}^{N_P-1} \underline{c}_{1,n} \cos(2\pi f_n t) \right) dt \int_0^{T_b} \left(n(\tau) \sum_{m=0}^{N_P-1} \underline{c}_{1,m} \cos(2\pi f_m t) \right) d\tau \right) \\
&= \int_0^{T_b} \int_0^{T_b} E(n(t)n(\tau)) \sum_{n=0}^{N_P-1} \underline{c}_{1,n} \cos(2\pi f_n t) \sum_{m=0}^{N_P-1} \underline{c}_{1,m} \cos(2\pi f_m t) dt d\tau \\
&= \int_0^{T_b} \int_0^{T_b} \frac{N_0}{2} \delta(t-\tau) \sum_{n=0}^{N_P-1} \cos^2(2\pi f_n t) dt d\tau \\
&= \frac{1}{2} \int_0^{T_b} \int_0^{T_b} \frac{N_0}{2} \delta(t-\tau) \sum_{n=0}^{N_P-1} (\cos(4\pi f_n t) + 1) dt d\tau \\
&= \frac{N_0 N_P}{4} \int_0^{T_b} \int_0^{T_b} \delta(t-\tau) dt d\tau \\
&= \frac{N_0 N_P T_b}{4}
\end{aligned} \tag{3.21}$$

where $E(N_1^2)$ denotes the expectation of N_1^2, and $E(n(t)n(\tau))$ is the auto-correlation of $n(t)$ as given in Equation (2.26). Thus, the analytical BER performance for user 1 in the MC-CDMA system can be obtained:

$$BER_{1,MC} = Q\left(\sqrt{\frac{S_{1\,power}}{W_1 + M_1}} \right)$$

$$= Q\left(\sqrt{\frac{\frac{N_P T_b^2 P}{2}}{\frac{N_0 N_P T_b}{4} + \frac{1}{2} \sum_{k=2}^{K} N_P T_b^2 \underline{R}_{k,1}^2 P}} \right)$$

$$= Q\left(\sqrt{\left(\frac{N_0}{2PT_b} + \sum_{k=2}^{K} \underline{R}_{k,1}^2\right)^{-1}}\right)$$

$$= Q\left(\left(\left(\frac{2E_b}{N_0}\right)^{-1} + \sum_{k=2}^{K} \underline{R}_{k,1}^2\right)^{-\frac{1}{2}}\right)$$

Following the same idea, for any user j in the system, the general BER performance for MC-CDMA can be obtained by:

$$BER_{MC} = Q\left(\left(\left(\frac{2E_b}{N_0}\right)^{-1} + \sum_{k=1,k\neq j}^{K} \underline{R}_{k,j}^2\right)^{-\frac{1}{2}}\right) \tag{3.22}$$

Therefore, from Equation (3.22), we can conclude that if without PTS scheme applied in MC-CDMA transmitter, the theoretical BER performance of synchronized MC-CDMA system is identical to that of synchronized DS-CDMA (see Equation (2.29)) while the signal is transmitted through AWGN channel.

The analytical BER performance of our proposed system is given in Figure 3.4. Note here we adopt the new chip sequences generated after the PTS scheme to estimate the MAI impact and original chip sequences are generated from Gold-sequence for 17 users. In Figure 3.4, the BER performance of MC-CDMA is significantly deteriorated by MAI as Eb/N_0 (SNR per bit) increases. Therefore, when SNR is high, the MAI is a dominant factor degrading the system performance in MC-CDMA.

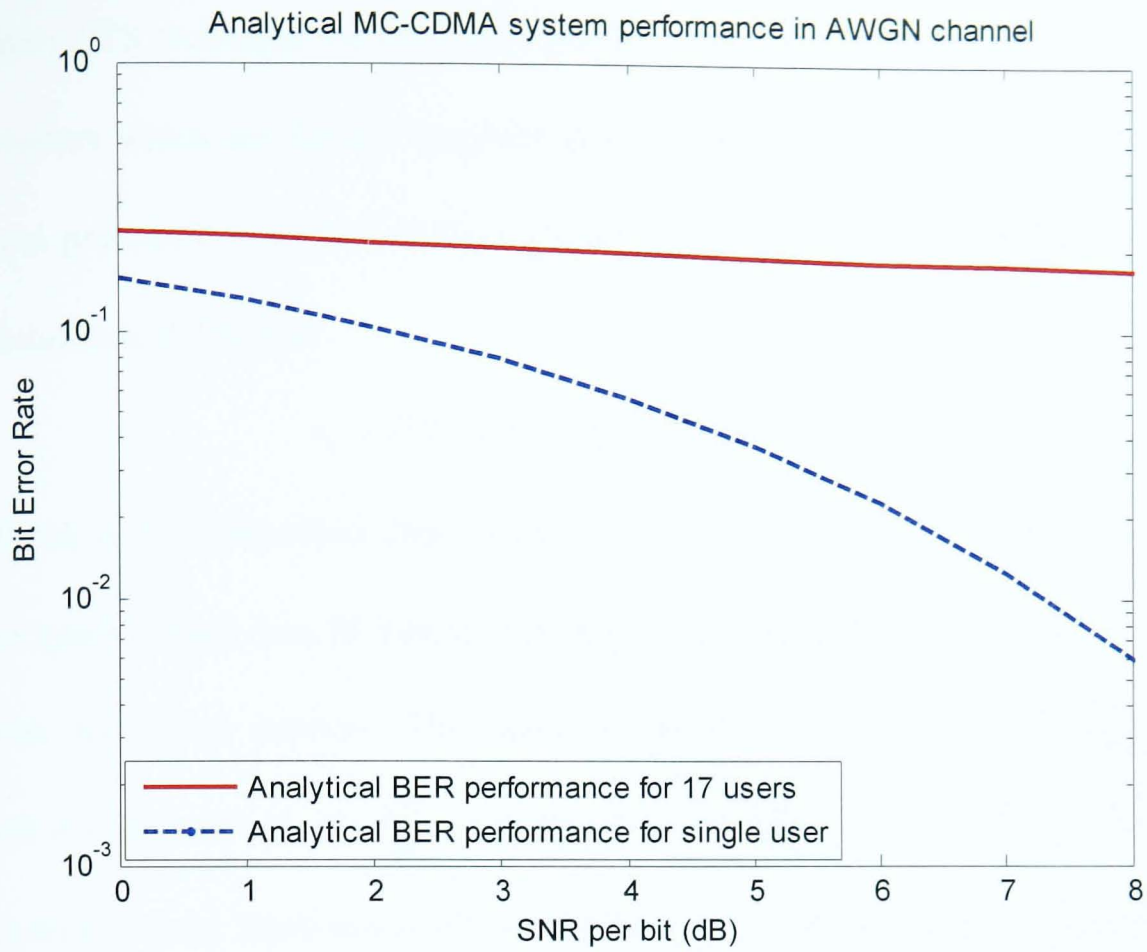

Figure 3.4 Analytical MC-CDMA system performance in AWGN channel using Gold-sequence as the spreading sequence and the PTS scheme in the transmitter

3.3 PTS Technique assisted PAPR Reduction in MC-CDMA System

In a transmitter of an MC-CDMA system, an input data block of N_P modulated samples (one OFDM modulated symbol) is partitioned into a number of disjointed sub-blocks after parallel-to-serial conversion. The subcarriers grouped in each sub-block are implemented by N_p points IFFT using zero interpolation and then weighted by a phase factor followed by superimposition. The phase factors for all sub-blocks are selected when the PAPR of the new combined and reconstructed signal is minimal. Figure 2.38 shows the block diagram of the PTS technique. In the

ordinary PTS technique the input data block is partitioned into disjointed sub-blocks or clusters which are further weighted and combined to minimize the PAPR. As a normal procedure in an MC-CDMA system without PTS, the data block after IFFT modulation is defined as

$$s_k = IFFT_N(S_k) = [s_k(0), s_k(1), ..., s_k(N_P - 1)] \tag{3.23}$$

where S_k is the transmitted chip vector of the k^{th} user. The PTS scheme divides the input symbol block into M disjoint sub-blocks and multiplies them by a set of phase factors for phase rotation. The value of phase factors is given by $b_w = e^{jw\theta}$, where $w = 0,1,...,W-1$, $\theta = \frac{2\pi}{W}$, and W is the number of phase factors (a random integer) in the set. Each sub-block is transformed into partial transmit sequence using IFFT and then rotated by its allocated phase factor. Therefore the crucial objective is to optimally combine the sub-blocks and corresponding phase factors in order to transmit the superimposed symbol block with the lowest PAPR. Furthermore, in order to precisely estimate the PAPR of the true continuous modulated chip signal in MC-CDMA system, the chip sequence S_k is oversampled by means of padding $(L-1)\times N_p$ zeros, where L is defined as an oversampling factor [99]. Accordingly, LN_p-point IFFT is needed for each sub-block with $(L-1)N_p$ zero-padding. It is shown that in [87] oversampling factor equal to or larger than 4 is sufficient to deal with the case. In this thesis, the oversampling factor L is chosen 4. Therefore, by using oversampling, the process of PTS is formulated as:

$$S_k = \sum_{m=0}^{M-1} S_k^m , \tag{3.24}$$

$$\underline{s_k} = \sum_{m=0}^{M-1} \left(IFFT_{LN_p} \left(S_k^m \right) \cdot b_w \right) \tag{3.25}$$

where S_k^m denotes the m^{th} sub-block and $\underline{s_k}$ represents the superimposed symbol block. Due to the linearity of discrete IFFT, we have

$$IFFT_{LN_p} \left(S_k \right) = \sum_{m=0}^{M-1} IFFT_{LN_p} \left(S_k^m \right). \tag{3.26}$$

Therefore, jointly selecting the optimum combination of the W phase factors in a phase vector whose length equals to the number of disjointed sub-blocks would be the key focus in the PTS technology. As mentioned earlier, one significant drawback of the PTS based PAPR reduction scheme is the large computational complexity of exhaustive iterative search, which is defined as W^M.

Another factor that may affect the PTS based PAPR reduction performance is the sub-block partitioning pattern, which is the method of dividing the subcarriers into multiple disjointed sub-blocks. There are three categories of sub-block partitioning: adjacent, interleaved and pseudo-random partitioning. Among them, pseudo-random partitioning has been found to be the best choice [100]. The PTS technique works with an arbitrary number of subcarriers and any modulation scheme. Without loss of generality, in the following analysis, we carry out research work based on disjoint subcarrier partitioning pattern for the simplicity of the system deployment.

3.3.1 Theoretical Analysis of PAPR Problem

According to [42], the PAPR issue can be mathematically expressed as

$$PAPR(s_k(t)) = 10\log_{10}\frac{\max\limits_{0\le t\le NT_c}|s_k(t)|^2}{E[s_k(t)^2]}(\text{dB}) \tag{3.27}$$

where $E[\cdot]$ denotes the expectation and $s_k(t)$ is the analog signal denoted in Equation (3.1). Practically, the analog signal is always sampled to become digital signal in order to efficiently simplify and analyze the implementation. Therefore, we can rewrite the Equation (3.1) and Equation (3.27) as

$$s_k \overset{\Delta}{=} s_k(vT_c) = \sqrt{\frac{P}{N_P}}\sum_{n=0}^{N_p-1} S_k e^{j\omega_n vT_c}, \tag{3.28}$$

and

$$PAPR(s_k) \overset{\Delta}{=} PAPR(s_k(vT_c)) = 10\log_{10}\frac{\max|s_k|^2}{E[s_k{}^2]} \tag{3.29}$$

where v=0,1,…,N_p-1. Equation (3.28) can be normalized as

$$s_k \overset{\Delta}{=} s_k(v) = \sqrt{\frac{P}{N_P}}\sum_{n=0}^{N_p-1} S_k e^{j\omega_n v} \tag{3.30}$$

$$= IFFT_{N_p}(S_k) = \left[s_k(0), s_k(1), \ldots, s_k(N_P-1)\right] \tag{3.31}$$

As the number of subcarriers increases, the hostile effect of high PAPR becomes severe in an MC-CDMA system. This may cause spectrum re-growth, in-band distortion and impairment of detection efficiency when signal is passed through nonlinear devices used for system signal processing. Additionally, the large PAPR can generate performance degradation unless the power amplifier has large power back-off and the power amplifier cost increases with its back-off value. Hence, reducing PAPR is a crucial research topic for the next-generation MC-CDMA based broadband wireless systems. The complementary cumulative distribution function (CCDF) or cumulative distribution function (CDF) are two common criteria to

measure how high the PAPR values are. The CCDF represents the probability of PAPR beyond a given threshold, which is defined as

$$\begin{aligned} CCDF &= 1 - CDF \\ &= \Pr\left(PAPR > PAPR_0\right) \end{aligned} \tag{3.32}$$

where $\Pr(\bullet)$ and PAPR_0 are symbol of probability and the given PAPR threshold, respectively. According to the central limit theorem [37], the real and imaginary values of $s_k(t)$ in Equation (3.28) become Gaussian distributed and MC-CDMA signal therefore has Rayleigh distribution with zero mean and a variance of P times the variance of one complex sinusoid. The power distribution of each MC-CDMA sample becomes a central chi-square distribution with 2 degrees of freedom and zero mean, with a cumulative distribution given by

$$CDF\left(PAPR_0\right) = \int_0^{PAPR_0} \frac{1}{2 \cdot \sigma^2} e^{-\frac{\mu}{2\sigma^2}} d\mu \tag{3.33}$$

where σ^2 is the variance of MC-CDMA signal $s_k(t)$. Provided the N_p MC-CDMA samples are mutually uncorrelated, which is the case of non-oversampling, the CDF of MC-CDMA symbol can be derived as

$$\begin{aligned} CDF\left(PAPR\left(s_k(t)\right) \le PAPR_0\right) &= \Pr\left(PAPR \le PAPR_0\right) \\ &= CDF\left(PAPR_0\right)^{N_P} \\ &= \left(1 - \exp\left(-\frac{1}{2} \cdot \frac{PAPR_0}{\sigma^2}\right)\right)^{N_P} \end{aligned} \tag{3.34}$$

Combining Equations (3.32) and (3.34), the mathematical expression of CCDF for PAPR reduction in MC-CDMA is given as

$$CCDF = 1 - \left(1 - \exp\left(-\frac{1}{2} \cdot \frac{PAPR_0}{\sigma^2}\right)^{N_P}\right) \tag{3.35}$$

CCDF offers a quantitative measure of PAPR reduction. It is shown in Figure 3.5 that the analytical CCDF vs. PAPR performance for Single-Carrier CDMA (DS-CDMA) and MC-CDMA with different subcarriers, which illustrates the PAPR problem in an MC communication system is severer than an SC communication system.

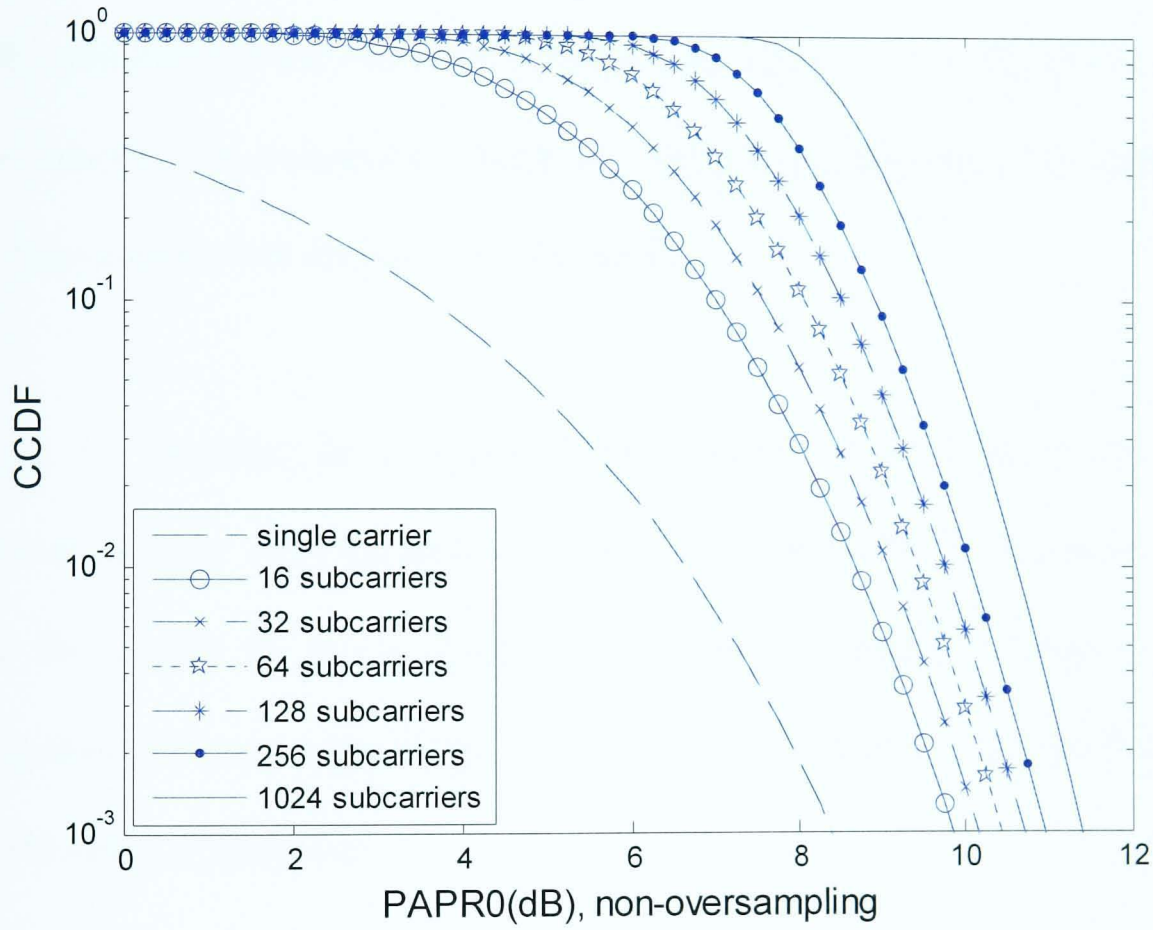

Figure 3.5 Analytical performance of PAPR vs. CCDF (non-oversampling) for Single-Carrier and MC-CDMA with subcarriers N_p=16, 32, 64, 128, 256, 1024 subcarriers

3.3.2 Iterative Search

As aforementioned, the computational complexity in ordinary PTS increases exponentially when the number of disjointed sub-blocks M and/or quantity of phase

factors W increase. Fortunately, as both W and/or M increase, the available searching space will be enlarged accordingly. Consequently, it will be more accurate to obtain the global minimum in a larger searching space and then PAPR reduction performance is further improved. Therefore, it is interesting to probe the nonlinear extent of the increment of the computational complexity along with two dimensions W and M, respectively, since it is assumed that there would be some saturated thresholds for both dimensions beyond which PAPR performance will not be dramatically improved. The observation is measured by CCDF, in which the saturated points are expected to be discovered for both dimensions, respectively.

Figure 3.6 illustrates the procedure of the iterative search, as mentioned in the previous sections. The computational complexity is determined by the phase factors and the number of the sub-blocks. Hence, we investigate the span of PAPR performance improvement through adjusting the phase factors W and the number of sub-blocks M, respectively.

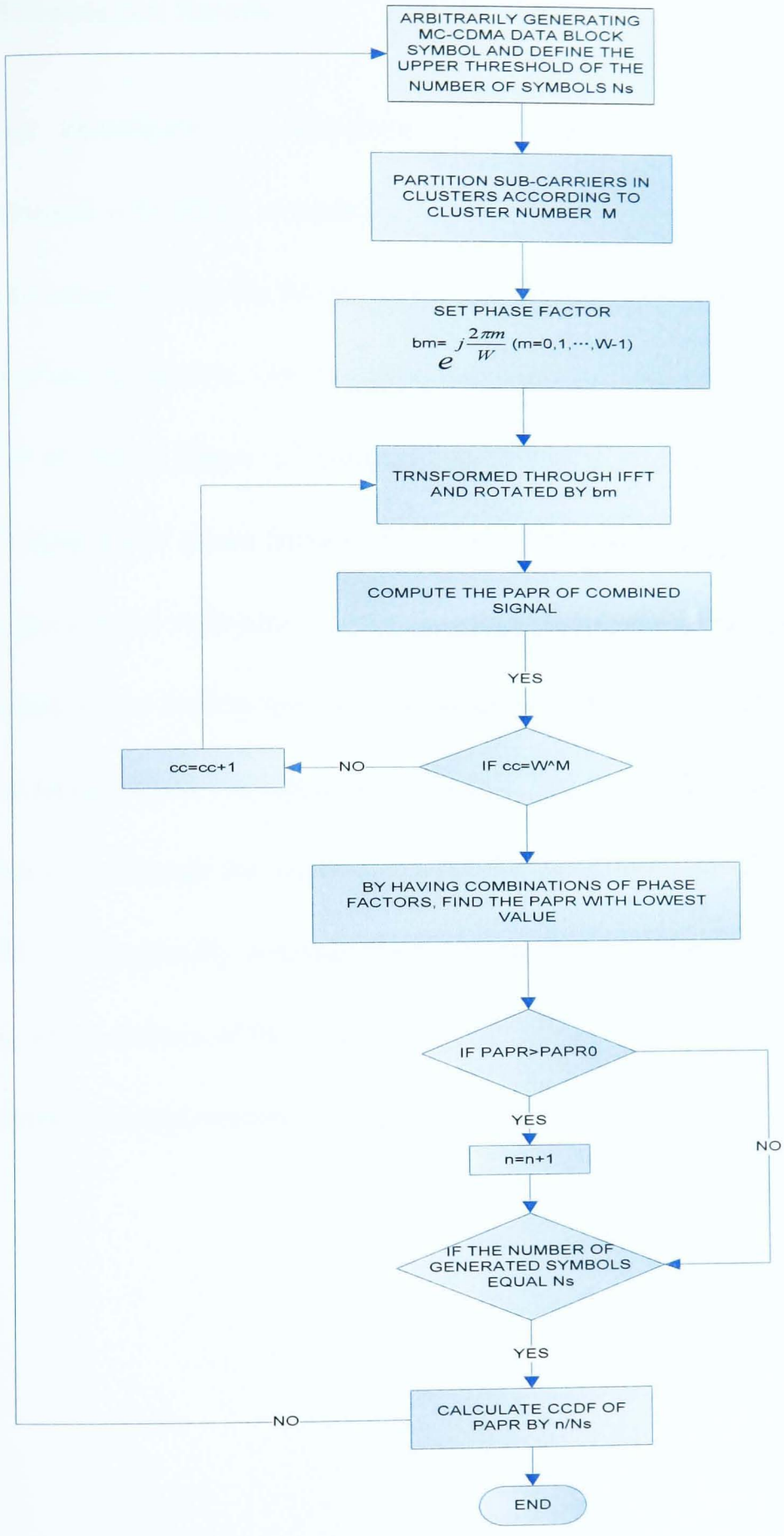

Figure 3.6 Flow chart of the iterative search PTS

3.3.3 Simulation Results

In our investigation, a simulator of 64-subcarriers MC-CDMA transmitter is constructed with BPSK modulation. Firstly, we choose the number of the clusters to be a constant. Hence, the 64 subcarrier are divided into 4 (M=4) clusters each having 16 (m=16) subcarriers. One thousand data symbols will be generated to calculate the CCDF of PAPR. Figure 3.7 compares the PAPR reduction performance based on the PTS using the W phase factors set {+1, -1} with the basic MC-CDMA without PTS. The green curve represents the reduced PAPR with the phase factors equal to 2 and the black curve depicts the basic MC-CDMA without PTS. Note that the number of phase factors set as 1 is actually equivalent to the basic MC-CDMA without PTS. It is salient that although the number of phase factors is increased slightly from 1 to 2, the PAPR is dramatically reduced. Based on the same probability of CCDF as 2×10^{-2}, using phase factors of two reduces the PAPR from 9dB to 6.5dB. Hence, the PAPR performance improvement is 9 - 6.5 = 2.5dB.

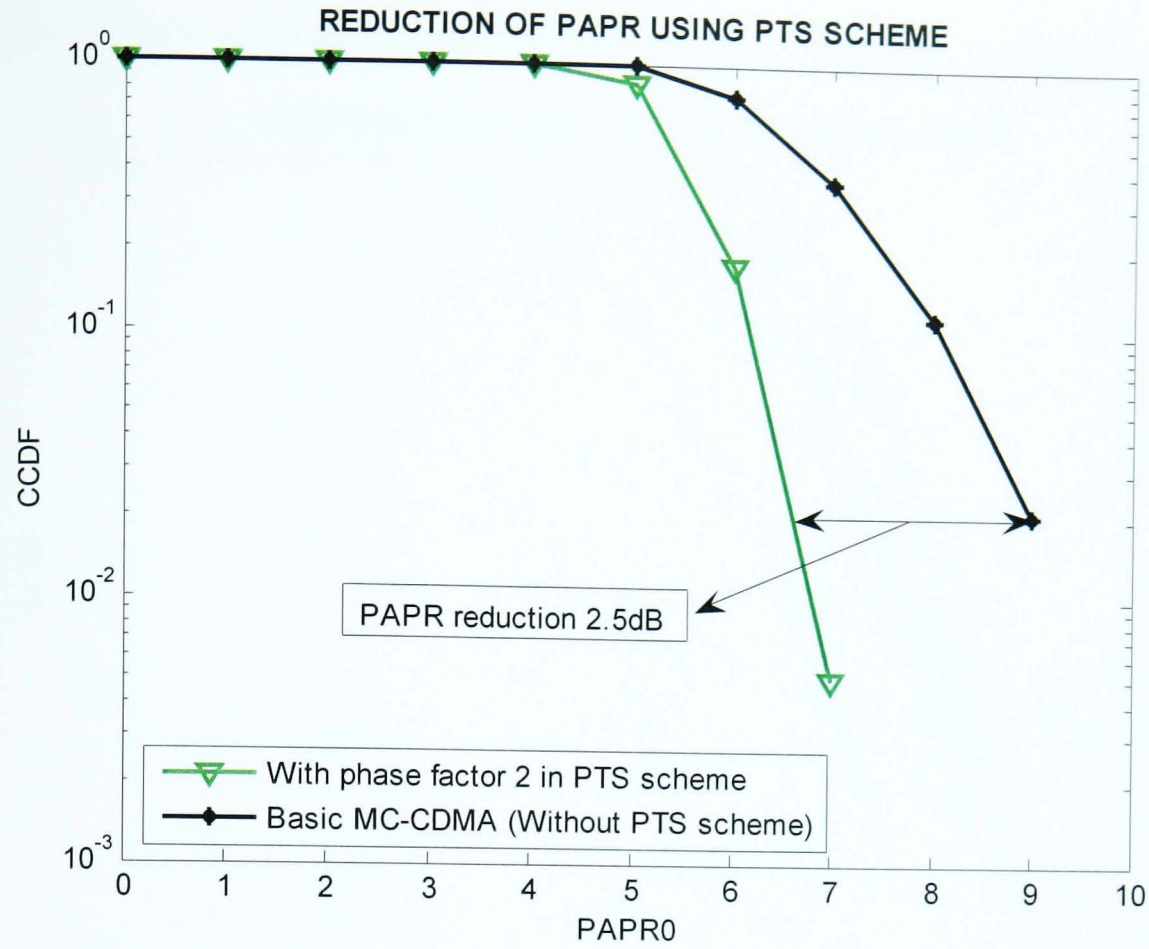

Figure 3.7 CCDF comparison of PAPR performance between the PTS assisted MC-CDMA and the basic MC-CDMA

Table 3.1 shows the values of probability that PAPR exceeds the given threshold PAPR0 for the basic MC-CDMA and the PTS-MC-CDMA when the number of phase factors is set as 2, respectively.

PAPR0	0-4	5	6	7	8	9	10-14
Prob(With PTS)	1	0.85	0.177	0.005	0	0	0
Prob(Unmodified)	1	0.982	0.758	0.366	0.114	0.021	0

TABLE 3.1 COMPARISON BETWEEN THE BASIC MC-CDMA AND THE PTS SCHEME

Figure 3.8 shows the original CCDF values vs. various numbers of subcarriers N_p for an MC-CDMA system without any PAPR reduction schemes. Table 3.2 records the

details of CCDF vs. discrete PAPR0 values for various numbers of subcarriers.

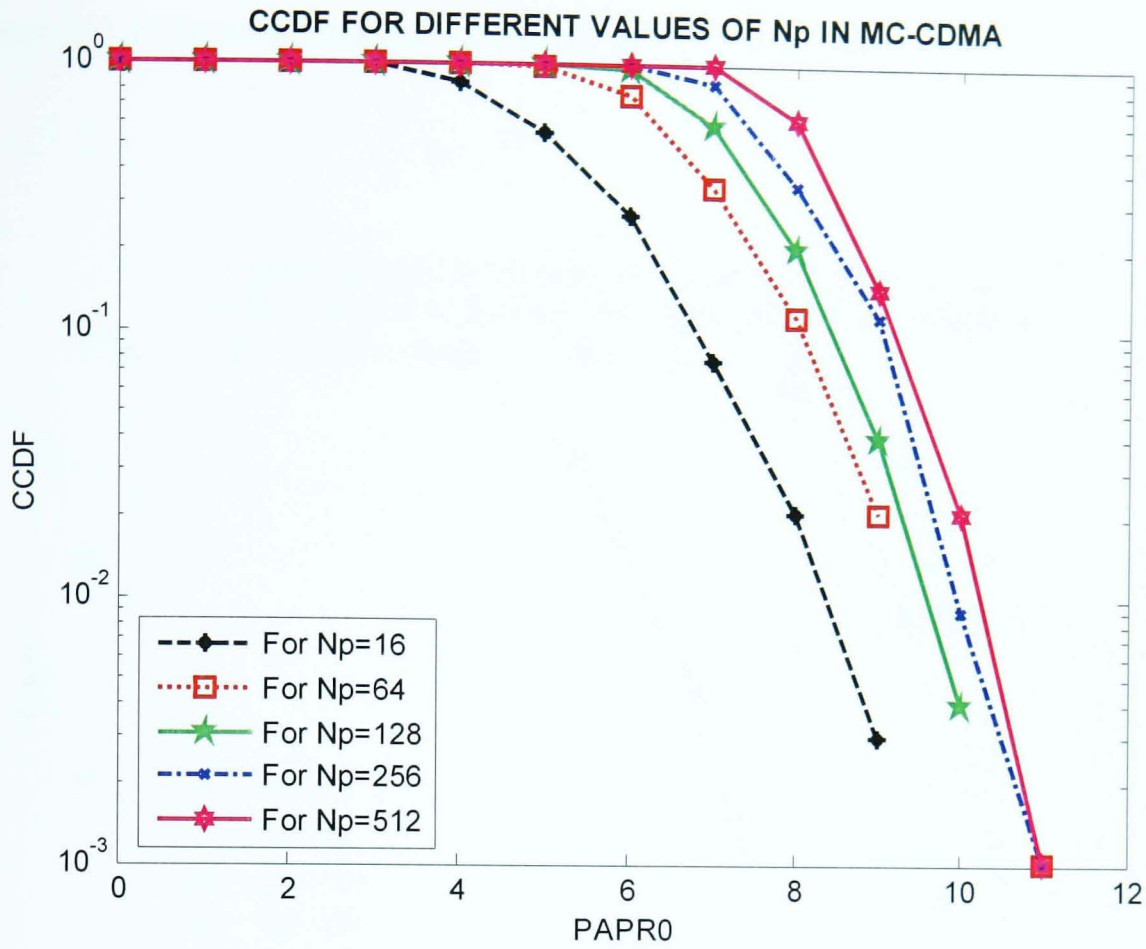

Figure 3.8 CCDF vs. various numbers of subcarriers of MC-CDMA

PAPR0	0-2	3	4	5	6	7	8	9	10	11
N_p=16	1	0.989	0.844	0.552	0.273	0.077	0.021	0.003		
N_p=64	1	1	1	0.978	0.762	0.348	0.115	0.021	0	0
N_p=128	1	1	1	1	0.944	0.581	0.205	0.04	0.004	0
N_p=256	1	1	1	1	0.997	0.835	0.351	0.114	0.009	0.001
N_p=512	1	1	1	1	1	0.986	0.616	0.146	0.021	0.001

TABLE 3.2 COMPARISON FOR DIFFERENT VALUES OF N_P

Figure 3.9 displays the CCDF vs. PAPR0 based on PTS scheme divided by 4

sub-blocks for diverse subcarriers. Number of clusters (M), number of subcarriers per cluster (m) and total MC-CDMA subcarrier (N_p) are related by

$$M = {}^{N_p}\!/_{m}. \tag{3.36}$$

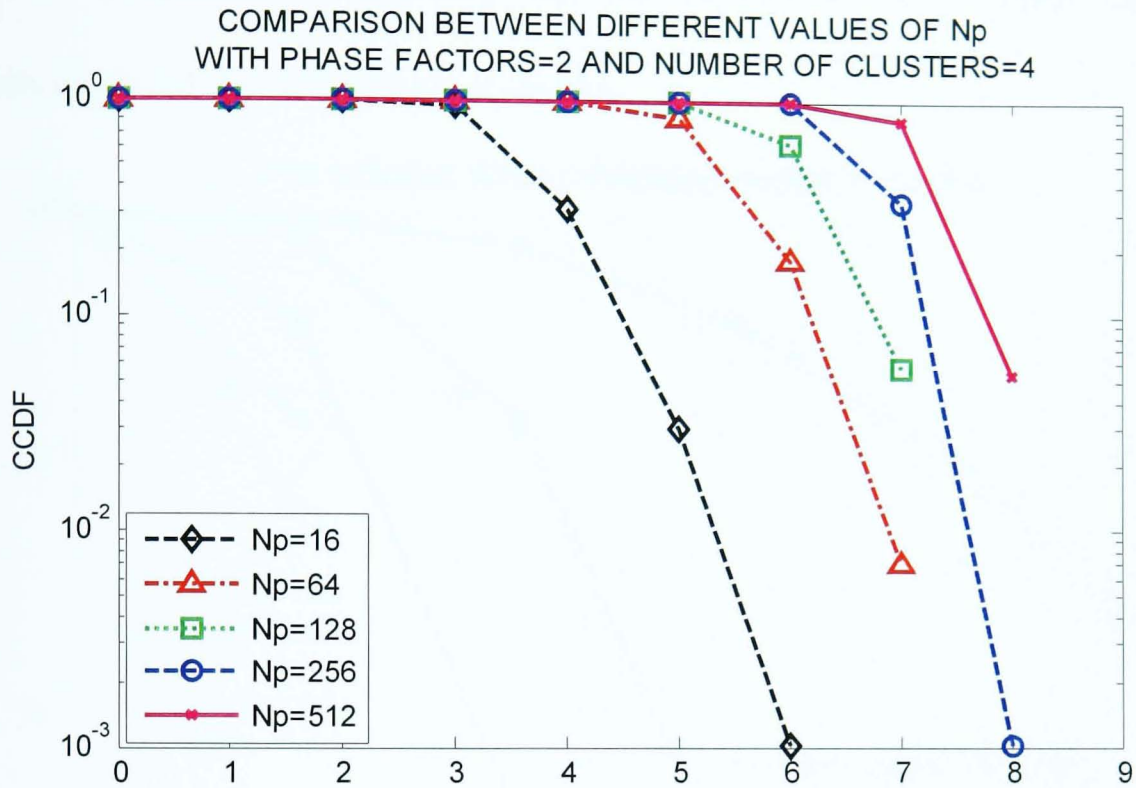

Figure 3.9 CCDF vs. PAPR0 for different subcarriers N_p using the number of phase factors W=2 and the number of clusters M= 4

In order to study the PAPR performance impacted by different phase factors, the number of clusters (M) is fixed to 4. We will vary the value of phase factors. Figure 3.10 presents the PAPR reduction performance based on setting different values of the phase factors. We have already shown that using PTS scheme we can improve the PAPR value by 2.5 dB when CCDF=2×10^{-2}. If the number of phase factors increases from 2 to 4, the PAPR will be reduced up to 0.75 dB according to CCDF=0.2. Enhancing the 4 phase factors to 6, the PAPR is further reduced up to 0.25 dB more. Observed from the increment of phase factors from 6 to 8, the PAPR performance

improvement approximately shrinks to 0.23dB, which is quite close to the PAPR reduction (0.25dB) from phase factors 4 to 6. Total PAPR reduction from phase factor 2 to phase factor 8 is 0.75+0.25+0.23=1.23dB with regard to CCDF=0.2. However, the total computational complexity also increases by $8^4/2^4$=256 times. Table 3.3 details the CCDF for different phase factors.

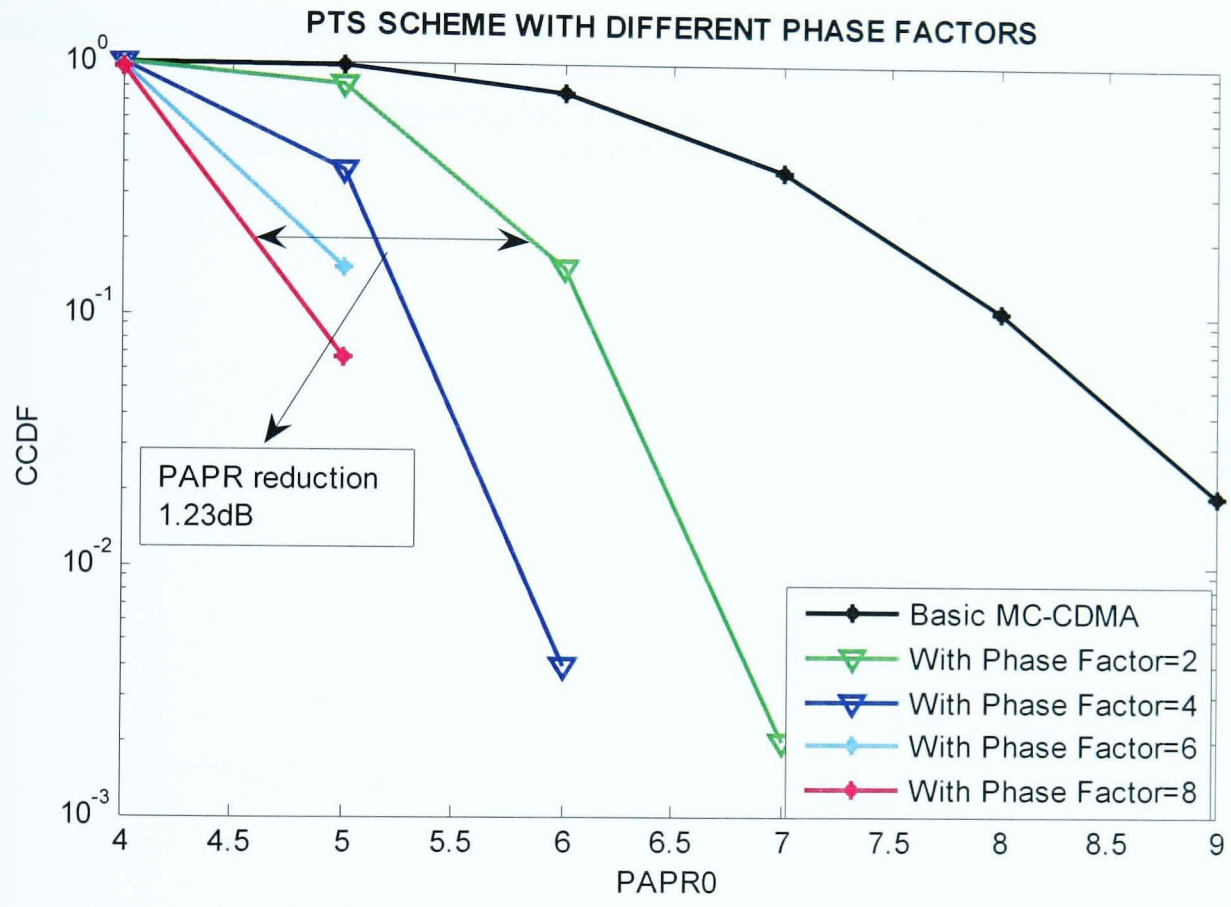

Figure 3.10 CCDF vs. PAPR0 based on different phase factors in PTS scheme

PAPR0	4	5	6	7
PF=2	1	0.822	0.153	0.002
PF=4	0.989	0.36	0.002	0
PF=6	0.97	0.143	0	0
PF=8	0.95	0.067	0	0

TABLE 3.3 CCDF VS. DIFFERENT VALUES OF W IN PTS SCHEME

Figure 3.11 shows an interesting comparison between the phase factors of 6 and 8. From Figure 3.11 and Table 3.4, the PAPR reduction performance is similar between setting phase factors as 6 and 8. However, the computational complexity magnified as $8^4/6^4 \approx 3$ times. Therefore, the tradeoff between approaching the global minimum of PAPR reduction and reasonably controlling the computational complexity needs careful consideration.

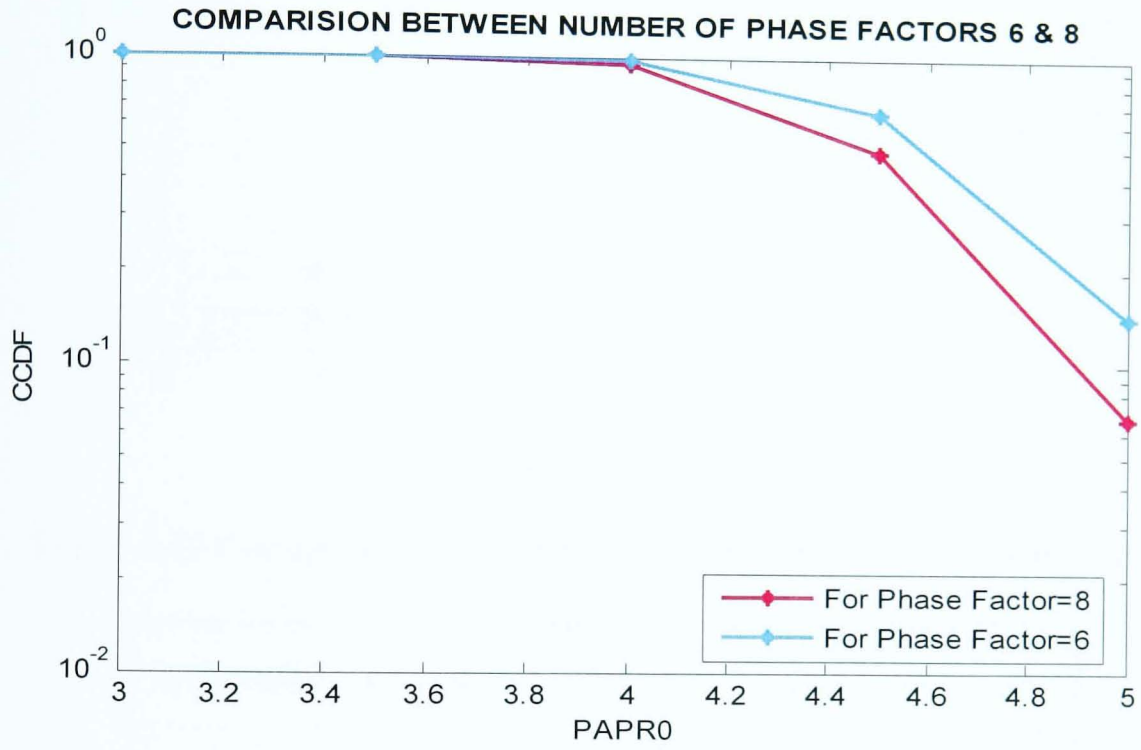

Figure 3.11 PTS based on phase factors W=6 & 8

PAPR0	3	3.5	4	4.5	5	6
PF=6	1	1	0.97	0.666	0.143	0
PF=8	1	1	0.941	0.492	0.067	0

TABLE 3.4 COMPARISON BETWEEN W=6 AND W=8

Figure 3.12 and Table 3.5 indicate the CCDF vs. phase factors for 64-subcarriers with the two clusters vs. four clusters, respectively. It is shown that when the number of clusters increases, the performance of PAPR reduction gets better. Furthermore, as the

number of phase factors increases, the difference of CCDF between the two clusters and the four clusters increases dramatically.

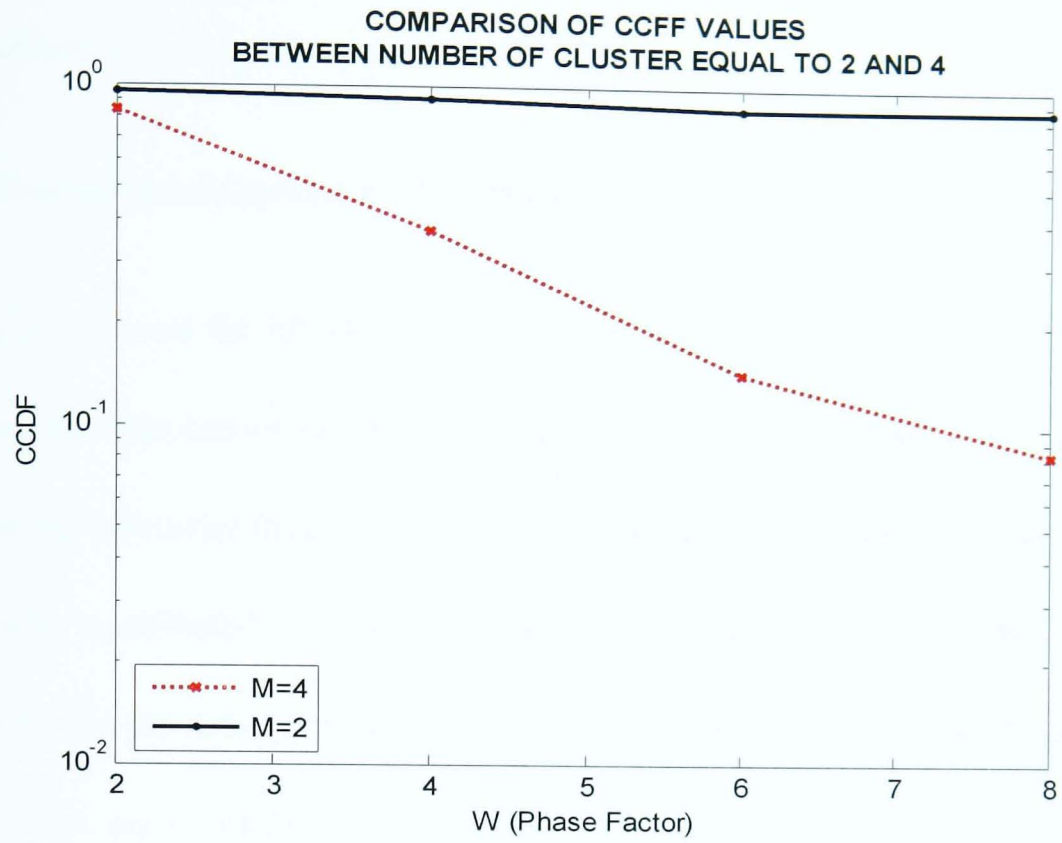

Figure 3.12 Comparing CCDF with number of clusters M= 2 & 4 for N_p=64

W (PHASE FACTORS)	2	4	6	8
CCDF when M=2	0.9540	0.9150	0.8680	0.8640
CCDF when M=4	0.8430	0.3720	0.1430	0.0830

TABLE 3.5 CCDF VALUES WITH M=2 & 4 WITH N_P=64

3.4 Optimum MUD of MC-CDMA Receiver

The motivation of optimum MUD in a synchronous MC-CDMA receiver is to eradicate the impact of MAI by sufficiently exploiting the information of all transmitted users. In this section, the conventional receiver structure of MUD [36] applied in synchronous MC-CDMA is first elaborated. Besides the introduction of

conventional MUD receiver, namely receiver I, a novel MUD receiver structure namely MUD receiver II is proposed in Section 3.4.2 for MC-CDMA system due to its simplicity evolving from current DS-CDMA system.

3.4.1 Conventional Optimum MUD Receiver I of Synchronous MC-CDMA

Figure 3.13 shows the MUD model of MC-CDMA receiver proposed in [36]. At the receiver, the data carried by each subcarrier is firstly de-modulated. The demodulated data on the subcarrier frequency f_0 yields a composite part of the spread signals of all the users, contributed by the 1^{st} chips of their respective spreading sequences. Similarly, for the subcarriers f_1 till f_{Np-1}, the contribution is from the 2^{nd} set of chips till the last set of chips of the spreading sequences from all users respectively.

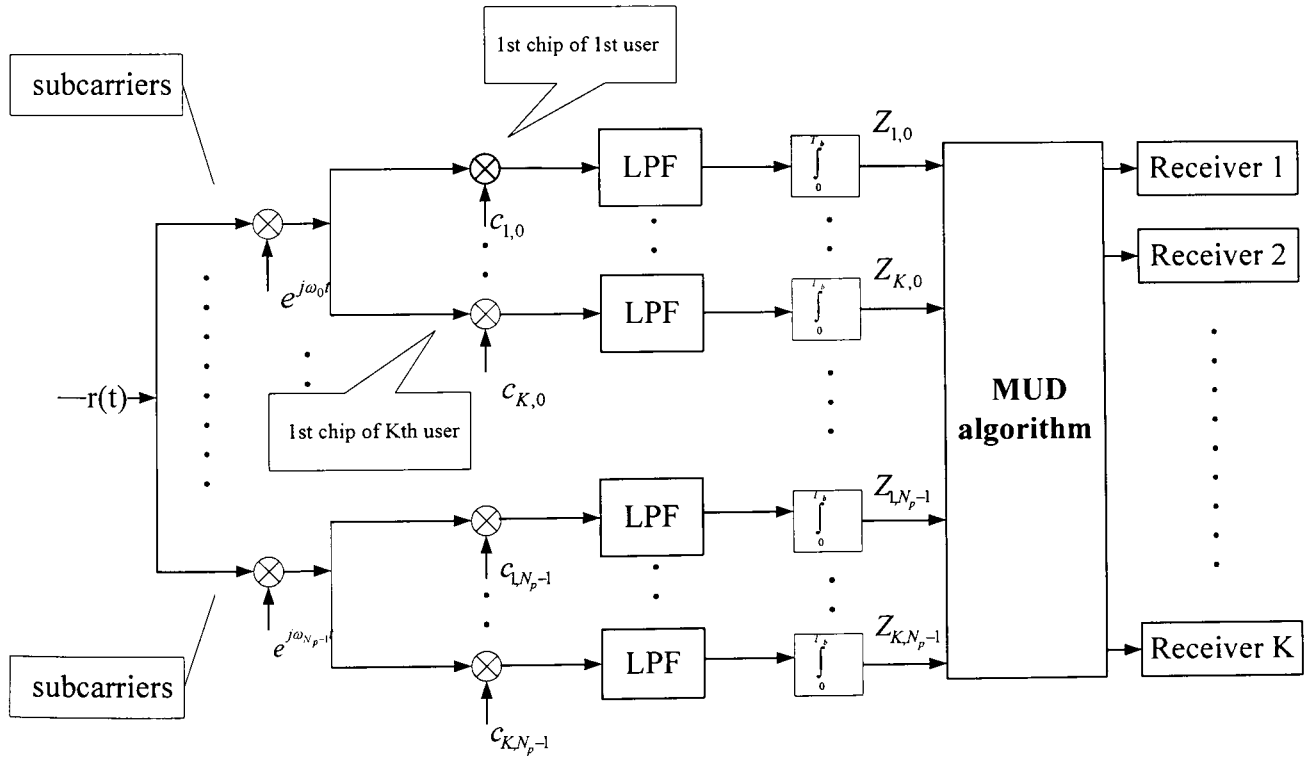

Figure 3.13 The block diagram of the conventional K-user synchronous MC-CDMA receiver assisted by MUD algorithm

The received signal on the m[th] subcarrier is expressed as,

$$r_m(t) = \sum_{k=1}^{K} \left[\sqrt{\frac{2E_k}{N_p}} c_{k,m}(t) \cdot d_k(t) \right] + n(t) \qquad (3.37)$$

where n(t) is the AWGN noise added onto the signal with two-sided power spectrum density $N_0/2$. The information of any particular bit of a user is carried by all of the subcarriers at any given time. The matrix representation of the corresponding transmitted signal expression on the m[th] subcarrier in Equation (3.37) can be represented as:

$$s_m(t) = C_m E d \qquad (3.38)$$

where,

$$C_m = \left[c_{1,m}, \ldots, c_{K,m} \right]$$

$$E = diag\left[\sqrt{\frac{2E_1}{N_p}}, \ldots, \sqrt{\frac{2E_K}{N_p}} \right] \qquad (3.39)$$

$$d = \left[d_1, \ldots, d_K \right]^T$$

As shown in Figure 3.13, the output from the matched filters can be represented in a form of vector "Z_m" [36]:

$$Z_m = [z_{1,m}, \ldots\ldots, z_{K,m}]^T = R_m E b + n \qquad (3.40)$$

where the cross-correlation matrix R_m is defined as

$$R_m = \begin{bmatrix} \rho_{11}^{(m)} & \rho_{12}^{(m)} & \cdots & \rho_{1K}^{(m)} \\ \rho_{21}^{(m)} & \rho_{22}^{(m)} & \cdots & \rho_{2K}^{(m)} \\ \vdots & \vdots & \vdots & \vdots \\ \rho_{K1}^{(m)} & \rho_{K2}^{(m)} & \cdots & \rho_{KK}^{(m)} \end{bmatrix} \qquad (3.41)$$

$\rho_{jk}^{(m)}$ is the value of cross-correlation ($j \neq k$) and the auto-correlation ($j=k$) of the spreading sequences contributing on the m[th] subcarrier and the noise vector n is represented as $n = \left[n_1, \ldots, n_K \right]^T$, where each component n_k (k=1,2...K) denotes the

noise item of output of MF for each user. MAI imposed by the cross-correlation between the spreading codes is the main problem in a MC-CDMA system. The Conventional Matched Filter Detector (CD) for the MC-CDMA system treats MAI as noise. However if we exploit the knowledge of the users' spreading sequences as auxiliaries, the MAI can be substantially reduced [36], and we could achieve capacity gains from the corresponding user. The joint optimum decision rule for a K-user synchronous CDMA system was discussed and derived in [16]. That model can be easily extended to a K-user MC-CDMA system model. The discrete time correlation metric on the m^{th} subcarrier can be expressed in a vector form as:

$$\Omega_m(d) = 2\,\mathrm{Re}[d^T E Z_m] - d^T E R_m E d \tag{3.42}$$

Since the data is transmitted over N_p orthogonal subcarriers, the contribution of all of such likelihood functions will yield an optimum vector $\hat{d}$

$$\Omega(d) = \sum_{m=0}^{N_p-1} \Omega_m(d) = \sum_{m=0}^{N_p-1} \{2\,\mathrm{Re}[d^T E Z_m] - d^T E R_m E d\} \tag{3.43}$$

Hence, the decision rule for the optimum K-user MC-CDMA MUD scheme based on the maximum likelihood criterion is to choose the specific bit combination $\hat{d}$ out of 2^K possible combinations, which maximizes the correlation metric of Equation (3.43). Therefore,

$$\hat{d} = \arg\left\{\max_{d}\left[\Omega(d)\right]\right\} \tag{3.44}$$

3.4.2 A Novel Optimum MUD Receiver II of Synchronous MC-CDMA

Figure 3.14 shows the model of our proposed MUD receiver of an MC-CDMA system. As similar to the conventional MUD receiver model illustrated in Figure 3.13, the first

step is the de-modulation which is carried on each subcarrier. In practice, we may only need one serial-to-parallel converter for the received signal. For the sake of clearness, there are K serial-to-parallel converters in Figure 3.13. Next, in contrast to the despreading conducted chip-wisely in conventional MUD receiver, the demodulated composite chip sequence is multiplied by each user's spreading sequence in the frequency domain and then the summations of each chip sequence product in frequency domain are passed to a bank of MFs. This process is the same as the MUD in conventional DS-CDMA receiver. Selecting novel optimum MUD receiver II in practice will reduce the cost evolving from DS-CDMA to future MC-CDMA networks due to the minimum change in the upgrading system.

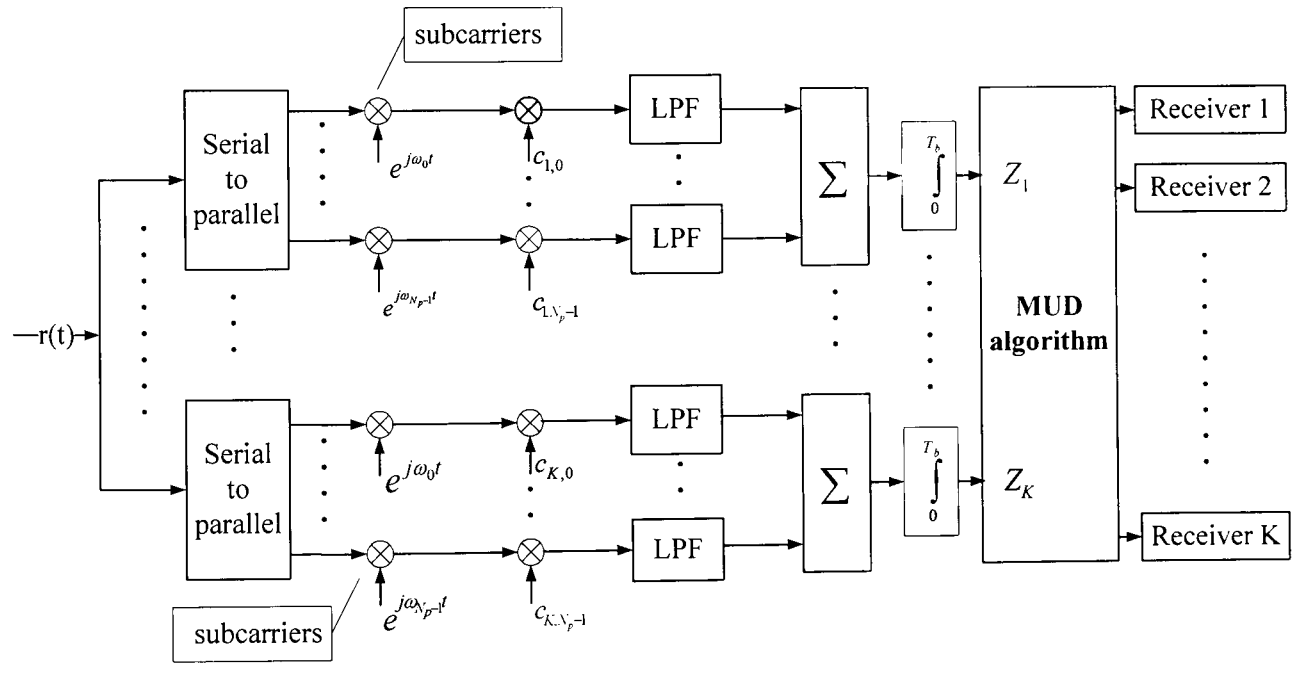

Figure 3.14 The block diagram of the K-user synchronous MC-CDMA receiver II assisted by MUD algorithm

After the output of k^{th} user's serial-to-parallel converter is demodulated, the received signal can be expressed as

$$r(t)=\sum_{k=1}^{K}\left[\sqrt{\frac{2E_k}{N_p}}c_k(t)\cdot d_k(t)\right]+n(t) \tag{3.45}$$

The matrix representation of the corresponding transmitted signal expression on all subcarriers in Equation (3.45) can be represented as:

$$s(t)=\sum_{k=1}^{K}C_kEd \tag{3.46}$$

where,

$$\begin{aligned} C_k &= \left[c_{k,0},\ldots, c_{k,N_p-1}\right] \\ E &= diag\left[\sqrt{\frac{2E_0}{N_p}},\ldots,\sqrt{\frac{2E_{N_p-1}}{N_p}}\right] \\ d &= \left[d_1,\ldots d_K\right]^T \end{aligned} \tag{3.47}$$

As shown in Figure 3.14, the output from the CDs (or MFs) can be represented in a form of vector Z:

$$Z=\left[Z_1,Z_2,\ldots.Z_K\right]^T=REd+n \tag{3.48}$$

where R is the cross-correlation matrix among spreading sequences ($\Re$) given by Equation (2.45) and the noise vector n is represented as $n=\left[n_1,\ldots,n_K\right]^T$, where each component n_k (k=1,2,..K) denotes the noise term of MF output for each user. Therefore, the complicated estimation in each subcarrier is simplified as the estimation for each user, which becomes to our more familiar expression of MUD for CDMA detailed in [16]. Furthermore, the objective likelihood function defined in Equation (3.43) can be modified as

$$\Omega(d)=2\,\mathrm{Re}[d^TEZ]-d^TEREd \tag{3.49}$$

Hence, the decision rule for the optimum K-user MC-CDMA MUD scheme based on

the maximum likelihood function become to select the specific bit combination $\hat{d}$ out of 2^K possible combinations in order to maximize the correlation metric of Equation (3.49). Therefore,

$$\hat{d} = \arg\left\{\max_{d}\left[\Omega(d)\right]\right\} \tag{3.50}$$

Figure 3.15 expatiates on the operational flow of an MC-CDMA system which is applicable for both two aforementioned structures of an MC-CDMA receiver. Note the only difference appears at the correlation metric (maximum likelihood function). One is based on the subcarrier-wise Z_m and R_m, and another is oriented by user-wise Z and R.

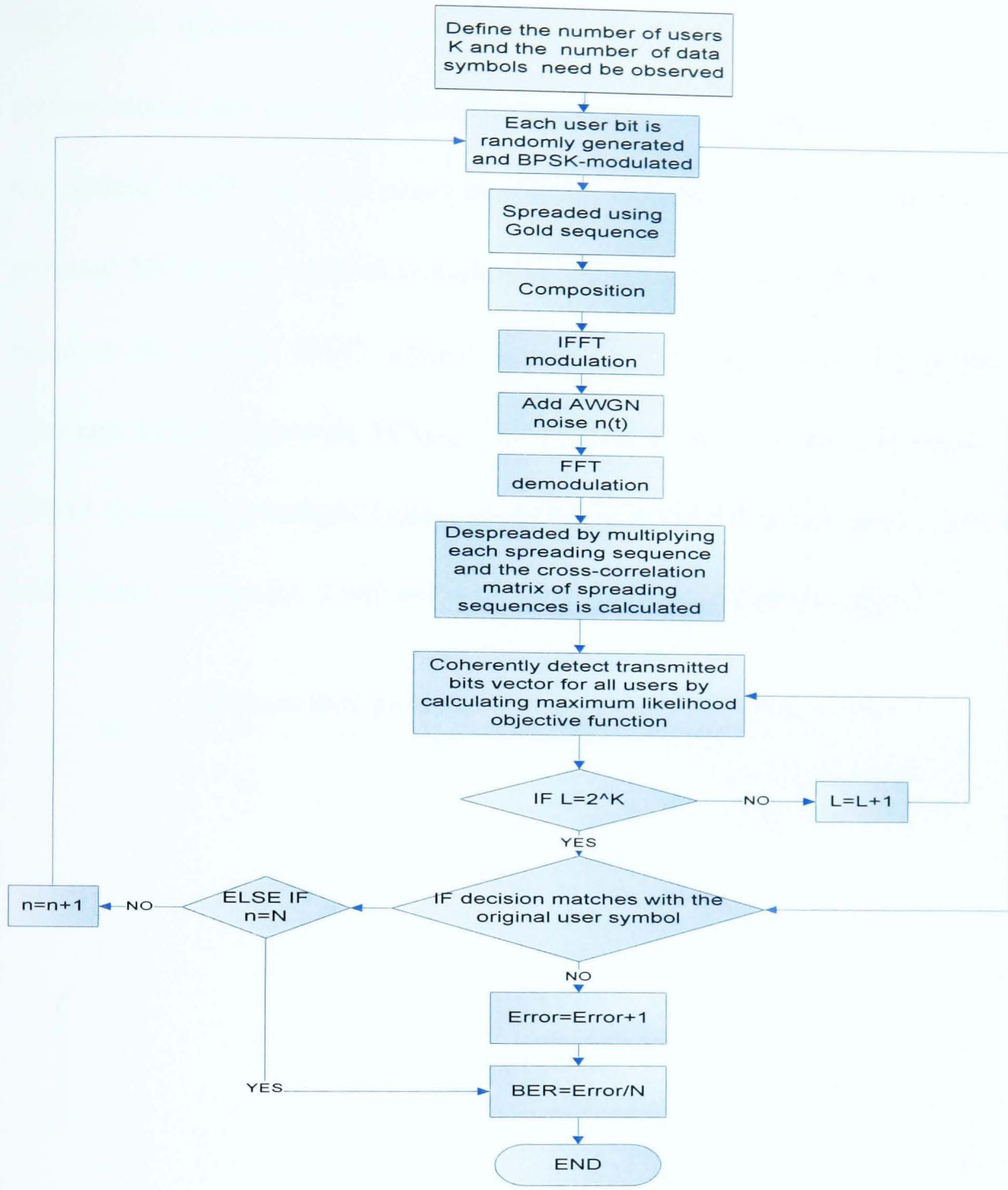

Figure 3.15 Flow chart of an MC-CDMA system applied by optimum MUD to the receiver

3.4.3 Simulation Results

In the simulation, 10000 binary bits are generated in transmitter to carry on the experiment for each MC-CDMA receiver. The BER performance vs. SNR per bit in Figure 3.16 is used to measure the optimal MUD performance assisted in two types of

MC-CDMA receivers. From the result, it is shown that the optimum MUD performance of our proposed MC-CDMA receiver II in Section 3.4.2 is identical to the optimal MUD assisted conventional MC-CDMA receiver I. Therefore, our proposed MC-CDMA receiver is equivalent to the conventional MC-CDMA receiver based on the optimal MUD scheme. It could be also understood that because the dominant factor to generate MAI in MC-CDMA is from the multiple access using CDMA spreading technique. Hence, no matter how OFDM demodulator is combined with CDMA despreader, it will not impact the optimal MUD performance.

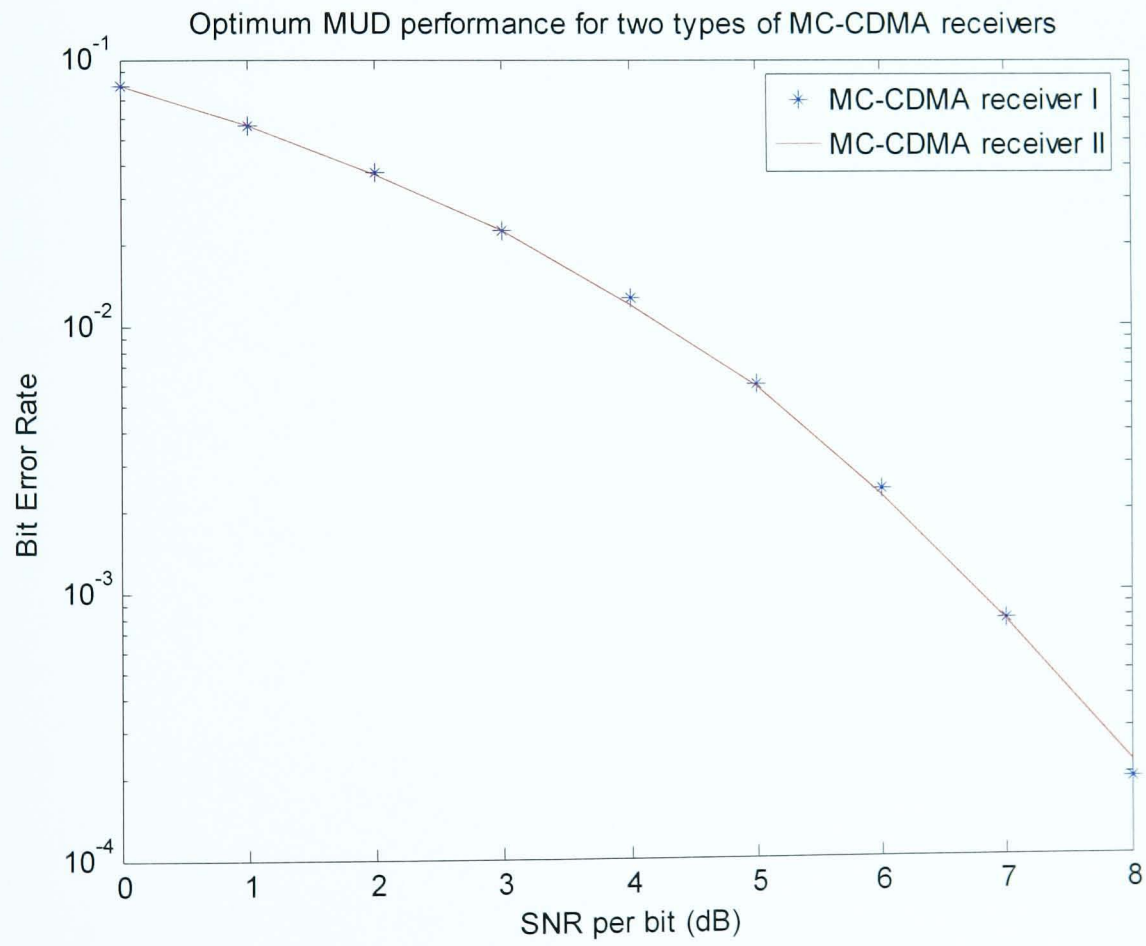

Figure 3.16 Optimum MUD performances for two types of MC-CDMA receivers

In practice, if the evolving cost from current 2G/3G system standard towards next generation broadband wireless system is controlled as minimum as possible, the

implementation cost will be significantly reduced and also the evolving procedure will become smooth and seamless. Our proposed novel MUD receiver II requires less modification of core chip algorithm design from the 2G/3G system than the conventional MUD receiver I for MC-CDMA, which offers good back-compatibility from the implementation point of view. Therefore, our proposed MC-CDMA receiver will be selected for the following analysis of MDGA aided MUD.

Chapter 4 An Intelligent Genetic Algorithm for PAPR Reduction in MC-CDMA Wireless System

As previously described, high computational complexity is the dominated barrier for PTS technology to be implemented in MC-CDMA transmitter in practice. Therefore, reducing computational complexity of PTS scheme and meanwhile keeping a good PAPR reduction performance become a hot research topic in the field. Recently, some research work [101, 102, 103, 104, 105] were proposed to reduce the computational complexity. However, to the best of our knowledge, either their computational complexity is still high, or the PAPR reduction performance is not good when complexity is reduced. In this Chapter, we propose a novel scheme called minimum distance guided genetic algorithm (MDGA) to dramatically reduce the computational complexity while achieving a good near-optimum performance close to the exhaustive search, which is validated by the experimental results.

4.1 Design of MDGA for PAPR Reduction

In order to avoid the problem of likely converging at local optimum, the conventional GA normally begins a random search at an experimental surface. However if the global optimum is actually close to some region, GAs started from random points of the experimental surface would be so time-consuming with low efficiency. Hence, with the help of some initial estimation, it is possible to accelerate the convergence to

the global optimum without being trapped at a local optimum. This is one main idea of our MDGA. Moreover, how to choose such a good estimation as a qualified guidance to lead and exploit the local search is also an important research issue.

4.1.1 Iterative Flipping assisted PTS

Firstly, the research interest has been focused on the proper selection of the local minimum. One of important criteria to be considered is that the local minimum should be easy to arrive, which means having the computational complexity as less as possible. If we spend too much time on locating the local minimum, the advantages of any improvements will be weakened. From the existing solutions proposed to reduce the computational complexity of exhaustive search of PTS [87, 101, 102, 103, 104, 105], iterative flipping (IF) [87] is recognized as a very simple scheme to achieve sub-optimum PAPR reduction performance with very low computational complexity. If binary (i.e., ±1) weighting phase factors are considered, the IF method works as follows: First, assume b_w=1 for all M clusters. Next, invert the first phase factor (b_1=-1) and re-compute the resulting PAPR. If the new PAPR is lower than the value in the previous step, retain b_1 as a part of the final phase vector; otherwise, b_1 reverts its previous value. The algorithm iteratively repeats in this fashion until all M phase factors have been measured. Hence, the combination of phase factors forms a sub-optimum solution for PAPR reduction. By considering that IF is a very simple method, we decide to use it as an initial guess point for the local minimum of our MDGA. This supposition can be confirmed by a comparison with the results of the

exhaustive search based PTS as shown in Figure 4.1 and Figure 4.2 for different numbers of subcarriers.

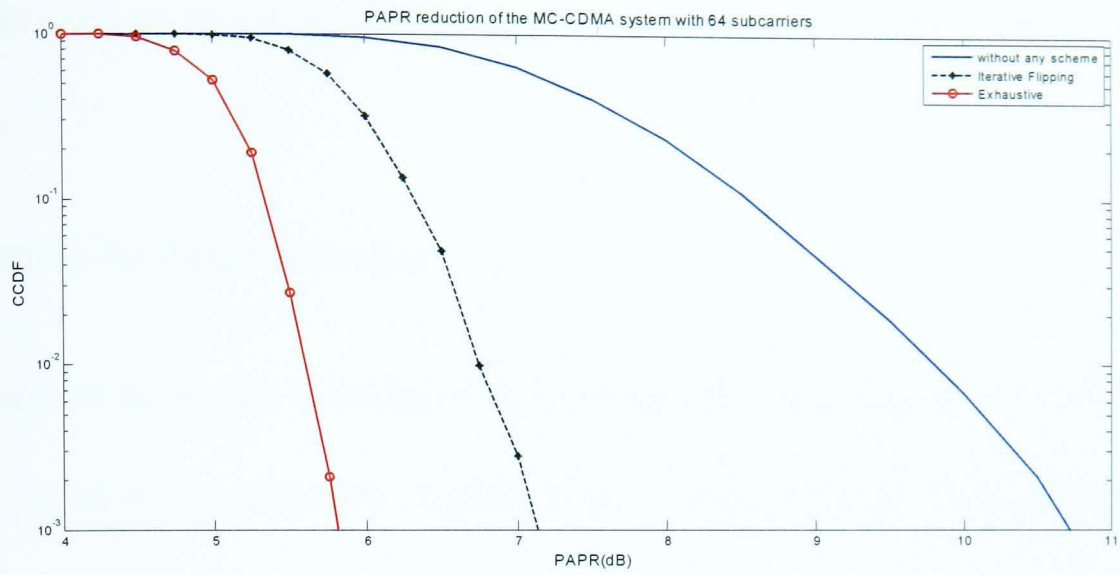

Figure 4.1 Iterative Flipping aided PAPR reduction performance vs. Exhaustive PTS for MC-CDMA system with 64 subcarriers

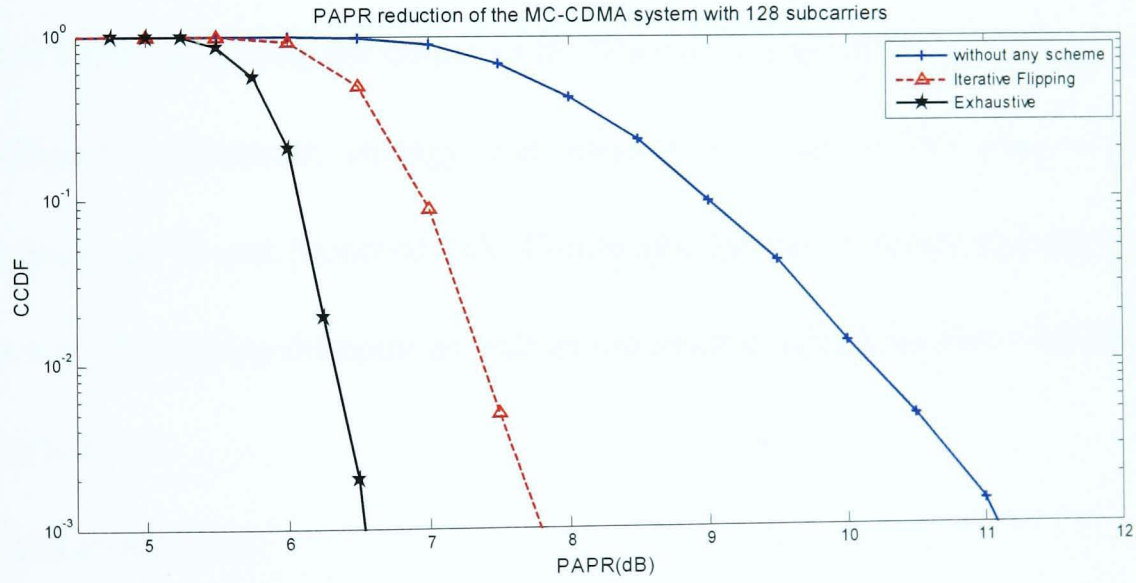

Figure 4.2 Iterative Flipping aided PAPR reduction performance vs. Exhaustive PTS for MC-CDMA system with 128 subcarriers

Since the IF mechanism works through tuning global variables to approach global minimum with linear computational complexity $\{(W-1)\times M\}$ as compared to any

random combination of variables (random local minimum) generated from experiment surface, the IF can be deemed as an appropriate jumping-off point in order to further carry on an efficient local search which is the motivation of our proposed scheme.

4.1.2 MDGA for PAPR Reduction

Our proposed novel GA is designed to accelerate the searching speed to find the optimal solution by adequately exploiting the output of the IF as guidance. As compared to the conventional GA, we introduce a novel replacement strategy in both initial population matrix and mating pools. The idea is to keep a balanced search throughout all GA generations. Initial population matrix replacement allows us to start the initial search guided by the output of IF. Whereas, replacement of mating pools is an intelligent replacement strategy that plays a key role in providing a quick convergence rate to our proposed GA. Combining the two schemes together offers MDGA a good jumping-off point as well as increased convergence rate. Our MDGA works as follows.

a) Initial Population

Considering that a good initial guess of the possible solutions is helpful for GA to obtain good performance, the selection of initial population to get better initial estimate is created up by mutating the output of the IF.

Let the total population of chromosomes be "N_{pop}". In order to ensure that each phase factor of IF's output experiences change at least once, we generate the initial "M"

(where M is the number of sub-blocks, hence $N_{pop} > M$) set of chromosomes by perturbing the IF's output in such a way that the Hamming Distance between the IF's output and the new individual keeps "one". That is why we call our scheme the "Minimum Distance Guided" approach. The IF's output is considered as a good estimate, yet there is a high probability that a search which is only guided by IF's output according to Hamming Distance of one may get stuck at local optima. In order to reduce this unwanted possibility and balance the trade-off between convergence rate and searching diversity, we make the rest of the population randomly generated in order to explore other possible optimum solutions in the search space as shown in Figure 4.3.

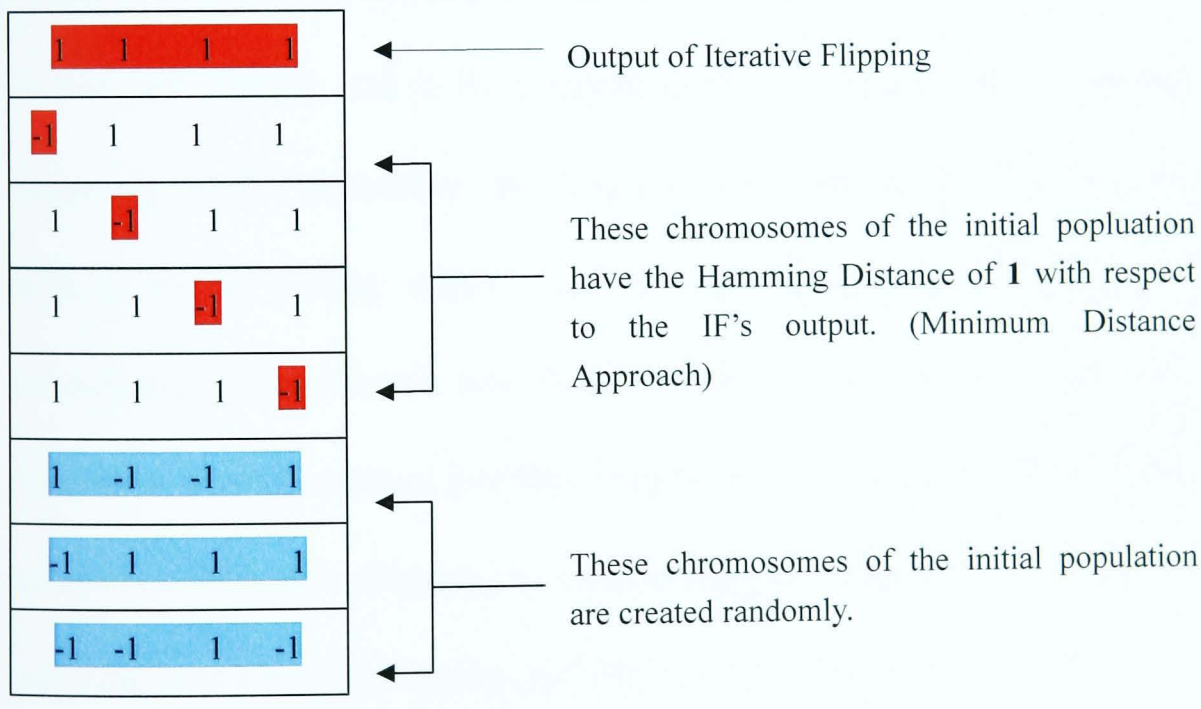

Figure 4.3 Formation of initial population in MDGA

b) Fitness Function

The fitness function is derived from Equation (3.25), which is rewritten as

$$\underline{\hat{s}_k} = \left\{\min\left(\underline{s_k}\right)\right\}_{\hat{b}_w} \tag{4.1}$$

Each combination of b_w is a vector of the phase factors, where the vector length is equal to the number of sub-blocks. The task of PTS is to measure all the phase factors jointly in order to discover a global minimum $\underline{\hat{s}_k}$ of searching space $\underline{s_k}$ by accurately positioning $\hat{b}_w$. In order to efficiently reduce PAPR in MC-CDMA system by using PTS technology, we need to find such a combination of vector "$\hat{b}_w$" that minimizes the above cost function.

c) Replacement Strategy

After a successful evaluation of the initial population, each chromosome is ranked according to the cost value from the minimum to the maximum. The truncation selection takes place according to some selection rate, "X*rate*" (e.g. X*rate* =1/2 is set in our case initially and to be dynamic further to prevent incest happens). In the beginning of each generation, the "$\lceil N_{pop}/2 \rceil$" best individuals in the ranking list are selected for the mating, where $\lceil N_{pop} \rceil$ denotes ceiling value of N_{pop}. For example, considering the population size of 30, we first select 15 best candidates by the truncation-selection method and then from the two fittest parents (with the lowest cost values) we form two offspring by performing uniformed crossover operation. Then, from the next two fittest mating parents we create two more offspring and so on till we form 13 new offspring. We design the mating process in a way that in each generation, the number of offspring generated is equal to N_{pop}- $(M+1)$ provided that the incest does not appear in the patent candidates.

After successful mating in each generation, we keep the fittest mate remained and generate the other M chromosomes by performing the same Minimum Distance approach using the fittest mate, i.e. the new pool will contain the fittest mate on the top along with the "M" individuals having the Hamming Distance of one between them and the previously formed "N_{pop}-$(M+1)$" number of offspring. This is how we exploit the attribute of best mate (local search) at each generation as well as we also create a reasonable number of offspring out of the mating pool for exploration.

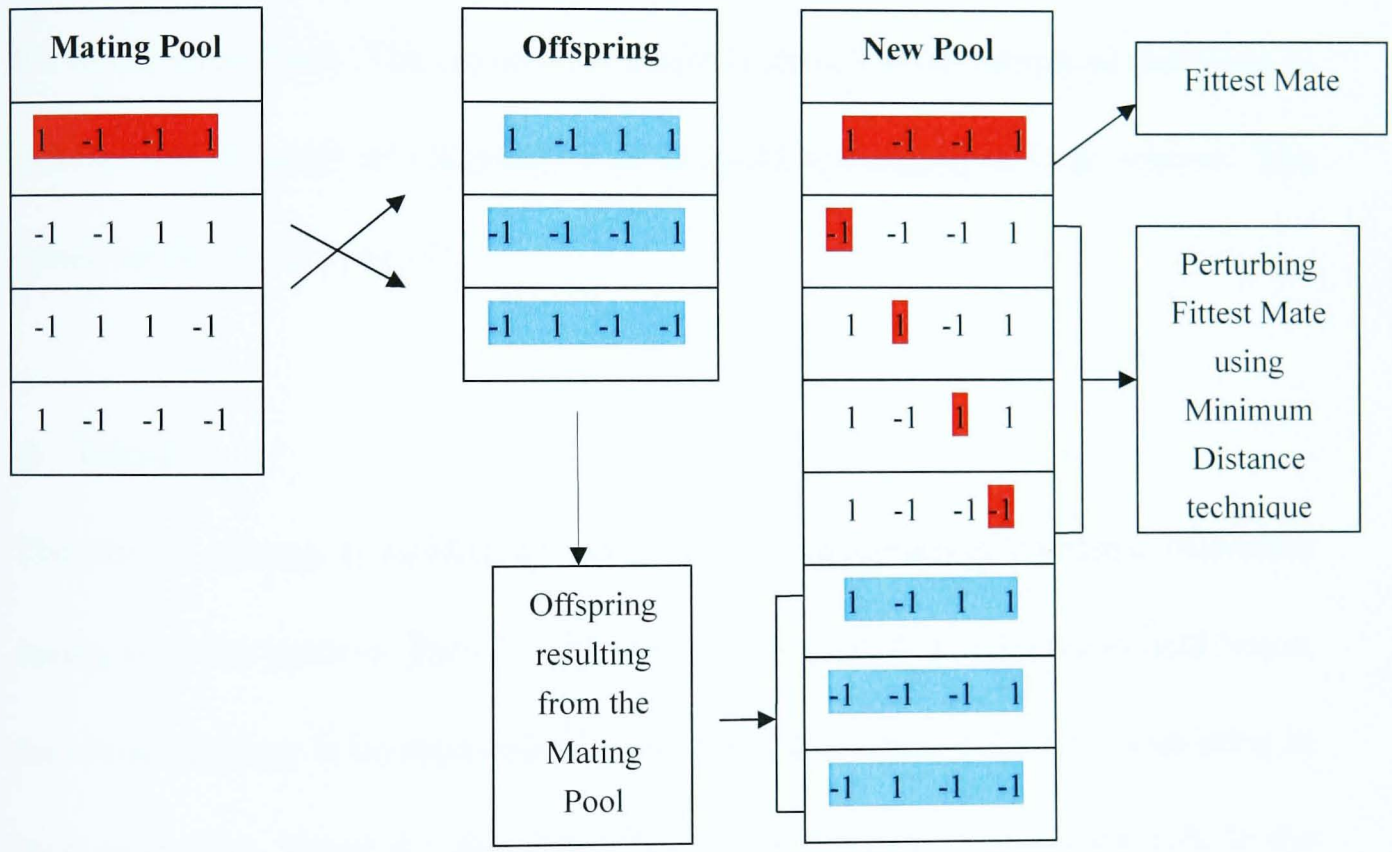

Figure 4.4.A Novel Replacement Strategy in MDGA

The MDGA is firstly guided by the output of IF and then in the following generations it is guided by the best mate selected from the mating pool. The fittest-initiated "M+1" individuals along with the "N_{pop}-(M+1)" offspring generated from the mating pool ensure that the GA would not likely be stuck at the local optimum. The process involved in the replacement strategy is shown in Figure 4.4, with an example

population size of 8 chromosomes for a case of four sub-blocks in an MC-CDMA system. Note that the schematic crossover point is taken after the 2^{nd} bit.

d) Type of Mutation & Crossover

The new pool undergoes mutation process which further ensures that our MDGA search would not get stuck around local optimum. Illuminated by the observation from conventional GA study [106], the constant mutation probability is chosen to be 0.2 in our experiment. The crossover operator is chosen to be uniformed crossover to increase the diversity of offspring so as to avoid converging at local minima. The crossover rate is set to be 1/2.

e) Elitism

The Elitism strategy is invoked to preserve the chromosome of the fittest individual during mutation process. There is only one optimum solution to be found, and hence, the elitism strategy is invoked only for one fittest individual of the total population in each generation. Figure 4.5 shows the flow of operation in the proposed GA. In the next section we show the comparison of the PAPR reduction performance and corresponding computational complexity between the proposed MDGA with other schemes.

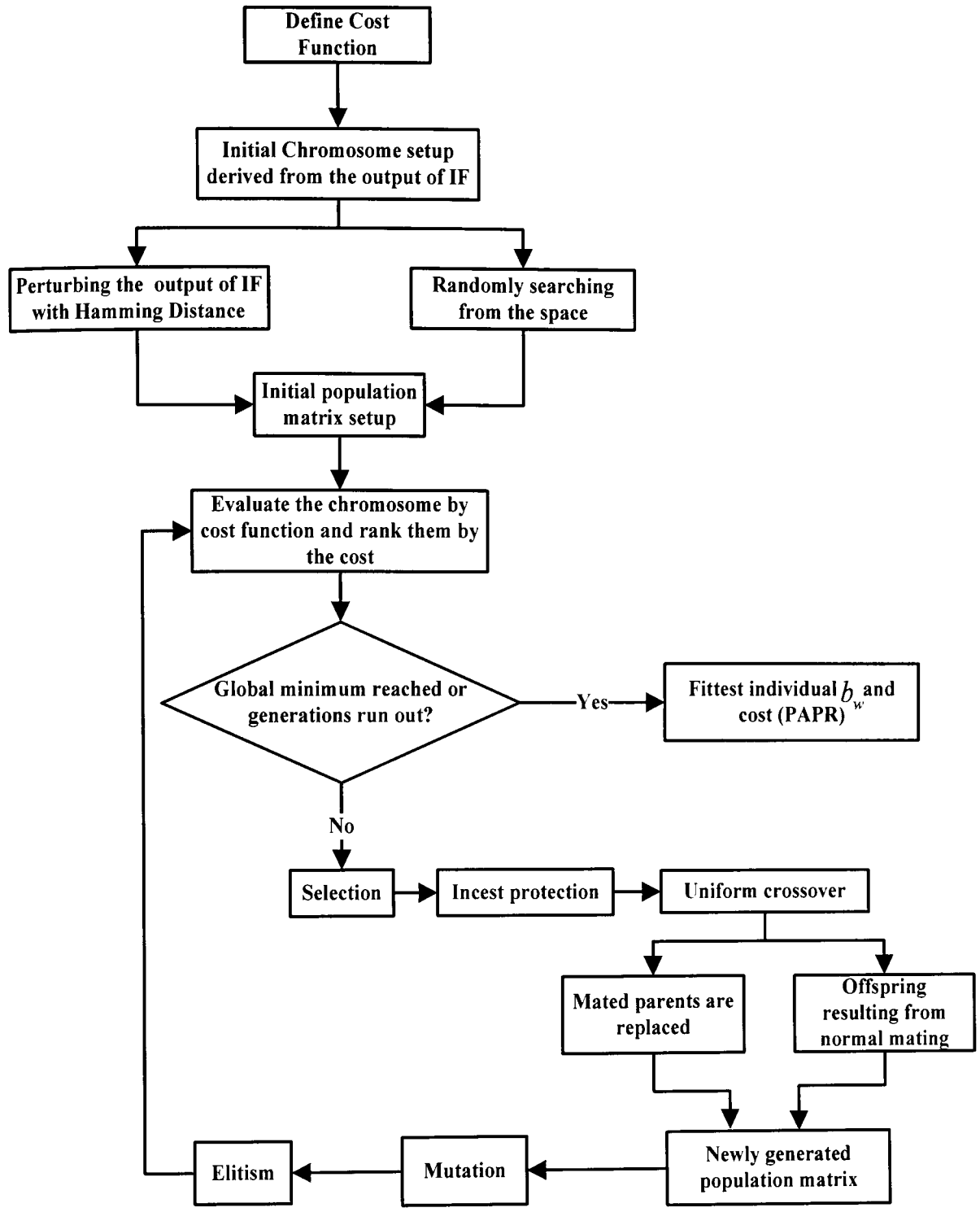

Figure 4.5 Flow chart of MDGA-PTS

4.2 Simulation Analysis

4.2.1 Parameters Configuration

The CCDF and computational complexity are the two main measurement criteria to

be used. The CCDF represents the probability of PAPR beyond the given threshold, whereas, the computational complexity of the GA, in the context of the total number of cost function evaluations which is defined as the product of the population size and the number of generations. Table 4.1 shows the configuration parameters used in the simulations.

TABLE 4.1
CONFIGURATION OF THE MDGA-PTS

SETUP/PARAMETER	METHOD/VALUE
Population size N_p	30
INITIALIZATION	Initial population setup strategy
Selection Method	Truncation Selection
Mating pool size	$\leq \lvert N_{pop}/2 \rvert$ depends on the number of non-identical individuals
Crossover operation	Uniformed crossover
Crossover rate	1/2
New pool	New pool created by Hamming Distance scheme
Mutation operation	Standard binary mutation
Mutation Probability p_m	0.2
Elitism	Yes
Incest protection	Yes
Termination Generation	5 or 10

4.2.2 Simulation Results

In Figure 4.6, some results of CCDF vs. PAPR are simualted for the MC-CDMA system with 64 subcarriers and BPSK modulation, in which 16 sub-blocks are

employed and binary phase factors are used for phase rotation on each sub-block. We choose the IF scheme and the conventional GA as comparison. It is noted that the IF method reduces the PAPR, but the performance is deteriorated as the sub-optimum. Using a conventional GA, the PAPR can be further reduced. However, the computational complexity is still high. The simulation results in Figure.4.6 show that the proposed MDGA can provide almost the same performance as exhaustive PTS, but with much lower computational complexity than conventional GA. Based on the same population size, the generations can be reduced at least half. Figure 4.7 is the detailed zoom-in version of Figure 4.6 It is shown that the performance of MDGA with five generations is even better than that of the conventional GA with ten generations, i.e., PAPR = 6.05dB using MDGA vs. PAPR = 6.07dB using conventional GA, for CCDF=10^{-3}. Furthermore, there is a significant improvement in PAPR reduction between our MDGA with 10 generations and the traditional GA with 20 generations, i.e. PAPR=5.86dB with ten generations, as compared to PAPR=5.91dB with 20 generations.

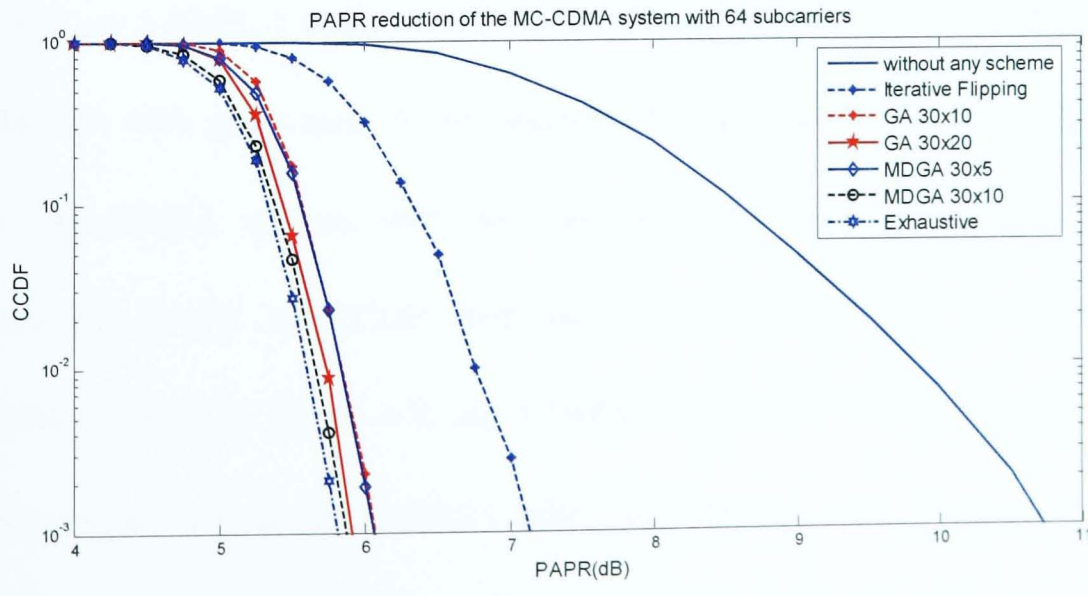

Figure 4.6 The CCDF vs. PAPR of the MC-CDMA system with 64 subcarriers

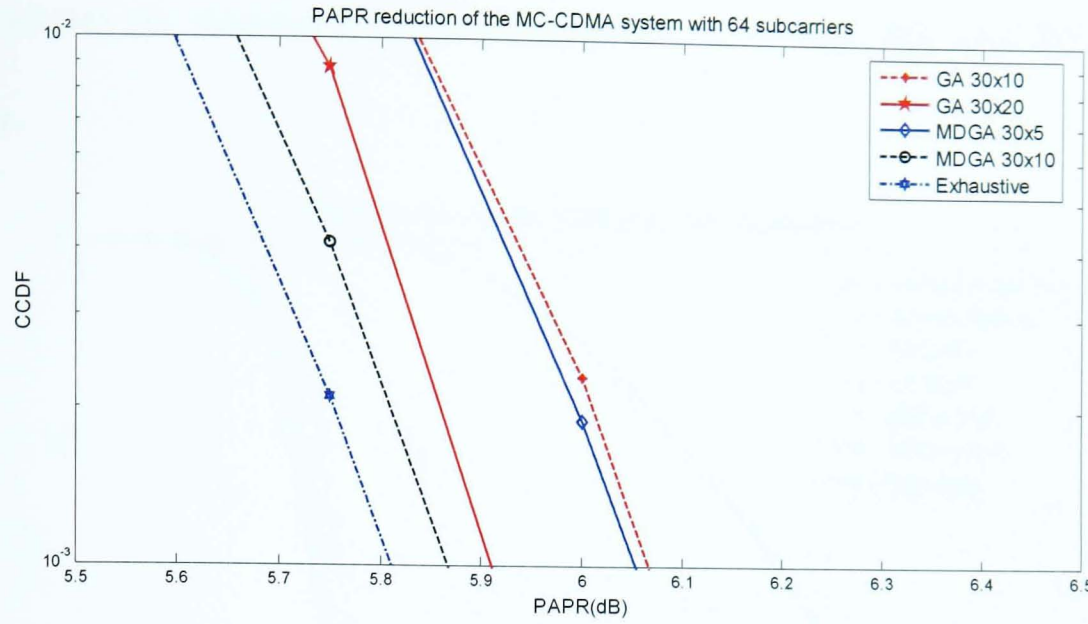

Figure 4.7 Zoom-in view of the CCDF vs. PAPR of the MC-CDMA with 64 subcarriers

In Figure 4.8, the simulation results are shown for the MC-CDMA system with 128 subcarriers, in which 16 sub-blocks are employed and binary phase factors are used for phase rotation on each sub-block. It is observed that the MDGA can stably perform regardless of an increase of subcarriers. When the CCDF=10^{-3}, the PAPR in Figure 4.7 are 6.07dB, 5.91dB, 6.05dB and 5.86dB for GA with generations 10, 20 and MDGA with generations 5, 10, respectively. Compared to the PAPR reduction of the MC-CDMA system with 64 subcarriers illustrated in Figure 4.7, the corresponding PAPR of CCDF with the value of 0.001 for 128 subcarriers MC-CDMA system in Figure 4.9, are 6.74dB, 6.61dB, 6.72dB and 6.56dB for GA with generations 10, 20 and MDGA with generations 5, 10, respectively, where Figure 4.9 is also the detailed zoom-in version of Figure 4.8. Therefore, our proposed

MDGA scheme is not affected by an increased number of subcarriers, which demonstrates its robustness of PAPR reduction in a high data rate MC-CDMA system.

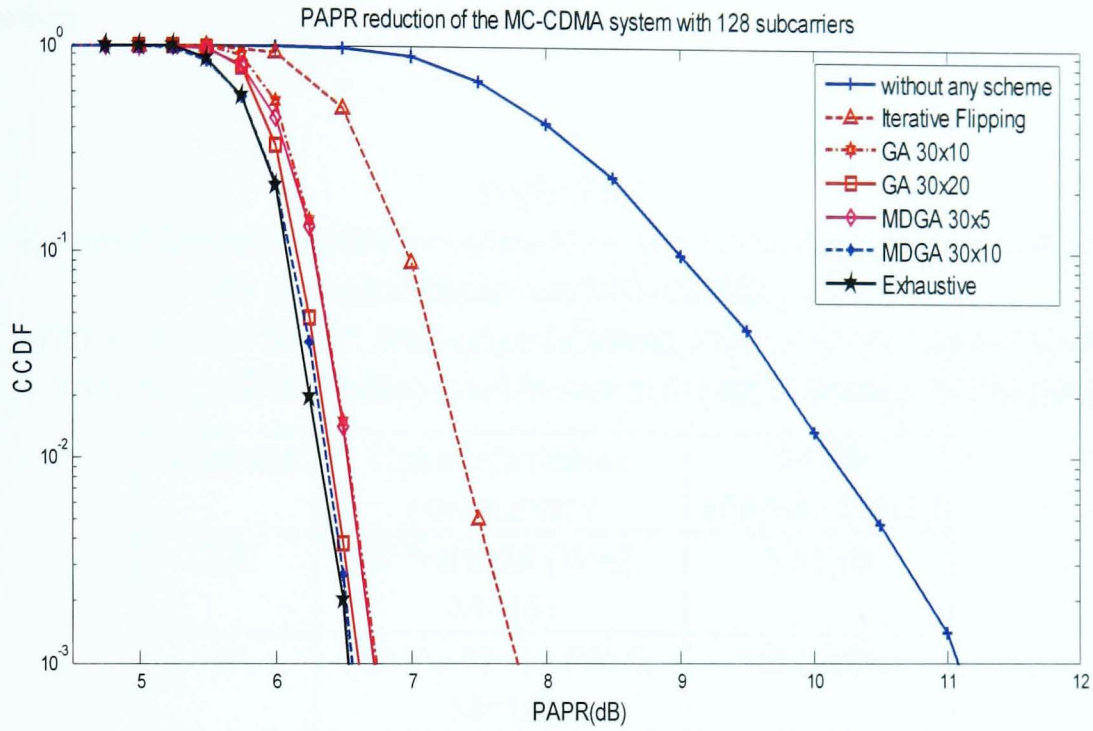

Figure 4.8 The CCDF vs. PAPR of the MC-CDMA system with 128 subcarriers

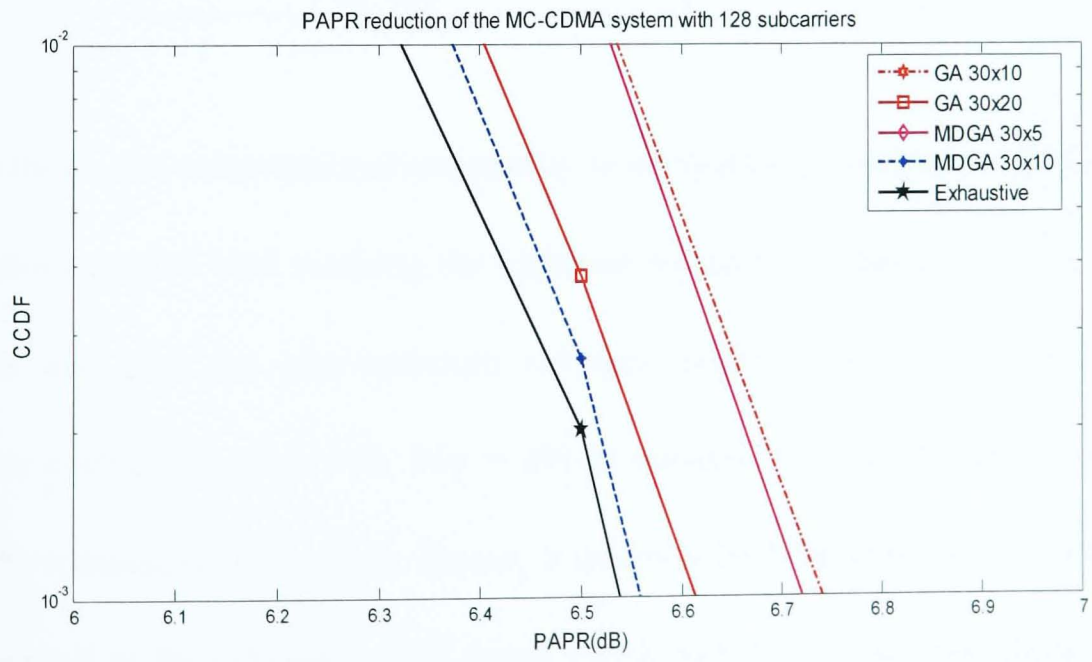

Figure 4.9 Zoom-in view of the CCDF vs. PAPR of the MC-CDMA with 128 subcarriers

The conventional GA with random search lacks the guidance from IF's output in each generation and is more likely to deviate the global minima and hence requires an increase in the number of generations to refine the optimal solutions before search termination.

TABLE 4.2

COMPARISON OF COMPUTATIONAL COMPLEXITY AMONG DIFFERENT SCHEMES BASED ON 64 SUBCARRIERS OF THE MC-CDMA SYSTEM

EX: EXHAUSTIVE PTS, IF: ITERATIVE FLIPPING, GA: CONVENTIONAL GENETIC ALGORITHM, MDGA: MINIMUM DISTANCE GUIDED GENETIC ALGORITHM

SCHEMES	COMPUTATIONAL COMPLEXITY	PAPR (CCDF=0.001)
EX	W^M=65536 (W=2, M=16)	5.81dB
IF	(W-1)×M=16 (W=2, M=16)	7.12dB
GA	P×G=600 (P=30, G=20)	5.91dB
MDGA	P×G+(W-1)×M=316 (P=30, G=10, W=2, M=16)	5.86dB

In this thesis, the computational complexity is defined as the number of cost function evaluations needed until reaching the optimum solution. As shown in Table 4.2, our MDGA can give the near-optimum solution within only $30 \times 10 + 16 = 316$ cost function evaluations (Gen =10, Pop = 30) as compared to 2^{16} (65,536) evaluations taken by exhaustive PTS search. Hence, it achieves 99.52% reduction in complexity as compared to the exhaustive PTS based PAPR reduction. Also from Figure 4.6, as compared to conventional GA with 600 (Pop=30, Gen=20) cost function evaluations, the MDGA reaches the optimum in only 316 (Pop=30, Gen=10) cost function

evaluations, ensuring 47.3% complexity reduction in terms of cost function evaluations. Note that as the number of generations increases, the complexity reduction can be further improved to 50+%.

Chapter 5 An Intelligent Genetic Algorithm assisted MUD in MC-CDMA Wireless System

As mentioned in Chapter 2, the key problem of applying optimum MUD in practice is its considerable computational complexity. Besides some sub-optimal MUD methods introduced in Chapter 2, a conventional GA assisted MUD was proposed for MC-CDMA [36]. In [36], the output of a bank of conventional single-user MF detectors (i.e. CDs) is used as suitable local minimum to carry on local search. The experiment results confirmed that GA can be used to address the complexity issue induced by optimum MUD. However, their idea of conventional GA in conjugation with local search is still both time- and efficiency-consuming. Interestingly, our novel MDGA proposed in the previous Chapter can also be adopted to address this MUD problem. In this Chapter, the details of the proposed MDGA algorithm for MUD are presented. The simulation results demonstrate the superiority of the MDGA as compared to the conventional GA solution.

5.1 Design of MDGA for MUD

With the analysis of Chapter 4, the premise to accelerate convergence rate with aid of our proposed algorithm is to exploit a favorable local minimum as jumping-off point. Using the output of a bunch of CDs to develop local search scheme for GA is considered to be feasible sustained by experimental performance in the study of [36].

Thus, the output of CDs which only have linear computational complexity is also considered as the elementary chromosome to initialize our population matrix. Based on initial population matrix, MDGA is deployed alone with each generation to maximize the gain of optimum MUD.

5.1.1 Matched Filter assisted MUD

Conventionally, a bunch of CDs deal with user's interference as noise. If the number of users goes infinite, the interference complies with Gaussian distribution according to the central limit theory [37]. The method of CD to detect user data is reasonable. For a certain number of users, the resulting performance of CD inevitably degrades as a sub-optimum solution. Due to its simplicity of implementation and global estimates for all users (a bunch of CDs), the output of CDs is deemed as a suitable candidate to carry on the local search in our MDGA.

5.1.2 MDGA for MUD

Our proposed novel MDGA is designed to accelerate the searching speed to find the optimal solution by adequately exploiting the output of a bunch of CDs as guidance. As compared to conventional GA mechanisms for MUD [107, 108], our MDGA-MUD proposes two main modifications, M1 and M2, namely. The idea is to keep a balanced search throughout all the GA generations: M1 allows us to start the initial search guided by CD's output together with a reasonable amount of randomness derived from general GA theory. M2 is an intelligent replacement

strategy that plays a dominant role in providing fast convergence rate. Combining the two modifications together offers our MDGA a good jumping-off point of search as well as increased convergence rate with low complexity while keeping the optimum performance. Next, we explain in detail how the MDGA operates.

a) Initial Population (M1)

This section explains the first modification - M1. Considering that a good initial estimation of the possible solutions is worthful for GA to obtain good performance at low cost of searching progress, the selection of initial population to approach optimal solution is created by mutating the output of the CDs. Let the total population of chromosomes be "N_{pop}". In order to ensure that each bit of the output of CDs experiences change at least once, we generate the initial "K+1" set of population by perturbing the output of CDs in such a way that the Hamming distance between the output of CDs and the new individual remains 1. The output of CDs is considered as a robust jumping-off point of search. However, there is a high probability that a search which is guided only by the output of CDs can get stuck at local optima at high SNR values. In order to ensure a certain proportional searching diversity we make the rest of the population generated from the mutation of output of CDs to explore optimum solution in the search space as shown in Figure.5.1.

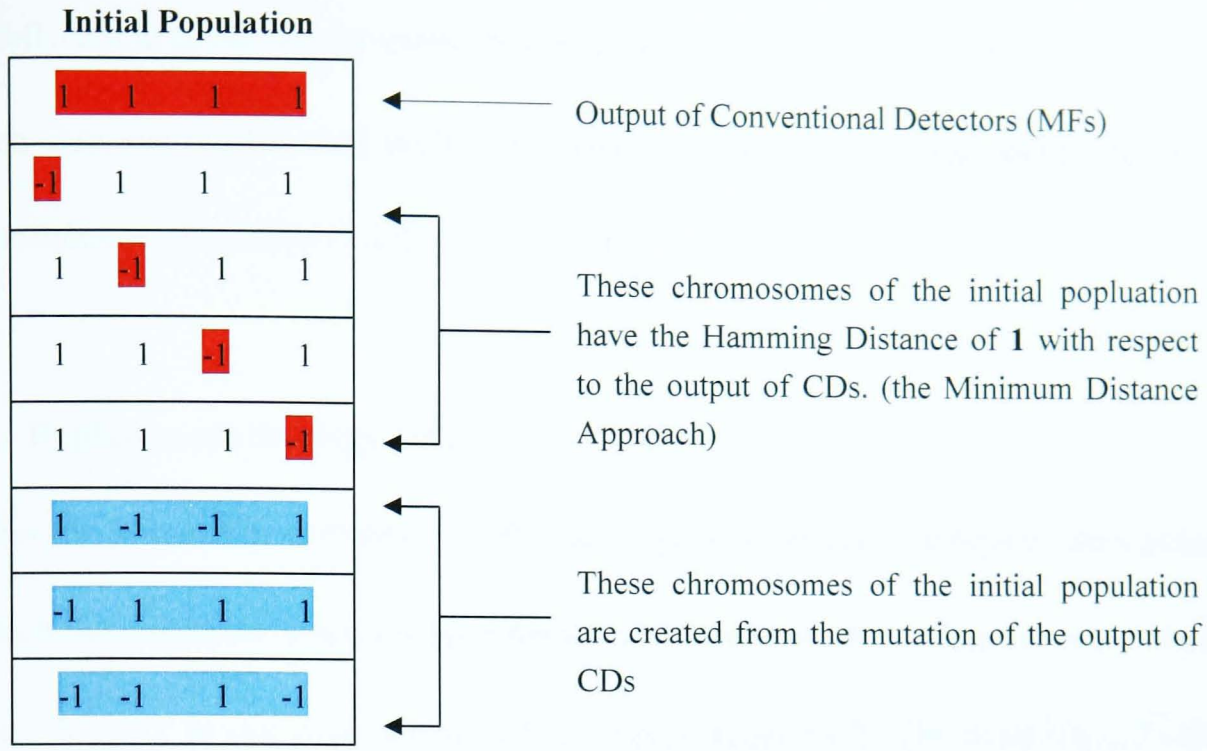

Figure 5.1 The formation of Initial pool for the proposed GA

It is noted here that this modification in the formation of initial population will create some dependency of the population size on the number of users. For example, if the number of users is "K" then population size is N_{pop} >K, so the algorithm will adjust the population size with the increasing number of users, which is actually in accordance with the study carried out by [36], indicating the need of properly increasing the population size when the number of users in the system is increased.

b) Fitness Function

In general GA, the goal of a fitness function is to evaluate the cost or status of each chromosome. In the MUD problem, the objective of the fitness function is the maximization of the cost (or objective) function, as defined in Equation (3.44), which is rewritten as

$$\Omega(d) = 2\,\mathrm{Re}[d^T EZ] - d^T ERE d \tag{5.1}$$

Each bit in vector "d" is actually representing a bit sent by a particular user. The task

of MUD is to detect all the users' bits coherently. In order to correctly detect the bit of each user, we need to find such a combination of vector "$\hat{d}$" that will maximize the cost function (Equation (5.1)).

c) Replacement Strategy (M2)

After the successful evaluation of the initial pool, truncation selection takes place in which the candidate solutions are ordered by fitness, and according to some selection rate, "X*rate*". In our case, we set a fixed value X*rate* =1/2. The most $\lceil N_{pop}/2 \rceil$ fittest individuals in the rank list are selected as candidates parents. For example, if the population size is 30, we first select 15 best candidates by the truncation-selection method and then starting from the fittest two parents we form two offspring by performing simple one-point crossover operation. Then, from the next two fittest mating parents we form two more offspring and so on till we have formed N_{pop}-(K+1)=30-(15+1)=14 new offspring. We designed the mating process in such a way that in each generation, the number of offspring generated is K+1-$\lceil N_{pop}/2 \rceil$ less than the selected parents, where symbol $\lceil N_{pop}/2 \rceil$ acquires the ceiling value of $N_{pop}/2$. After successful mating, we replace K prior chromosomes in the rank except fittest mate from the population matrix by performing the same Minimum Distance approach using the fittest mate, i.e. the population matrix will contain the fittest mate on the top along with the "K+1" individuals having Hamming Distance of **1** between them and the previously formed "N_{pop}-(K+1)" number of offspring. This is how we exploit the information of best mate (local search) at each generation as well as we

also create a reasonable number of offspring out of the mating pool for exploration.

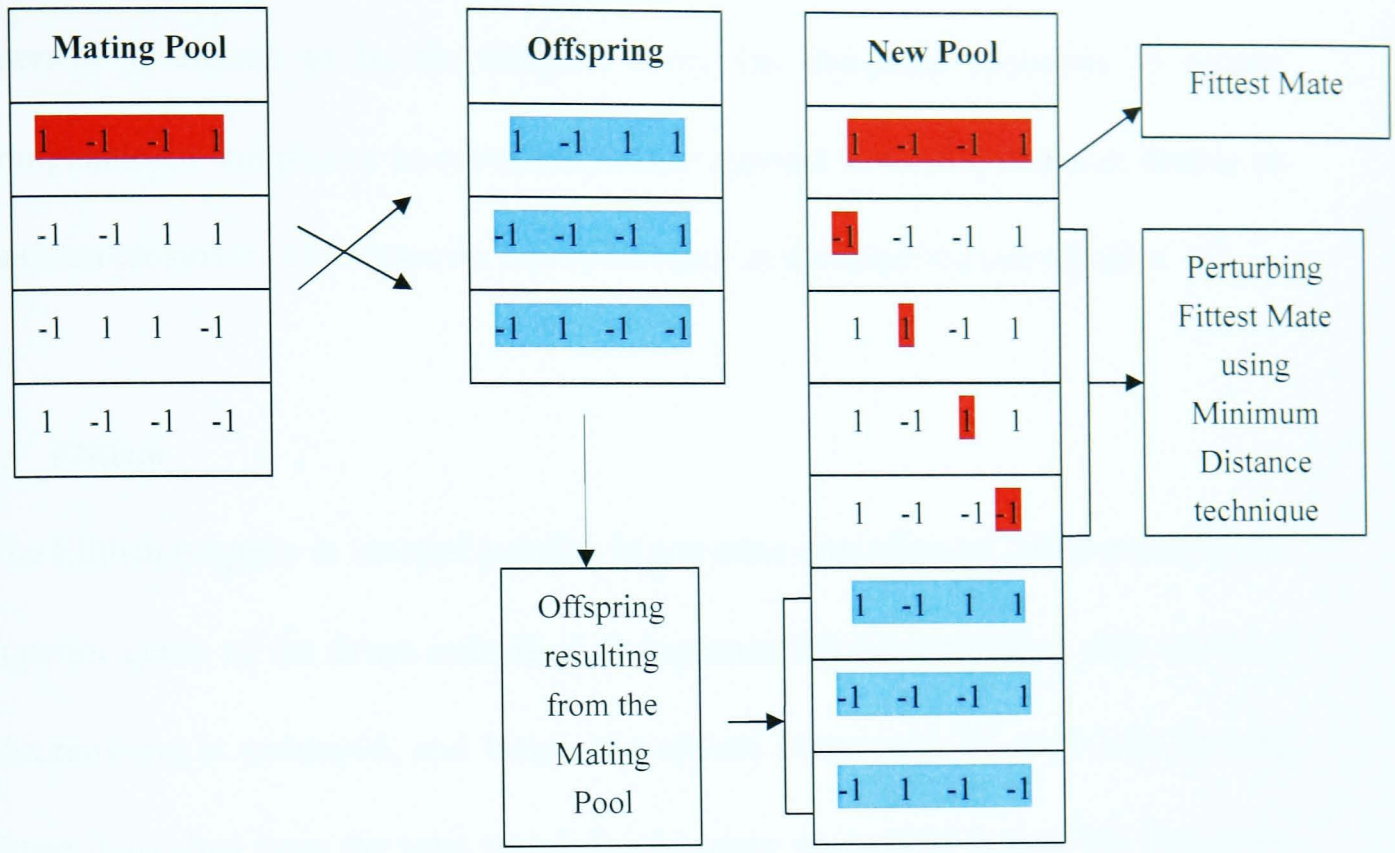

Figure 5.2 A Novel Replacement Strategy for MDGA

In MDGA, the GA is firstly guided by the CD's output and then in the following generations it is guided by the best mate created from the population matrix in each generation. The fittest-initiated "K+1" individuals along with the "N_{pop}-(K+1)" offspring generated from the mating pool ensure that the GA would not be stuck at the local maximum. The process involved in the replacement strategy is shown in Figure 5.2, with an example population size of 8 chromosomes for a 4-user MC-CDMA system. Note that the crossover point is taken after the 2nd bit.

d) Type of Mutation & Crossover

The new population matrix undergoes mutation process which further ensures that our MDGA search will not get stuck around local minimum. Usually, the mutation

probability is chosen close to 0 (in our case, it is chosen to be 0.1). The crossover operator is chosen to be the simplest form, i.e. one-point crossover to reduce computational complexity as compared to conventional GA [108] that uses double or uniform crossover. The crossover rate is set equal to the selection rate which is 1/2.

e) Elitism

The Elitism property is invoked just like in any other conventional GA to preserve the superior genes of the fittest individual during mutation process. Here, only one best chromosome is preserved, and hence, the elitism property is invoked only for one fittest individual from the total population in every generation. Figure 6.3 shows the flow of operations in the proposed GA. In the next section we define the simulation parameters and show the performance and the convergence rate of the highlighted MDGA based MUD.

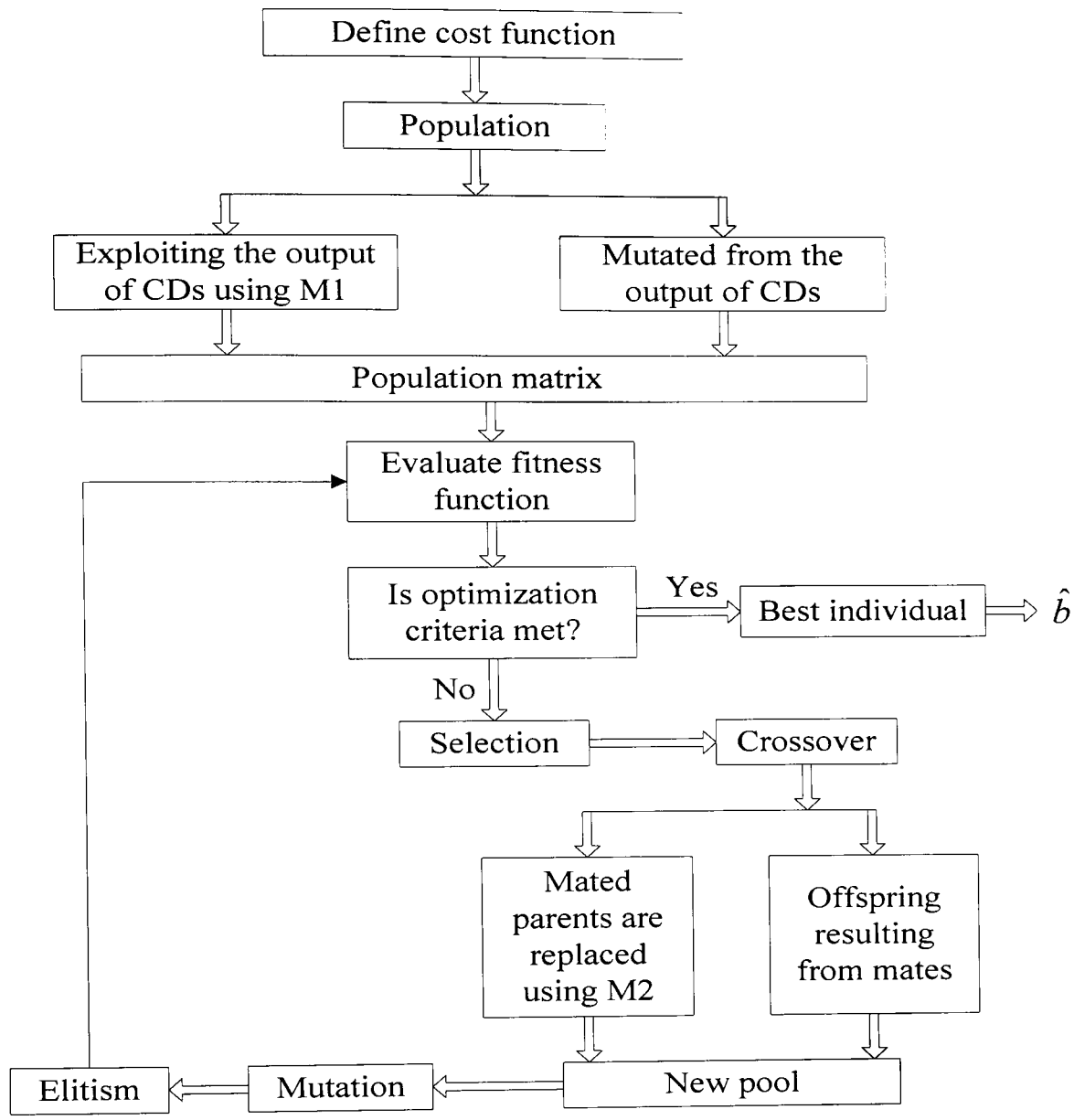

Figure 5.3 The flow chart of MDGA-MUD

5.2 Simulation Analysis

5.2.1 Parameters Configuration

The BER, optimum solution searching time and the computational complexity are the three main performance criteria to be measured. The detection time is governed by the number of generations required to obtain a reliable decision. The computational complexity is determined by the total number of objective function evaluations. Table

5.1 shows the configuration parameters used in the simulations. BPSK modulation type is chosen in the system as an example.

TABLE 5.1 CONFIGURATION OF THE MDGA-MUD

PARAMETERS	METHODS/VALUES
Population size N_{pop}	30
Initialization	Initial population generated using M1
Selection method	Truncation Selection
Selection rate	50%
Crossover operation	Single-point crossover
Crossover rate	1/2
New pool	New pool created using M2
Mutation operation	Standard binary mutation
Mutation probability p_m	0.1
Elitism	Yes
Termination generation	5
Spreading factor (SF)	15

5.2.2 Simulation Results

As shown in Figure 5.4, MDGA can converge very close to the optimum within only 5 generations with a population size of 30 when the number of users is 15. This is

because that not only can MDGA find a good starting point but also achieve a high final convergence rate due to the proposed two methods (M1 and M2). The number of cost function evaluations taken by MDGA is only 150 till it obtains near-optimum solution.

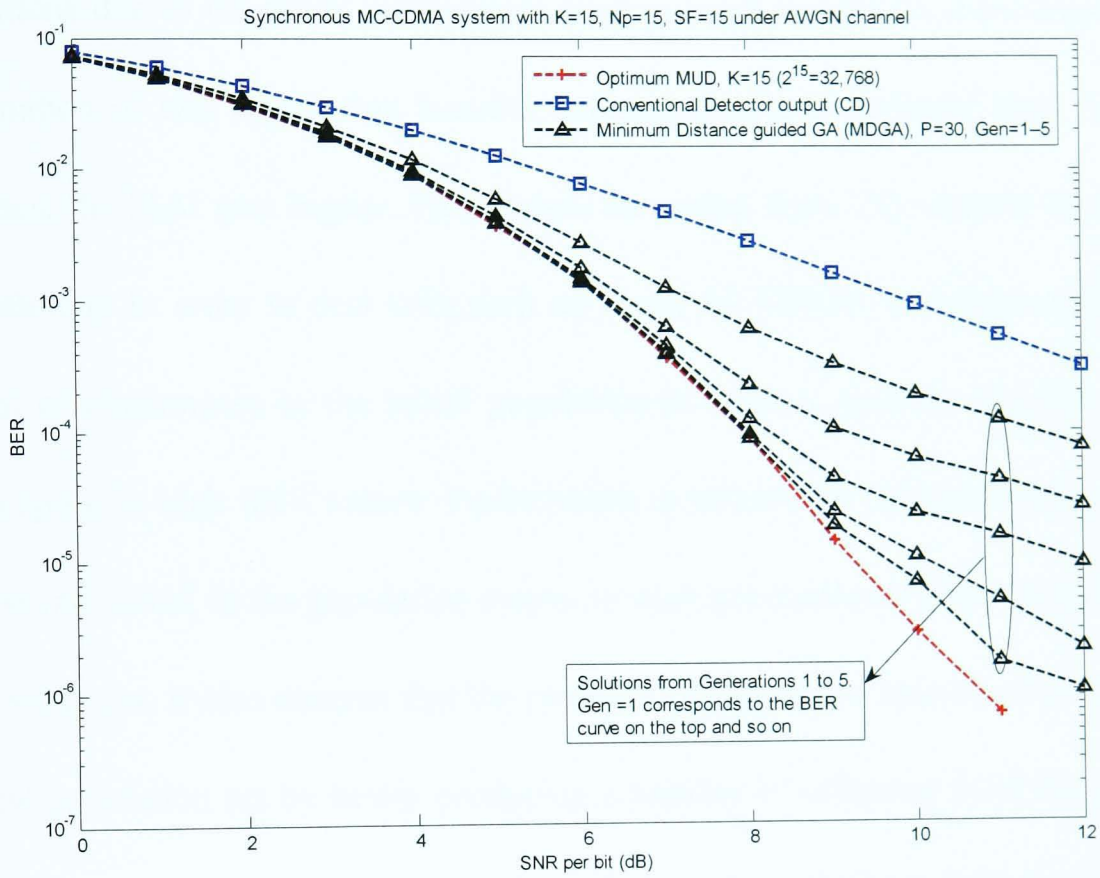

Figure 5.4 The BER performance of the first 5 generations of MDGA assisted MUD in MC-CDMA over an AWGN channel. The MDGA-MUD can converge very close to the optimum in as low as 5 generations with a population size of 30 for a 15-user synchronous MC-CDMA system (SF=15 & N_p=15)

In Figure 5.5, we investigate the individual impact of each modification (M1 and M2). Please note that the convergence graphs of the two modifications actually cross each other after the first generation. Although M1 has a good start due to the Minimum

Distance aproach used to initiate the population and poor convergence due to the conventional replacement strategy. Whereas M2 has a poor start because of the conventional approach used in initializing the GA population which it actually happens in the first geneation, but it also provides a fast convergence in the successive generations due to the novel replacement strategy used in MDGA. Furthermore, the combination of two approaches benefits both schemes and performs best. As SNR increases, the MAI gets higher. This causes the output from CDs further away from the optimum. In order to deal with such an issue, the MDGA introduces reasonable amount of randomness in the initial population in order to gain the diversity in the search space at high SNR values. Furthermore, it utilizes the information carried by the best individual in the population matrix in each generation so as to get better and better solutions. It also ensures that the presence of significant amount of diversity in the new population set by newly producing a number of offspring from the selected mates. The new comers (offspring) along with those individuals exploited best mate's by the Minimum Distance approach react in our MDGA to converge very fast towards the optimum. The conventional GA lacks this ability and is more likely to get stuck at local minimum and hence requires an increase in the number of generations before search terminates. The population size in MDGA is associated with the number of users "K" in the system. The simulation results in Figure 5.6 show that with the increasing number of users in the system, MDGA still closely inosculates the optimum solution. This indicates that the robustness of MDGA with various number of users, if we set $N_{pop} = 2K$. Also, our scheme is robust with the increasing number

of users in the system.

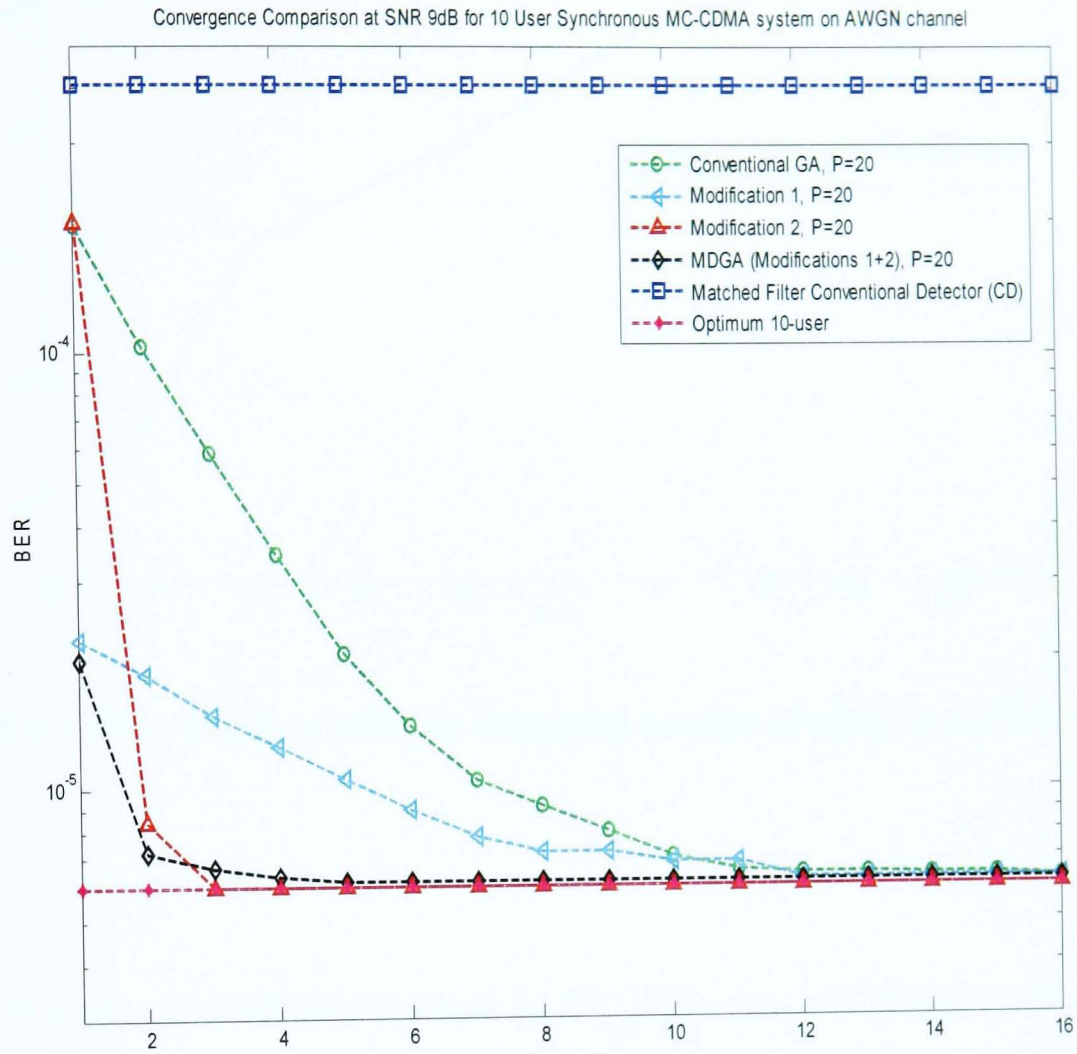

Figure 5.5 Convergence comparison of MDGA vs. Conventional GA [108] for 10-user MC-CDMA system under 9dB SNR

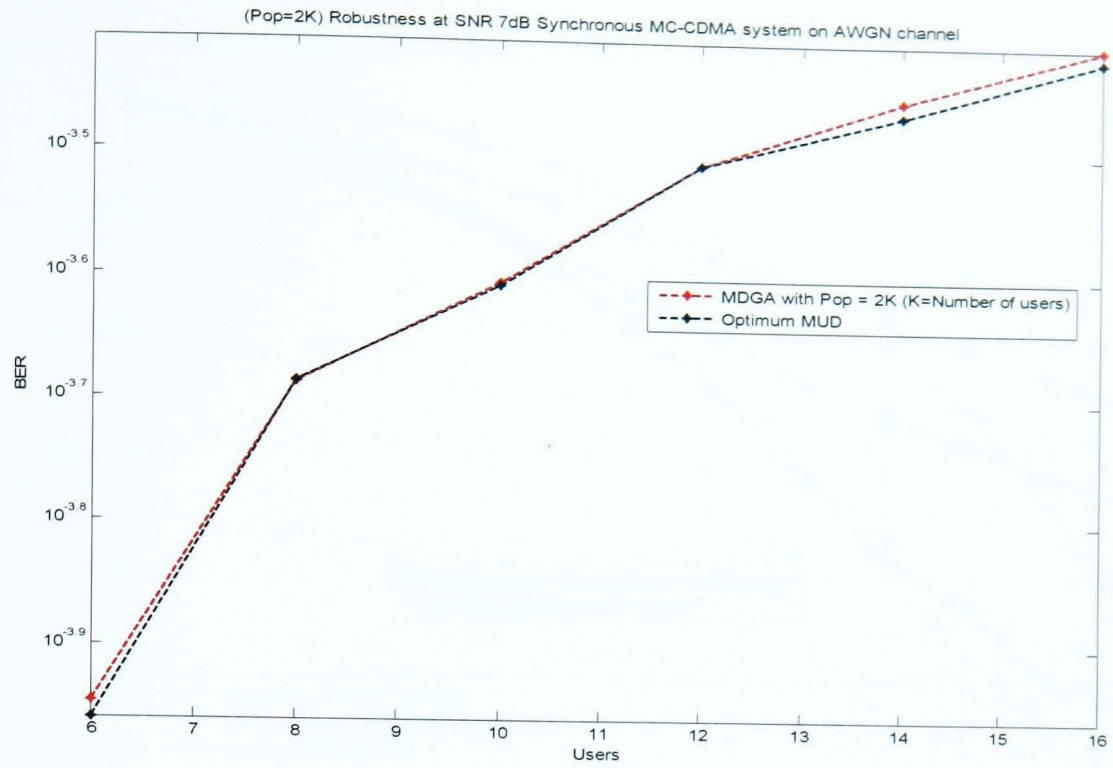

Figure 5.6 MDGA is robust with the increasing number of users in the MC-CDMA system

The percentage of complexity involved is $\left(\frac{Pop \times Gen}{2^K}\right) \times 100\%$. As shown in Figure 5.5, MDGA can give the near-optimum solution within only 150 cost function evaluations (Gen = 5, Pop = 30) as compared to 2^{15} (32,768) evaluations taken by exhaustive search. Hence, it achieves 99.54% reduction in complexity as compared to optimum MUD. Also from Figure 5.5, as compared to conventional GA [108] with 240 (Gen=12, Pop=20) cost function evaluations, the MDGA reaches the optimum in only 100 (Pop=20, Gen=5) cost function evaluations, ensuring 58.3% complexity reduction in terms of cost function evaluations.

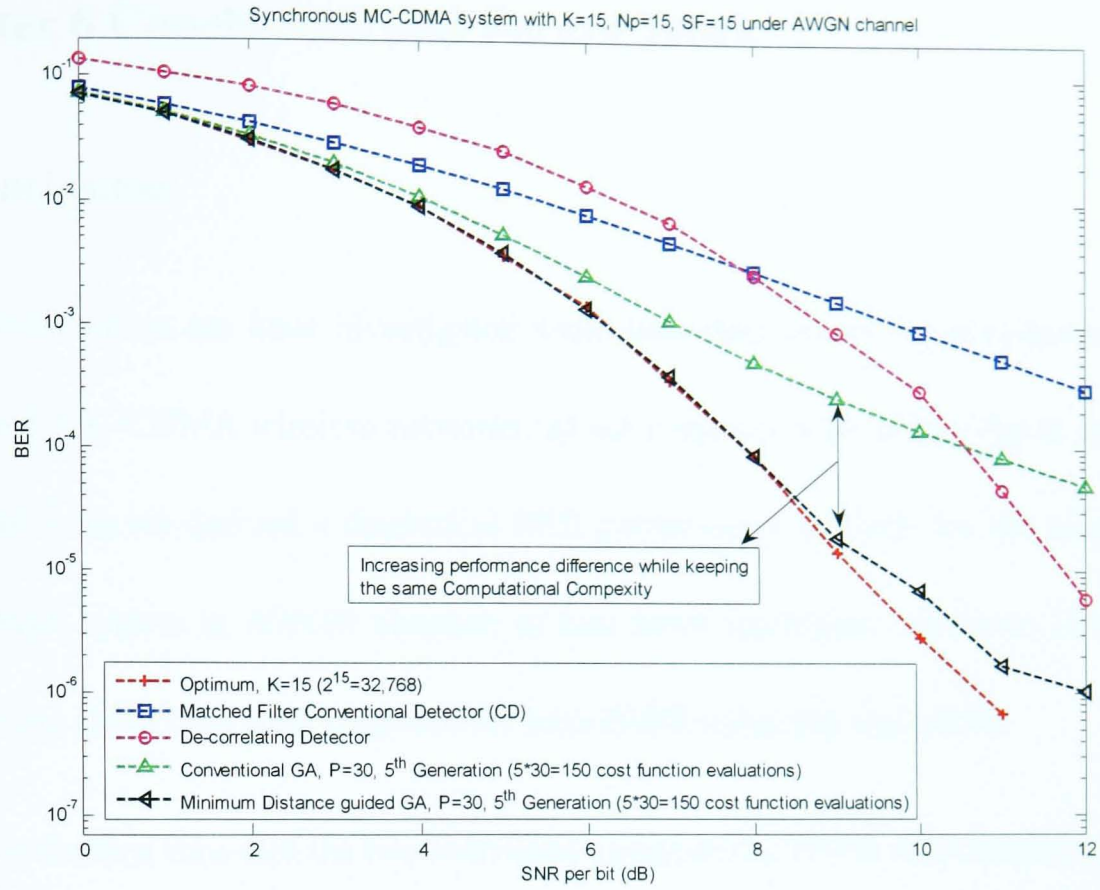

Figure 5.7. BER Comparison of MDGA vs. Conventional GA [108] with the same computational complexity (P=30 and Gen=5) vs. De-Correlating. The MDGA based MUD in 15-user synchronous MC-CDMA (SF=15 & N_p=15) system, outperforms Conventional GA with significant reduction in the BER

The relation between the population size and the number of users in MDGA helps us to further generalize the computational complexity in terms of number of users. For constant termination generation (Gen = 5) the number of cost function evaluations are: $Pop \times Gen = 2K \times 5 = 10K$, if we set $Pop=2K$. Hence, the complexity becomes $\left(\frac{10\boldsymbol{K}}{2^{K}}\right) \times 100\%$. The amount of computational complexity introduced is ten times the number of users, i.e. the number of evaluations = $10K$, where K = (1, 2, 3, … K_{max}).

Chapter 6 Conclusions and Future Work

6.1 Conclusions

In this dissertation we have investigated some important issues for next-generation broadband MC-CDMA wireless networks: a) we proposed a novel intelligent system architecture; b) we derived a theoretical BER performance analysis for the proposed MC-CDMA system in AWGN channel; c) two novel intelligent Minimum Distance guided GAs (MDGAs) were proposed for both PAPR reduction and MUD.

First, it is the first time that the two individual components, PAPR reduction block and MUD block are integrated in an emerging MC-CDMA system, where our new intelligent system design offers a robust structure against both complex issues. The unified system architecture allows one core MDGA block to be used by both transmitter and receiver for both issues which can significantly reduce the implementation cost of practical systems.

Second, we derived a theoretical BER performance analysis for the proposed MC-CDMA system and our analytical results demonstrated that the theoretical BER performance of synchronized MC-CDMA system is the same as that of the synchronized DS-CDMA system under AWGN channel.

Third, in contrast to traditional GAs, our MDGAs start with a balanced ratio of exploration and exploitation which is maintained throughout the process. In our algorithms, a new replacement strategy is designed which increases significantly the

convergence rate and reduces dramatically computational complexity as compared to the conventional GAs. Our simulation results show that, if compared to those schemes using exhaustive search and traditional GAs, our MDGA-based PAPR reduction scheme achieves 99.52% and 50+% reductions in computational complexity, respectively; our MDGA-based MUD scheme achieves 99.54% and 50+% reductions in computational complexity, respectively.

6.2 Future Work

The future work would include:

- Complex phase factors of PTS: Currently, the phase factor selected is binary phase factor set {+1, -1} in the favor of simplicity of the research problem. The future work would be carried on the optimization of the complex phase factor set based on our proposed novel GA.
- Channel conditions: In the current research, the channel is assumed as AWGN channel. The future work will investigate more sophisticated channel conditions such as Rayleigh and Ricean Fading channels.
- Modulation techniques: For the current research, only BPSK modulation is considered. Various higher-order modulation schemes like Quadrature Phase Shift Keying (QPSK), M-ary Quadrature Amplitude Modulations (QAMs), would be further considered.
- Asynchronous system: Only synchronous model MC-CDMA system is assumed in the thesis. Therefore, asynchronous system model should be investigated later.

References

[1] C. Zhen-Wei Qiang, B. Lanvin, M. Minges, E. Swanson, B. Wellenius, G. R. Clarke, N. Halewood, A. Adamali, J. O. Coffey, and Z. Safdar, "Global Trends and Policies-2006: Information and Communications for Development," *World Bank Publications*, January 2006.

[2] R. F. Bellaver, "Wireless: from Marconi to McCaw," *University as a Bridge from Technology to Society. IEEE International Symposium on Technology and Society*. pp. 197-200. Sept. 2000

[3] "People of AT&T Meet People of McCraw." *AT&T Public relations* 1994

[4] J. Korhonen, *Introduction to 3G Mobile Communications.* London: Artech House Publishers, 2001.

[5] S. C. Yang, *3G CDMA 2000 Wireless System Engineering*. London: Artech House, 2004

[6] TDSCDMA forum, [WWW] available from: http://www.tdscdma-forum.org/EN/ (Accessed on 18/01/08)

[7] S. Ohmori, Y. Yamao, and N. Nakajima, " The Future Generations of Mobile Communications based on Broadband Access Technologies, " *IEEE Communications Magazine*, vol. 38 (12), pp. 134-142, Dec 2000

[8] IEEE 802.11 Wireless Local Area Network standard, [WWW] available from: http://ieee802.org/11/IEEE 802.11 (Accessed on 19/01/08)

[9] IEEE 802.16 Wireless Metropolitan Area Network (MAN) standard, [WWW] available from: http://wirelessman.org/ (Accessed on 19/01/08)

[10] Intel UWB Technology, [WWW] available from: http://www.intel.com/technology/comms/uwb/ (Accessed on 20/01/08)

[11] LTE standard, [WWW] available from: http://www.3gpp.org/Highlights/LTE/lte.htm (Accessed on 20/01/08)

[12] N. Yee, J. P. Linnartz and G. Fettweis, "Multi-Carrier CDMA in Indoor Wireless Radio Networks," in *Proceedings IEEE International Symposium on Personal, Indoor and Mobile Radio Communucations (PIMRC '93)*, Yokohama, Japan, 1993

[13] K. Fazel, and L. Papke, "On the performance of Convolutionally- Coded CDMNOFDM for Mobile Communication System," in *Proceedings IEEE International Symposium on Personal, Indoor and Mobile Radio Communications (PIMRC '93)*, pp. 468-472, Yokohama, Japan, 1993

[14] A. Pandharipande, "Principles of OFDM," in *IEEE Potentials,* vol. 21 (2). pp. 16 - 19 April-May 2002

[15] B. Sklar, *Digital Communications Fundamentals and Applications.* USA: Prentice-Hall 1988

[16] S. Verdu, *Multiuser Detection.* UK: Cambridge University Press 1998

[17] N. Abramson, "Development of the ALOHANET," *IEEE Transactions on Information Theory*, vol. 31 (2). pp. 119-123, Mar 1985

[18] C. Namislo, "Analysis of Mobile Radio Slotted ALOHA Networks," *IEEE Transactions on Vehicular Technology*, vol. 33 (3). pp. 199-204, Aug 1984

[19] N. Meisner, J.Segal, and M. Tanigawa, "An Adaptive Retransmission Technique for Use in a Slotted-ALOHA Channel, " *IEEE Transactions on Communications*, vol 28. (9). Part 1, pp. 1776 – 1778, Sep 1980

[20] M. Ferguson, "On the Control, Stability, and Waiting Time in a Slotted ALOHA Random-Access System," *IEEE Transactions on Communications*, vol. 23 (11). pp. 1306-1311, Nov 1975

[21] L. Kleinrock, and F. Tobagi, "Packet Switching in Radio Channels: Part I--Carrier Sense Multiple-Access Modes and Their Throughput-Delay Characteristics" *IEEE Transactions on Communications,* vol. 23 (12). pp. 1400 – 1416, Dec 1975

[22] K.-T. Ko, and B. Davis, "A Space-Division Multiple-Access Protocol for Spot-Beam Antenna and Satellite-Switched Communication Network," *IEEE Journal on Selected Areas in Communications*, vol. 1 (1). pp. 126 – 132, Jan 1983

[23] K. L. Bell, J. Capetanakis, and V. A. Marshall, "Optimal traffic scheduling in SDMA/FDMA/TDMA MILSATCOM systems," *IEEE Military Communications Conference (MILCOM '91), Conference Record, 'Military Communications in a Changing World,* vol.2. pp. 653 – 657. 4-7 Nov. 1991

[24] M. I. Silventoinen, and H. Posti, "Radio resource management in a novel indoor GSM base station system," *The 8th IEEE International Symposium on Personal, Indoor and Mobile Radio Communications, 'Waves of the Year 2000' (PIMRC '97)*, vol. 3. pp. 776 – 780. 1-4 Sept. 1997

[25] D. Gerlach, and P. Arogyaswami. "Base station transmitter antenna arrays with mobile to base feedback," *1993 Conference Record of The Twenty-Seventh Asilomar Conference on Signals, Systems and Computers,* vol.2. pp.1432 – 1436. 1-3 Nov. 1993

[26] M. Tangemann, "Near-Far Effects in Adaptive SDMA Systems," *The 6th IEEE International Symposium on Personal, Indoor and Mobile Radio Communications, 1995. (PIMRC'95). 'Wireless: Merging onto the Information Superhighway'*, vol. 3. pp. 1293. 27-29 Sept. 1995

[27] T. Halonen, J. Romero, and J. Melero, *GSM, GPRS, and EDGE Performance: Evolution towards*

3G/UMTS- 2nd ed. UK: John Wiley & Sons, Ltd. 2003

[28] T. Ojanpera, and R. Prasad, *Wideband CDMA for Third Generation Mobile Communications.* Norwood, MA, USA: Artech House, Inc. 1998

[29] M. K. Simon, J. K. Omura, R. A. Scholtz, and B. K. Levitt, *Spread Spectrum Communications Handbook.* USA: McGraw Hill, 1994.

[30] U. Grob, A. L. Welti, E.Zollinger, R. Kung, and H.Kaufmann, "Microcellular Direct-Sequence Spread-Spectrum Radio System using N-path RAKE Receiver," *IEEE Journal on Selected Areas in Communications*, vol. 8 (5). pp. 772 – 780. June 1990

[31] C. Kchao, and G. L. Stubeer, "Analysis of a Direct-Sequence Spread-Spectrum Cellular Radio System," *IEEE Transactions on Communications,* vol. 41 (10). pp. 1507 – 1517. Oct 1993

[32] E. Le Strat, "Architecture Simplications for an Improved Performance RAKE Receiver," *IEEE 43rd Vehicular Technology Conference,* pp. 726 – 729. 18-20 May 1993

[33] A. Baier, U.-C. Fiebig, W. Granzow, W. Koch, P. Teder, and J. Thielecke, "Design study for a CDMA-based Third-Generation Mobile Radio System," *IEEE Journal on Selected Areas in Communications*, vol. 12, pp. 733–743, May 1994

[34] T. Ottosson and A. Svensson, "On Schemes for Multirate Support in DS-CDMA Systems,"

Wireless Personal Communications (Kluwer), vol. 6, pp. 265–287, Mar 1998

[35] S. Ramakrishna and J. M. Holtzman, "A Comparison between Single Code and Multiple Code Transmission Schemes in a CDMA System," in *Proceedings of the IEEE Vehicular Technology Conference (VTC)* (Ottawa, Canada), pp. 791–795, May 18-21 1998

[36] L. Hanzo, L.-L. Yang, E.-L. Kuan, and K. Yen, *Single- and Multi-Carrier CDMA: Multi-User Detection, Space-Time Spreading, Synchronization, Standards and Networking*. Piscataway, NJ: IEEE Press/Wiley, 2003.

[37] J. G. Proakis, *Digital Communications-4th ed.* USA: McGraw Hill, 2001

[38] L. Hanzo, B. J. Choi, T. Keller, and M. Münster, *OFDM and MC-CDMA for Broadband Multi-User Communications, WLANs, and Broadcasting*, John Wiley and Sons, 2003

[39] S. B.Weinstein and P. Ebert, "Data Transmission by Frequency-Division Multiplexing Using the Discrete Fourier Transform," *IEEE Transactions on Communication Technology*, vol. 19. pp. 628–634, October 1971.

[40] J. Bingham, "Multi-Carrier Modulation for Data Transmission: An Idea Whose Time Has Come," *IEEE Communications Magazine*, pp. 5–14, May 1990.

[41] I. Kalet, "The Multitone Channel," *IEEE Transactions on Communications*, vol. 37, pp. 119–124, February 1989.

[42] R. V. Nee, and R. Prasad, *OFDM for Wireless Multimedia Communications*. USA: Artech House, 2000.

[43] J. J. Gledhill, "OFDM for digital terrestrial television," *IEE Colloquium on Digital Terrestrial Television,* pp. 2/1 - 2/8, 10 Nov 1993

[44] X. D. Wang, "OFDM and Its Application to 4G," International Conference on Wireless and Optical Communications. 14th Annual WOCC 2005, pp. 69, 22-23 April 2005

[45] R. Nogueroles, M. Bossert, and V. Zyablov, "Capacity of MC-FDMA in Mobile Communications," *The 8th IEEE International Symposium on Personal, Indoor and Mobile Radio Communications, 1997. 'Waves of the Year 2000'. PIMRC '97,* vol. 1. pp. 110 – 114, 1-4 Sept. 1997

[46] S. Kaiser, "MC-FDMA and MC-TDMA vs. MC-CDMA and SS-MC-MA: Performance Evaluation for Fading Channels," *in Proceedings IEEE 5th International Symposium on Spread Spectrum Techniques and Applications*, vol. 1. pp. 200 – 204, 2-4 Sept. 1998

[47] B. Jabbair, and D. McDysan, "Performance of Demand Assignment TDMA and Multi-Carrier TDMA Satellite Networks," *IEEE Journal on Selected Areas in Communications,* vol. 10 (2). pp. 478 – 486, Feb. 1992

[48] B. Xu, C. Y. Yang, and G. G. Bi, "MC-TDMA Scheme for Downlink Broadband Wireless Communications," *IEEE International Conference on Communications, 2005. ICC 2005.* vol. 2. pp. 944 – 948, 16-20 May 2005

[49] N. Yee, J.-P. Linnartz, and G. Fettweis, "Multi-Carrier CDMA in Indoor Wireless Radio Network," *IEICE Transactions on Communications*, vol. E77-B, pp. 900–904, July 1994

[50] B. Popov'c, "Spreading Sequences for Multi-Carrier CDMA Systems," *IEEE Transactions on Communications*, vol. 47. pp. 918–926, June 1999

[51] A. Chouly, A. Brajal, and S. Jourdan, "Orthogonal Multi-Carrier Techniques Applied to Direct Sequence Spread Spectrum CDMA Systems," in *Proceedings of the IEEE GLOBECOM '93*, (Houston, USA), pp. 1723–1728, November 1993

[52] S. Kondo and L. Milstein, "On the Use of Multi-Carrier Direct Sequence Spread Spectrum Systems," in *Proceedings of IEEE MILCOM'93*, (Boston, MA), pp. 52–56, Oct. 1993

[53] S. Kondo and L. Milstein, "Performance of Multi-Carrier DS CDMA Systems," *IEEE Transactions on Communications*, vol. 44, pp. 238–246, February 1996

[54] V. Dasilva and E. Sousa, "Multi-Carrier Orthogonal CDMA Signals for Quasi-Synchronous Communication Systems," *IEEE Journal on Selected Areas in Communications*, vol. 12. pp. 842–852. June 1994

[55] V. M. DaSilva and E. S. Sousa, "Performance of Orthogonal CDMA Codes for Quasi-Synchronous Communication Systems," in *Proceedings of IEEE ICUPC'93* (Ottawa, Canada), pp. 995–999. Oct. 1993

[56] Y. Sanada and M. Nakagawa, "A Multiuser Interference Cancellation Technique Utilizing Convolutional Codes and Multi-Carrier Modulation for Wireless Indoor Communications," *IEEE Journal on Selected Areas in Communications*, vol. 14, pp. 1500–1509, October 1996

[57] E. Sourour and M. Nakagawa, "Performance of Orthogonal Multi-Carrier CDMA in a Multipath Fading Channel," *IEEE Transactions on Communications*, vol. 44, pp. 356–367, March 1996

[58] A. Matsumoto, K. Miyoshi, M. Uesugi, and O. Kato, "A Study on Time Domain Spreading for OFCDM," The 5th International Symposium on Wireless Personal Multimedia Communications, vol. 2, pp.725 – 728, 27-30 Oct. 2002

[59] N. Maeda, H. Atarashi, S. Abeta, and M. Sawahashi, "Performance of Forward Link Broadband OFCDM Packet Wireless Access Using MMSE Combining Scheme Based on SIR Estimation" *IEEE 55th Vehicular Technology Conference, VTC Spring 2002*, vol. 2, pp. 1045 – 1049, 6-9 May 2002

[60] M. Tanno, H.Atarashi, K.Higuchi, and M.Sawahashi, "Three-Step Fast Cell Search Algorithm Utilizing Common Pilot channel for OFCDM Broadband Packet Wireless Access," IEEE 56th

Vehicular Technology Conference, 2002. Proceedings. VTC 2002-Fall, vol. 3, pp. 1575 – 1579, 24-28 Sept. 2002

[61] A. Morimoto, S. Abeta, and M.Sawahashi, "Cell Selection Based on Shadowing Variation for Forward Link Broadband OFCDM Packet Wireless Access," IEEE 56th Vehicular Technology Conference, 2002. Proceedings. VTC 2002-Fall, vol. 4, pp. 2071 – 2075, 24-28 Sept. 2002

[62] N. Miki, S.Abeta, and M. Sawahashi, "Evaluation of Throughput Employing Hybrid ARQ Packet Combining in Forward Link OFCDM Broadband Wireless Access," The 13th IEEE International Symposium on Personal, Indoor and Mobile Radio Communications, vol. 1, pp. 394 – 398, 15-18 Sept. 2002

[63] L. Vandendorpe, "Multitone Direct Sequence CDMA System in an Indoor Wireless Environment," in *Proceedings of IEEE First Symposium of Communications and Vehicular Technology in the Benelux, Delft, The Netherlands*, pp. 4.1–1–4.1–8, Oct. 1993

[64] L. Vandendorpe, "Multitone Spread Spectrum Multiple Access Communications System in a Multipath Rician Fading Channel," *IEEE Transactions on Vehicular Technology*, vol. 44, no. 2, pp. 327–337, 1995

[65] R. Prasad and S. Hara, "Overview of Multi-Carrier CDMA," *IEEE Communications Magazine*, vol. 35, pp. 126–133, Dec. 1997.

[66] H. Steendam, M. Moeneclaey, and H. Sari, "The Effect of Carrier Phase Jitter on the Performance of Orthogonal Frequency-Division Multiple-Access Systems," *IEEE Transactions on Communications,* vol. 46 (4), pp. 456-459, Apr 1998

[67] S. Zhou, and G. B. Giannkis, "Generalized Frequency Hopping OFDMA Through Unknown Frequency-Selective Multipath Channels," *IEEE Wireless Communications and Networking Conference, WCNC 200,* vol.1, pp. 56 – 60, 23-28 Sept. 2000

[68] A. Stamoulis, L. Zhiqiang, and G. B. Giannakis, "Space-Time Block-Coded OFDMA with Linear Precoding for Multirate Services," *IEEE Transactions on Acoustics, Speech, and Signal Processing,* vol. 50, Issue 1, pp. 119 – 129, Jan. 2002

[69] S. B. Weinstein, P. M. Ebert, "Data Transmission by Frequency Division Multiplexing Using the Discrete Fourier Transform," *IEEE Transactions on Communication Technology,* vol. COM-19, pp. 628-634, October 1971

[70] S. Kondo and L. Milstein, "On the Use of Multi-Carrier Direct Sequence Spread Spectrum Systems," in *Proceedings of IEEE MILCOM'93*, (Boston, MA), pp. 52–56, Oct. 1993

[71] S. Kondo and L. Milstein, "Performance of Multi-Carrier DS CDMA Systems," *IEEE Transactions on Communications*, vol. 44, pp. 238–246, February 1996

[72] V. Dasilva and E. Sousa, "Multi-Carrier Orthogonal CDMA Signals for Quasi-Synchronous

Communication Systems," *IEEE Journal on Selected Areas in Communications*, vol. 12. pp. 842–852. June 1994

[73] V. M. DaSilva and E. S. Sousa, "Performance of Orthogonal CDMA Codes for Quasi-Synchronous Communication Systems," *in Proceedings of IEEE ICUPC'93, (Ottawa, Canada)*, pp. 995–999, Oct. 1993.

[74] Y. Sanada and M. Nakagawa, "A Multiuser Interference Cancellation Technique Utilizing Convolutional Codes and Multi-Carrier Modulation for Wireless Indoor Communications," *IEEE Journal on Selected Areas in Communications*, vol. 14, pp. 1500–1509, October 1996

[75] E. Sourour and M. Nakagawa, "Performance of Orthogonal Multi-Carrier CDMA in a Multipath Fading Channel," *IEEE Transactions on Communications*, vol. 44, pp. 356–367, March 1996

[76] A. Matsumoto, K. Miyoshi, M. Uesugi, and O. Kato, "A Study on Time Domain Spreading for OFCDM," *The 5th International Symposium on Wireless Personal Multimedia Communications,* vol. 2, pp. 725 – 728, 27-30 Oct. 2002

[77] Y. Q. Zhou, J. Z. Wang, and T.-S. Ng, "Two Dimensionally Spread OFCDM Systems for 4G Mobile Communications," *IEEE Region 10 Conference TENCON 2007,* pp. 1 – 4, Oct. 30 2007-Nov. 2 2007

[78] C. Rapp, "Effects of HPA-Nonlinearity on a 4-DPSWOFDM Signal for a Digital Sound Broadcasting System," in *Proceedings of the Second European Conference on Satellite Communications, Lihge, Belgium*, pp. 179- 184, October 22-24, 1991,

[79] X. D. Li and L. J. Cimini. Jr., "Effects of Clipping and Filtering on the Performance of OFDM," *IEEE 47th Vehicular Technology Conference,* vol. 3, pp. 1634 – 1638, 4-7 May 1997

[80] R. V. Nee and A. D. Wild, "Reducing the Peak-to-Average Power Ratio of OFDM," *48th IEEE Vehicular Technology Conference, VTC 98,* vol. 3, pp. 2072 – 2076, 18-21 May 1998

[81] X. B. Wang, T. T. Tjhung, and C. S. Ng, "Reduction of Peak-to-Average Power Ratio of OFDM System Using a Companding Technique," *IEEE Transactions on Broadcasting*, vol. 45, no.3, Sept.1999

[82] A. Mattsson, G. Mendenhall, and T. Dittmer, "Comments on 'Reduction of Peak-to-Average Power Ratio of OFDM System Using a Companding Technique'," *IEEE Transaction on Broadcasting*

[83] X. B. Wang, T. T.Tjhung, and C. S. Ng, "Reply to the comments on 'Reduction of peak-to-average power ratio of OFDM system using a companding technique'," *IEEE Transactions on Broadcasting,* vol. 45. (4), pp. 420 – 422, Dec. 1999

[84] X. Huang, J. H. Lu, J. L. Zheng, J. Chuang, and J. Gu, "Reduction of Peak-to-Average Power Ratio of OFDM Signals with Companding Transform," *Electronics Letters,* vol 37, Issue 8, pp. 506 – 507, 12 Apr 2001

[85] R. D. J. Van Nee, "OFDM Codes for Peak-to-Average Power Reduction and Error Correction," *IEEE Global Telecommunications Conference,* London, pp. 740-744, 18-22, Nov. 1996.

[86] N. Ohkubo and T. Ohtsuki, " A Peak to Average Power Ratio Reduction of Multi-Carrier CDMA Using Selected Mapping," in *Proceedings of Vehicular Technology Conference (VTC),* vol.4 pp.2086-2090, 24-28 Sept. 2002

[87] L. J. Cimini. Jr. and N.R. Sollenberger, "Peak-to-Average Power Ratio Reduction of an OFDM Signal using Partial Transmit Sequences," *IEEE International Conference on Communications. (ICC'99),* vol. 1, pp. 511-515, 6-10 June. 1999

[88] S. H. Muller and J. B. Huber, "OFDM with Reduced Peak-to-Average Power Ratio by Optimum Combination of Partial Transmit Sequences," *Electronics Letters,* vol.33 (5), pp. 368-369, Feb. 1997

[89] Y. S. Li, J.-H. Kyung, J.-W. Son, and H.-G. Ryu, "PAPR Reduction in MC/DS CDMA System by DFT Spreading Codes," *Third International Conference on Information Technology and Applications, 2005. ICITA 2005,* vol. 2, pp. 326 – 329, 4-7 July 2005

[90] J. Armstrong, "Peak-to-Average Power Reduction for OFDM by Repeated Clipping and Frequency Domain Filtering," Electronics Letters, vol. 38, Issue 5, pp. 246 – 247, 28 Feb. 2002

[91] T. A. Wilkinson and A. E. Jones, "Minimisation of the Peak to Mean Envelope Power Ratio of Multi-Carrier Transmission Schemes by Block Coding," *IEEE 45th Vehicular Technology Conference*, vol. 2, pp. 825 – 829, 25-28 July 1995

[92] F. Danilo-Lemoine, D. Falconer, C.-T. Lam, M. Sabbaghian, and K. Wesołowski, "Power Backoff Reduction Techniques for Generalized Multi-Carrier Waveforms," *EURASIP Journal on Wireless Communications and Networking*, vol. 2008, Article ID 437801, 13 pages, 2008

[93] W. V. Etten, "Maximum Likelihood Receiver for Multiple Channel Transmission Systems," *IEEE Trans. Commun.*, vol. 24, pp. 276-283, Feb. 1976

[94] S. Moshavi, "Multiuser Detection for DS-CDMA Communications," *IEEE Communications Magazine*, October 1996

[95] S. L. Miller and B. J. Ranbolt, "MMSE Detection of Multi-Carrier CDMA," *IEEE Journal on Selected Areas in Communications*, vol. 18, pp. 2356-2362, Nov 2000

[96] M. Kavehrad and J. Salz. "Cross-Polarization Cancellation and Equalization in Digital Transmission over Dually Polarized Multipath Fading Channels," *AT&T Technical Journal*, 64:2211-2245, Dec. 1985

[97] J. H. Holland, *Adaptation in Natural and Artificial Systems*, University of Michigan Press, Ann Arbor, 1975

[98] R. L. Haupt and S. E. Haupt, "Practical Genetic Algorithms", *Second Edition, John Wiley & Sons, Inc*, 2004

[99] C. Tellambura, " Phase Optimization Criterion for Reducing Peak-to-Average Power Ratio in OFDM," *Electronics Letters,* vol. 34 (2), pp. 169-170, 22 Jan. 1998

[100] D.-H. Park and H.-K. Song, "A New PAPR Reduction Technique of OFDM System with Nonlinear High Power Amplifier," *IEEE Transactions on Consumer Electronics,*vol. 53, Issue 2, pp. 327 – 332, May 2007

[101] W. S. Ho, A. Madhukumar, and F. Chin, "Peak-to-Average Power Reduction Using Partial Transmit Sequences: A Suboptimal Approach Based on Dual Layered Phase Sequencing," *IEEE Trans. Broadcasting*, vol. 49, no. 2, pp. 225–231, June 2003.

[102] Y.-H. You, W.-G. Jeon, J.-H. Paik, and H.-K. Song, "A Simple Construction of OFDM-CDMA Signals With Low Peak-to-Average Power Ratio," *IEEE Trans. Broadcasting*, vol. 49, no. 4. pp. 403–407, Dec. 2003.

[103] O.-J. Kwon and Y.-H. Ha, "Multi-Carrier Pap Reduction Method Using Sub-Optimal PTS with Threshold," *IEEE Trans. Broadcasting*, vol. 49, no.2, pp. 232–236, June 2003.

[104] D.-W. Lim, S.-J. Heo, J.-S. No, and H. Chung, "A New PTS OFDM Scheme with Low Complexity for PAPR Reduction," *IEEE Trans. Broadcasting*, vol. 52, no. 1, pp. 77–82, Mar. 2006.

[105] L. Yang, R. S. Chen, Y. M. Siu, and K. K. Soo, "PAPR Reduction of an OFDM Signal by Use of PTS with Low Computational Complexity," *IEEE Trans. Broadcasting*, vol. 52, no. 1, pp. 83–86, Mar. 2006

[106] J. J. Grefenstette, "Optimization of Control Parameters for Genetic Algorithms," IEEE Transactions on Systems, Man and Cybernetics, vol. 16, Issue 1, pp. 122 – 128, Jan. 1986

[107] M. J. Juntti, "Genetic Algorithms for Multiuser Detection in Synchronous CDMA," *IEEE International Symposium on Inform Theory*, pp. 492, 1997

[108] H. Wei, and L. Hanzo, "Reduced-Complexity Near-Optimum Genetic Assisted Multiuser Detection for Synchronous Multi-Carrier CDMA", *Proc. of 2004 IEEE VTC-Spring Conf.*, Milan (I), vol. 3, pp. 1717-1721, May 17-19 2004